

**SPLICE STRENGTH OF EPOXY-COATED
HIGH RELATIVE RIB AREA BARS**

By

CHANGZHENG TAN

DAVID DARWIN

MICHAEL L. THOLEN

JUN ZUO

A Report on Research Sponsored by

THE NATIONAL SCIENCE FOUNDATION

Research Grants No. MSS-9021066 and CMS-9402563

THE U.S. DEPARTMENT OF TRANSPORTATION

FEDERAL HIGHWAY ADMINISTRATION

THE CIVIL ENGINEERING RESEARCH FOUNDATION

Contract No. 91- N6002

THE REINFORCED CONCRETE RESEARCH COUNCIL

Project 56

**STRUCTURAL ENGINEERING AND ENGINEERING MATERIALS
SL REPORT 96-2**

UNIVERSITY OF KANSAS CENTER FOR RESEARCH, INC.

LAWRENCE, KANSAS

MAY 1996

This report was prepared by the University of Kansas Center for Research, Inc. as an account of work sponsored by the National Science Foundation (NSF), the Federal Highway Administration, and the Civil Engineering Research Foundation (CERF).

Any opinions, findings, and conclusions or recommendations expressed in this material are those of the authors and do not necessarily reflect the views of the National Science Foundation or the Federal Highway Administration.

Neither CERF, nor any persons acting on behalf of either:

- a. Makes any warranty or representation, express or implied, with respect to the accuracy, completeness, or usefulness of the information contained in this report, or that the use of any apparatus, method, or process disclosed in this report may not infringe third party rights; or
- b. Assumes any liability with respect to the use of, or for damages resulting from the use of, any information, apparatus, method; or process disclosed in this report.
- c. Makes any endorsement, recommendation or preference of specific commercial products, commodities or services which may be referenced in this report.

SPLICE STRENGTH OF EPOXY-COATED HIGH RELATIVE RIB AREA BARS

ABSTRACT

The effect of epoxy coating on the splice strength of high relative rib area bars with and without confining transverse reinforcement is described. Test results for 47 beam splice specimens containing No. 5, No. 8, or No. 11 (16, 25 or 36 mm) bars with relative rib areas ranging from 0.101 to 0.141 and seven deformation patterns are included in the analysis. Twenty-seven of the 47 beam splice tests are reported for the first time. Average coating thickness ranged from 7.1 to 16.8 mils (0.18 to 0.43 mm). Forty-three specimens were bottom-cast and four were top-cast. The test results for the high relative rib area bars are combined with 44 previous splice tests using conventional bars. Epoxy coating was found to have a much less detrimental effect on splice strength for high relative rib area bars than for conventional bars. The average splice strength ratio of coated to uncoated bars C/U is 0.89, compared to 0.74 for conventional reinforcement. C/U is approximately the same for splices with and without transverse reinforcement. The test results of the current study indicate that the development length modification factor required by the ACI Building Code (318-95) and the AASHTO Bridge Specifications (1992) can be reduced from 1.5 to 1.2 for epoxy-coated high relative rib bars.

Keywords: bond (concrete to reinforcement); bridge specifications; building codes; deformed reinforcement; development; epoxy coating; reinforcing steels; relative rib area; splicing; structural engineering.

ACKNOWLEDGMENTS

The authors gratefully acknowledge the financial and material support received by this project. Support for this research was provided by the National Science Foundation under NSF Grants No. MSS-9021066 and CMS-9402563, the U.S. Department of Transportation - Federal Highway Administration, the Civil Engineering Research Foundation under CERF Contract No. 91-N6002, the Reinforced Concrete Research Council under RCRC Project 56, ABC Coating, Inc., AmeriSteel (formerly Florida Steel Corporation), Birmingham Steel Corporation, Chaparral Steel, Fletcher Coating Company, Morton Powder Coatings, Inc., North Star Steel Company, O'Brien Powder Products, Inc., and 3M Corporation. Epoxy coating was applied to the C bars by ABC Coating, Inc., to the F bars by AmeriSteel, and to the N bars by Simcote, Inc. The basalt coarse aggregate was supplied by Geiger Ready-Mix and Iron Mountain Trap Rock Company. Form release agent, curing compound, and mounting hardware were supplied by Richmond Screw Anchor Company.

INTRODUCTION

Epoxy-coated reinforcing steel is used in a wide variety of reinforced concrete structures where the concrete is exposed to a corrosive environment. An important consideration in design is the effect of epoxy coating on the bond strength of the reinforcing steel to concrete. Because of the detrimental effects of epoxy coating on the bond strength of reinforcing steel, the ACI Building Code (318-95) and the AASHTO Bridge Specifications (1992) require the use of longer development and splice lengths for epoxy-coated reinforcing steel than for the uncoated steel. A development length modification factor of 1.5 must be used for the epoxy-coated bars with a cover less than 3 bar diameters or a clear spacing less than 6 bar diameters, and a factor of 1.2 must be used for coated bars under other conditions. The 1.5 factor is based on an average ratio of coated to uncoated bar bond strength, C/U , of 0.66 obtained from 21 beam splice tests (Treece and Jirsa 1987, 1989) using bars with a deformation pattern that is no longer in use due to difficulties of applying the epoxy coating. Later studies (Choi et al. 1990, 1991; Hester et al. 1991, 1993; Hadje-Ghaffari et al. 1991, 1992, 1994), however, have demonstrated that a value of $C/U = 0.74$ more accurately represents the effects of epoxy coating on bond strength.

Research by Choi et al. (1990, 1991) also demonstrated that an increase in the relative rib area of deformed bars, R_r (ratio of projected rib area normal to bar axis to the product of the nominal bar perimeter and the center-to-center rib spacing – see Fig. 1), results in a reduction in the negative effects of epoxy coating on bond strength. That research strongly suggested that an increase in R_r above the values of 0.055 – 0.085 obtained with conventional reinforcement could significantly improve the bond strength of epoxy-coated reinforcing steel to concrete.

A large-scale study has been underway at the University of Kansas since 1991 to better understand the bond characteristics of both uncoated and coated reinforcing steel. In the initial portion of the study, Darwin and Graham (1993a, 1993b) demonstrated that, for uncoated reinforcement, the higher the relative rib area, R_r , the higher the bond strength between concrete and reinforcing bars confined by transverse reinforcement. Based on those results, bars with relative rib areas ranging from 0.101 to 0.141 were produced commercially and tested using full-scale beam splice specimens. Tests by Darwin et al. (1995a, 1996a) included 10 matched pairs of specimens containing coated and uncoated high R_r bars that produced an average C/U ratio of

0.88, strongly supporting the initial observations of Choi et al. (1990, 1991).

This report combines test results of the original 20 specimens with those of 27 additional specimens to determine the effect of epoxy coating on the splice strength of high relative rib area bars, both with and without confining transverse reinforcement.

EXPERIMENTAL PROGRAM

The total experimental program consisted of 47 beam splice specimens. Forty-four specimens were cast as 22 matched pairs with the same parameters except for bar surface condition (epoxy-coated or uncoated). The remaining 3 specimens contained epoxy-coated bars without matching specimens containing uncoated bars. All 47 specimens are listed in Table 1. The results for the first 20 specimens were reported by Darwin et al. (1995a, 1996a). In Table 1, the specimen number identifies the group and the order of casting and testing within the group. The specimens were cast in 16 groups containing one to three matched pairs per group and one group (22) containing three coated specimens.

The key test parameters were bar surface condition (epoxy-coated or uncoated) and relative rib area (0.101 to 0.141). Other parameters included bar size [No. 5, No. 8, or No. 11 (16, 25 or 36 mm)], concrete cover, bar spacing, degree of confinement provided by transverse reinforcement, casting position (bottom-cast or top-cast), and the concrete strength as part of a larger study.

Among the 22 matched pairs, seven pairs contained splices with confining reinforcement, and fifteen pairs contained splices without confining reinforcement; twenty pairs contained bottom-cast bars and two pairs contained top-cast bars with more than 12 in. (305 mm) of concrete below the test bars. Concretes containing two different coarse aggregates (described below) were used to evaluate the effect of aggregate properties on bond strength (Darwin et al. 1995a, 1996a).

The bars used in the study are shown in Fig. 2. Bar properties are summarized in Table 2.

Test Specimens

Beam specimens, 13 or 16 ft (4 or 4.9 m) long, were tested as inverted simply supported beams with two concentrated loads in the span to produce, respectively, a 4 or 6 ft (1.2 or 1.8 m)

constant moment region, as shown in Figs. 3, 4, and 5, except for specimens 23b.5 and 23b.6 and the specimens in group 22. The specimens in group 22 were tested as simply supported beams with one concentrated load at the middle of the beams, as shown in Fig. 6, and specimens 23b.5 and 23b.6 were tested with two concentrated loads in the span, as shown in Fig. 7, to study the effect of shear on splice strength.

Most specimens contained two or three longitudinal bars spliced at the center of the beam. The specimens in group 22 and specimens 23b.5 and 23b.6 contained splices located 17 in. (432 mm) away from the closest concentrated load. Distances between the ends of splices and the supports were greater than the depth of the beam for all specimens.

No. 3, No. 4, or No. 5 (9.5, 13, or 16 mm) closed stirrups were spaced evenly within the splice region in those specimens used to study the effects of transverse reinforcement on bond strength. The outer stirrups within the splice region were located one-half of the spacing between stirrups from the ends of the splice. No. 3 (9.5 mm) stirrups were placed outside of the constant moment region to provide shear strength. No. 4, No. 5, and No. 6 (13, 16, and 19 mm) bars were used as compression reinforcement for specimens with No. 5, No. 8, and No. 11 (16, 25, and 35 mm) test bars, respectively.

Beams had a nominal width of 12 or 18 in. (305 or 457 mm) and nominal depths of 15.5 to 17 in. (394 to 432 mm). Nominal values for bottom cover ranged from 1.25 to 3 in. (32 to 76 mm), and side covers on the splices ranged from 1 to 3 in. (25 to 76 mm). Nominal values for bar clear spacing were no less than one bar diameter, d_b . Splice length ranged from 16 to 40 in. (406 to 1016 mm). Beam configurations are shown in Figs. 4 to 7, and actual member dimensions are given in Table 1.

Materials

Reinforcing Steel -- Seven experimental deformation patterns were used in the current study. The bars met the requirements of ASTM A 615, with the exception that some did not have bar markings. The new bars consisted of two No. 5 (16 mm) bars, designated 5C2 and 5C3; four No. 8 (25 mm) bars, designated 8C1, 8F1, 8N1, and 8N3; and one No. 11 (35 mm) bar, designated 11F3 (Note: the first number in the designation is the bar size, the letter identifies the manufacturer, the trailing number identifies an experimental deformation pattern). The new bars

generally have closer and higher ribs than conventional bars. Bars of each size and deformation pattern were made from the same heat of steel. No bar markings were within splice regions.

The epoxy coatings were applied commercially in accordance with ASTM A 775 to bars of the same heat of steel as the uncoated bars. Average coating thicknesses for the bars in a specimen ranged from 7.1 to 16.8 mils (0.18 to 0.43 mm). Coating thicknesses were measured using a pull-off type gauge (Mikrotest III Thickness Gauge). Measurements were made at ten points along each of the two longitudinal ribs of the bar within the splice length. This method was used because the probe of the pull-off gauge could not be placed between the bar ribs which are much closer than those of conventional bars.

To compare the measured thickness of epoxy coating obtained using this method to that obtained using the method specified in ASTM A 775, four No. 8 (25 mm) conventional bars were measured using both methods. The results, presented in Appendix B, show that the overall average readings for coating thickness for the ASTM method and the method used in the current study are 7.7 and 8.8 mils (0.20 and 0.22 mm) respectively, with the standard deviations of 1.320 and 1.830 and coefficients of variation of 0.172 and 0.209.

The average coating thicknesses for the bars being spliced in each specimen are reported in Table 1. Both the longitudinal reinforcement and the transverse reinforcement within the splice regions had the same surface properties (epoxy-coated or uncoated). Bar properties for the spliced bars are given in Table 2. Yield strengths for transverse reinforcement are given in Table 1. The yield strengths reported in Tables 1 and 2 are based on tests of three samples of each bar type. Conventional Grade 60 bars were used for transverse and compression reinforcement.

Concrete -- Concrete was supplied by a local ready mix plant. Water-cement ratios ranging from 0.33 to 0.44 were used to produce concrete strengths ranging from 4090 psi to 9080 psi (28 to 63 MPa). Superplasticizer (ASTM C 494 TYPE F or G) and silica fume were used in some mixes to produce concretes with a compressive strength greater than 6000 psi (42 MPa). All of the specimens in a group were cast using the same batch of concrete. Testing ages ranged from 5 to 30 days. Mix proportions and concrete properties are summarized in Table 3.

Two types of coarse aggregate (crushed limestone and basalt) with a 3/4 in. (19 mm) maximum nominal size were used, along with Type I Portland cement and Kansas River sand. Limestone specimens tested as 1 in. (25 mm) square by 3 in. (76 mm) prisms have a compressive

strength of about 15,000 psi (103 MPa), while basalt specimens of similar dimensions have a compressive strength of about 50,000 psi (345 MPa).

Specimen Manufacture

Forms were constructed using 3/4 in. (19 mm) thick plywood, 2 x 4 studs, and all-thread rods. The majority of the plywood was manufactured with a polymeric resin coating (DriForm 90 No-Oil panels, manufactured by Champion International Corp.) that did not require the use of a release agent. All-thread rods were used to hold the forms together and to hold the reinforcing steel cage in place. Joints in the forms were sealed with flexible caulk to prevent leakage.

Reinforcing cages were fabricated inside the forms using wire ties. For bottom-cast specimens, test bars were placed on steel chairs at the bottom of the forms, with no chairs within splice regions. For top-cast specimens, test bars were tied to stirrups outside of the splice regions which were supported by steel chairs at bottom of the form. The test bars were also supported by and tied to all-thread rods outside of the splice regions. The all-thread rods were located 3 in. (76 mm) and 66 in. (1.7 m) from the ends of the form. Each splice consisted of two bars which were tied together with 4 or 6 steel ties. Portions of the bars with markings were not included in the splice length. To prevent interlocking of the ribs, spliced bars were positioned so that one had the longitudinal ribs horizontal while the other was vertical. Bottom cover was controlled by the steel chairs. Side cover was controlled by tying the top and bottom reinforcement to the all-thread rods which extended through the inside of the forms. Covers and bar spacings were measured after the forms had been moved to the casting position and are given in Table 1. Two No. 8 (25 mm) lifting bars, one at each of the quarter points of the beams, were used to help move the specimens. Bars were cleaned with acetone before being placed in forms and again before concrete was placed.

Concrete Placement

The concrete was placed in two lifts of half of the beam depth each. In the first lift, the end regions of all beams in a group were placed first, followed by the splice regions. In the second lift, the splice regions were placed first, followed by the end regions. This was to ensure that the concrete within the splice regions was as uniform in quality as possible from specimen to

specimen. Each lift of concrete was mechanically vibrated with a 1.5 in. (38 mm) square vibrator on each side of the beams at about one foot (305 mm) intervals.

For the high-strength concrete [$f'_c > 6000$ psi (42 MPa)], the water, sand, and cement were loaded and mixed together in the truck first at the ready-mix plant. Then the superplasticizer and silica fume were added and mixed for about 2 minutes. Finally the coarse aggregate was added. This procedure was used to ensure both uniformity and workability in the high strength mixes.

After initial set of the concrete, the beams were covered with wet burlap on the top surface and then covered with plastic. Standard 6 x 12 in. (152 x 305 mm) test cylinders were cast in steel molds and cured in the same manner as the test specimens. The burlap was kept wet until the forms were stripped after the concrete had reached a compressive strength of at least 3000 psi (21 MPa) and the specimens were left to dry until the time of test.

Test Procedures

Most specimens were tested as shown in Fig. 2, except the specimens in group 22 were tested as shown in Fig. 5 and specimens 23b.5 and 23b.6 were tested as shown in Fig. 6.

Beams were supported at two points by pin and roller supports mounted on concrete pedestals. A 3/4 in. (19 mm) thick steel plate was attached to the bottom of the beam at each support location with a layer of high strength gypsum cement (Hydrostone) to distribute the reaction.

For most specimens, loads were applied at the ends of the beams to produce a constant moment region between the two supports (Figs. 2, 3, and 4). The loads were applied to two spreader beams, one at each end of the specimen, by four hydraulic jacks through four 1.5 in. (38 mm) diameter load rods. The load rods were attached to the steel beam with semi-cylindrical rollers so that the applied load remained vertical as the ends of the test beam rotated. Beams were loaded continuously to failure at a rate of about 3 kips (13 kN) per minute at each load point. Load on the beam was measured using each of the four load rods which were instrumented as load cells using four strain gauges in a full bridge configuration. Deflections were measured at each load point and at the middle of the beams using spring-loaded linear variable differential transformers (LVDTs).

For specimens 23b.5 and 23b.6 and specimens in group 22, similar loading and support-

ing methods were used except that the loads were applied within the span of the beams, the specimens were supported at the ends, and deflections were measured only at the middle of the beams.

The load cells and LVDTs were connected through a Hewlett-Packard data acquisition system to a computer, allowing the data to be saved on a computer disk. Load-deflection curves were plotted as tests progressed. Tests lasted 15 to 20 minutes. Each group of specimens was tested in a 12 hour period. Three or more standard 6 x 12 in. (152 x 305 mm) concrete cylinders were tested in compression soon after completing the tests.

SPECIMEN BEHAVIOR AND ANALYSIS OF TEST RESULTS

Results and Observations

Load-deflection curves for the test specimens are shown in Appendix A. Solid lines represent specimens containing coated bars, while dashed lines represent specimens with uncoated bars (unless otherwise specified). Failure loads, moments, and bar stresses calculated using the working stress method are given in Table 1.

The load-deflection curves for all of the beams within the same group are virtually identical up to the point of failure of the weaker specimens. All specimens failed by spitting of the concrete cover at the tension face of beams within the splice region. Beams containing epoxy-coated bars failed at a lower load than the corresponding beams with uncoated bars, with the exception of the single pair of beams containing bottom-cast 5C3 bars; the 5C3 bars have the highest value of R_r (0.141) used in the current tests.

Beams without stirrups failed suddenly, and the load dropped quickly after it reached the ultimate load. Beams with stirrups behaved in a more ductile fashion, with the load dropping slowly after the peak load. Beams with stirrups also exhibited much more cracking and smaller crack widths in the splice failure than did specimens without stirrups. However, the width and number of the cracks within splice region showed no clear dependence on the presence or absence of epoxy coating.

Specimens containing high strength concrete [$f'_c > 6000$ psi (42 MPa)], shown in Figs. A.13 to A.15, failed in a more brittle manner than specimens containing normal-strength con-

crete, with more concrete splitting off within the splice region.

Typically, failure was preceded by extensive longitudinal and transverse cracking in the splice region. Longitudinal cracks formed initially along the top of the spliced bars on the tension face of the beams, and later on the sides of the beams at the level of the splices. Transverse cracks formed at each end of the splices and at the stirrup locations (when used) on the tension face of the beam, and ran across the full width of the beam, extending to the sides. Typical sections following failure are shown in Figs. 8a and 8b.

Following the splice tests, the concrete cover was removed to study the nature of the interaction at the steel-concrete interface. For uncoated bar specimens, both with and without stirrups, the concrete between the bar ribs at the steel-concrete interface showed signs of crushing or shearing. Concrete damage between the bar ribs was higher near the discontinuous ends of the spliced bars than near the continuous ends. This variation in damage was more evident for the 11F3 bars confined by stirrups than for the other cases. Some concrete residue remained on the bar shaft between the ribs, with the concrete exhibiting good adhesion to the bars.

For the epoxy-coated bar specimens, the concrete at the interface had a smooth, glassy surface, and exhibited little damage. But generally, the higher the failure load of the coated bar specimen relative to the matched uncoated bar specimen, the greater the damage at the steel-concrete interface. This behavior was more evident for the 5C3 bars than for the other cases. In contrast to the uncoated bars, there was little concrete left on the shaft of the coated bars; in most cases, the concrete exhibited no adhesion to coated bars.

Evaluation of the Experimental Results

The principal goal of this project is to evaluate the effects of new bar deformation patterns and transverse reinforcement on splice strength of epoxy-coated bars.

To evaluate the test results, bar stresses at failure for the 20 bottom-cast splice specimens containing epoxy-coated bars are compared to those of the corresponding uncoated bar specimens in Table 4. All of the specimens had a concrete cover less than 3 bar diameters, or a clear spacing less than 6 bar diameters. Seven out of the twenty matched pairs contained splices that were confined by transverse reinforcement. The splice strength ratios for each matched pair of coated and uncoated bar specimens are normalized with respect to the equations developed by Darwin et al.

(1995b, 1996b) to eliminate the effects of minor differences in concrete cover and bar clear spacing between the two matched beams.

The equations were developed to predict the development and splice strength for the uncoated bars, based on a statistical analyses of 133 splice and development specimens in which the bars were not confined by transverse reinforcement and 166 specimens in which the bars were confined by transverse reinforcement. These equations accurately represent the development and splice strength of uncoated reinforcing bars, both with and without confining reinforcement, for values of f'_c between 2,500 to 16,000 psi (17 to 110 MPa). The equations also take into account the effects of cover, bar spacing, development/splice length, and the geometric properties of the developed/spliced bars. For the specimens without stirrups, the equation is

$$\frac{A_b f_s}{f'_c{}^{1/4}} = [63 l_s (c_m + 0.5 d_b) + 2130 A_b] \left(0.1 \frac{c_M}{c_m} + 0.9\right) \quad (1)$$

For the specimens with stirrups the equation is

$$\frac{A_b f_s}{f'_c{}^{1/4}} = [63 l_s (c_m + 0.5 d_b) + 2130 A_b] \left(0.1 \frac{c_M}{c_m} + 0.9\right) + 2226 t_r t_d \frac{N A_{tr}}{n} + 66 \quad (2)$$

in which

$$t_r = 9.6 R_r + 0.28$$

$$t_d = 0.72 d_b + 0.28, \text{ in.}$$

$$f_s = \text{steel stress at failure, psi}$$

$$f'_c = \text{concrete compressive strength, psi; } f'_c{}^{1/4}, \text{ psi}$$

$$l_s = \text{splice or development length, in.}$$

$$c_m, c_M = \text{minimum or maximum value of } c_s \text{ or } c_b \text{ (} c_M/c_m \leq 3.5 \text{), in.}$$

$$c_s = \text{Min } (c_{si} + 0.25, c_{so}), \text{ in.}$$

$$c_{si} = \text{one-half of clear spacing between bars, in.}$$

$$c_{so}, c_b = \text{side cover or bottom cover of reinforcing bars, in.}$$

$$A_b = \text{area of bar cross-section, in.}^2$$

$$N = \text{the number of transverse reinforcing bars (stirrups or ties) crossing } l_s$$

$$n = \text{number of bars being developed or spliced along the plane of splitting}$$

$$A_{tr} = \text{area of each stirrup or tie crossing the potential plane of splitting adjacent to the reinforcement being developed or spliced, in.}^2$$

The comparisons in Table 4 are made separately for the specimens without and with stirrups and are given in Tables 5 and 6, respectively. In addition to the 20 matched pairs of bottom-cast splice specimens tested in the current study, the test results of 7 matched pairs of splice tests by Choi et al. (1990, 1991) and 15 matched pairs of splice tests by Hester et al. (1991, 1993) are used for the overall evaluation (see Table 7). Next, the splice strength ratios for the high R_r bars are compared with those of the conventional bars. The effects of R_r , confining reinforcement, and total confinement provided by concrete and transverse steel on the splice strength ratio, C/U , are addressed. The effect of bar rib face angle on C/U ratio is also evaluated. The effect of casting position on the splice strength is addressed briefly.

Splice Strength Ratio, C/U – The comparisons made in Table 4 show that the ratios of the splice strengths of the coated (C) to the uncoated (U) bars range from 0.787 to 1.081, with an overall average of 0.894. The comparisons made in Table 5 and Table 6 show that the average ratios for the specimens without and with stirrups are 0.909 and 0.865, respectively.

These values contrast strikingly with the average splice strength ratio of 0.66 for the 21 beam splice tests (Treece and Jirsa 1987, 1989) used to establish the current development length modification factors for the epoxy-coated bars (ACI 318-95, AASHTO 1992), as well as the average splice strength ratio of 0.82 for the 14 beam splice tests by Choi et al. (1990, 1991), the average splice strength ratio of 0.72 for the 30 beam splice tests by Hester et al. (1991, 1993), and the overall average splice strength ratio of 0.74 for a data base including 113 splice tests (Hester, Salamizavaregh, Darwin, and McCabe 1991, 1993).

These comparisons indicate that high relative rib area bars will require lower development length modification factors than those in current use (ACI 318-95, AASHTO 1992). The average value of C/U , 0.894, obtained in this study represents the effect of epoxy coating on the splice strength of the bottom-cast high R_r bars with and without confining transverse reinforcement. Replacing N by l_s/s in Eq. 2, dropping the term of 66, and solving for l_s gives

$$l_s = \frac{A_b \left[\frac{f_s}{f'_c{}^{1/4}} - 2130 \left(0.1 \frac{c_M}{c_m} + 0.9 \right) \right]}{63 \left[(c_m + 0.5d_b) \left(0.1 \frac{c_M}{c_m} + 0.9 \right) + \frac{35.3 t_r t_d A_{tr}}{sn} \right]} \quad (3)$$

in which s = center-to-center spacing of the stirrups within the splice region, in.

For epoxy-coated bars, Eq. (3) becomes

$$l_{s,epoxy} = \frac{A_b \left[\frac{f_s}{f'_c{}^{1/4} C/U} - 2130 \left(0.1 \frac{c_M}{c_m} + 0.9 \right) \right]}{63 \left[(c_m + 0.5d_b) \left(0.1 \frac{c_M}{c_m} + 0.9 \right) + \frac{35.3 t_r t_d A_{tr}}{sn} \right]} \quad (4)$$

The development length modification factor for epoxy-coated bars can be obtained dividing Eq. 4 by Eq. 3 and assuming $c_M = c_m$

$$MF = \frac{l_{s,epoxy}}{l_s} = \frac{\frac{f_s}{f'_c{}^{1/4} C/U} - 2130}{\frac{f_s}{f'_c{}^{1/4}} - 2130} \quad (5)$$

For grade 60 steel and concrete compressive strengths ranging from 4000 to 10,000 psi (28 to 69 MPa), Eq. 5 yields modification factors ranging from 1.16 to 1.19, demonstrating that the development length modification factor could be dropped, conservatively, from 1.5 to 1.2 for the epoxy-coated high relative rib area bars with concrete cover less than $3 d_b$ or clear spacing less than $6 d_b$. This 20 percent reduction would apply whether or not the bars are confined by transverse reinforcement.

Relative Rib Area, R_r . -- The effect of relative rib area on relative bond strength is illustrated for the specimens without transverse reinforcement tested in the current study, for the specimens without transverse reinforcement tested in current and previous studies, and for all of the specimens with and without transverse reinforcement tested in current and previous studies, in Figs. 9, 10, and 11, respectively. In these figures, the splice strength ratio of coated to uncoated bars normalized to Eq. (1) or (2), C/U , is plotted as a function of the relative rib area, R_r .

Using the technique of dummy variables (Draper and Smith, 1981), the best-fit lines for each bar size and study are obtained based on the assumption that, while there may be differences in C/U due to bar size and study, the change in C/U due to relative rib area is the same for all the bar sizes.

Figs. 9 and 10 show that the scatter in the test results is high, but that, overall, relative rib area has an effect on the splice strength ratio. C/U increases, on the average, by 0.10 as R_r increases from 0.10 to 0.14 for the current specimens without stirrups (Fig. 9); and C/U increases, on the average, by 0.20 as R_r increases from 0.07 to 0.14 for the specimens without stirrups tested in the current and previous studies (Fig. 10).

Fig. 11 shows that the positive effect of R_r on C/U applies to all of the specimens, with and without transverse reinforcement, tested in the current and previous studies. As with Fig. 10, the best-fit lines in Fig. 11 indicate that C/U increases by about 0.20 as the R_r increases from 0.07 to 0.14. Thus, the use of high relative rib area bars could significantly reduce the detrimental effects of epoxy coating on the splice strength of reinforcing steel, whether or not the spliced bars are confined by transverse reinforcement.

Transverse Reinforcement – The effect of transverse reinforcement on the normalized splice strength ratio is illustrated in Figs. 12 to 15. In these figures, the normalized splice strength ratio is plotted as a function of K_{tr} , a measure of the degree of confinement provided by transverse reinforcement within splice region (Darwin et al. 1995a, 1996a). K_{tr} includes the effect of relative rib area, since it includes the term t_r .

$$K_{tr} = 35.3 \frac{A_{tr}}{s n} t_r t_d \quad (6)$$

K_{tr} has units of in.

Fig. 12 shows the effect of transverse reinforcement on the splice strength ratio for the specimens with stirrups from the current study. Using dummy variables analysis, the best-fit lines are based on bar size. Fig. 12 shows that, for the specimens tested in this study, K_{tr} has a significant effect on C/U , with C/U increasing, on the average, by 0.186 as K_{tr} increases from 0.0 to 3.0 in. (0.0 to 76.2 mm).

The effect of K_{tr} on C/U , however, disappears when the specimens without transverse steel are included in the analysis, as shown in Fig. 13. The slope of the best-fit lines in Fig. 13 is

-0.003, showing no effect.

Similar analyses for both current and previous studies are presented in Figs. 14 and 15. The results are similar. For the specimens with stirrups, Fig. 14 suggests that there is an effect of K_{tr} on C/U ; the slope of the best-fit lines is 0.061. But Fig. 15 shows that, overall, K_{tr} has no effect on C/U . The slope of the best-fit lines is -0.009.

These results raise a question as to the role of additional confinement provided by concrete cover and clear spacing, on C/U . This can be evaluated by considering the effect of $(c + K_{tr})$, a measure of the total confinement provided by concrete cover, clear spacing, and transverse reinforcement, on C/U , where

$$c = (c_{\min} + 0.5 d_b) \left(0.1 \frac{c_M}{c_m} + 0.9 \right) \quad (7)$$

Total Confinement— The effect of total confinement, $(c + K_{tr})$, on C/U is studied using the combined test results. C/U is plotted as a function of $(c + K_{tr})$ for specimens with stirrups and for all specimens tested in current and previous studies in Figs. 16, and 17, respectively. The best-fit lines are obtained using dummy variables analysis. Fig. 16 shows that $(c + K_{tr})$ has an effect on C/U for the specimens with stirrups, with C/U increasing, on average, by 0.081 as $(c + K_{tr})$ increases from 2.5 to 4.0 in. (63.5 to 101.6 mm). This result matches the effect of K_{tr} on C/U shown in Fig. 14.

Fig. 17, however, demonstrates that, generally, the total confinement provided by concrete and transverse steel, $(c + K_{tr})$, has no effect on C/U . The slope of the best-fit lines in Fig. 17 is -0.013, suggesting that the confinement provided by transverse steel or by transverse steel plus concrete does not affect the splice strength ratio, C/U .

Rib Face Angle, γ — The effect of rib face angle on the splice strength ratio, C/U , is studied using the 20 pairs of beam splice specimens tested in the current study. The rib face angle is the angle between the profile of a bar rib and the longitudinal axis of the bar.

Rib face angle has long been considered as one of the parameters that affect the bond behavior of reinforcing steel. Clark (1946) observed that the more gradual the inclination of the face of bar deformation, the greater the slip for a given force. Lutz (1970) observed that additional slip occurs when friction is reduced by the use of grease, even for rib face angles in excess of 45° , but that ribs with flatter face angles are affected more than ribs with steeper face angles.

This observation is of special interest because it may explain a great deal about the performance of epoxy-coated bars. In contrast, research by Soretz and Holzehnbein (1979) demonstrates that the rib face angle is a relatively small factor compared to rib bearing area for uncoated bars. They observed that bars with a lower rib face angle exhibited more slip, but provided the same strength as bars with equal rib heights and steeper rib face angles. As a result, the rib face angle was not included in the guidance used to design commercially produced high R_t bars.

The normalized splice strength ratio, C/U , is plotted as a function of rib face angle in Figs. 18 and 19 for the specimens without stirrups and in Figs. 20 and 21 for the specimens with stirrups. The test results are compared with a theoretical relation developed by Hadje-Ghaffari, Darwin and McCábe (1991):

$$C/U = \frac{(\tan \gamma + \mu_c)(1 - \mu_u \tan \gamma)}{(\tan \gamma + \mu_u)(1 - \mu_c \tan \gamma)} \quad (8)$$

in which γ = bar rib face angle

μ_c = the coefficient of friction for the epoxy-coated bars

μ_u = the coefficient of friction for the uncoated bars

Average values of μ_c and μ_u equal 0.491 and 0.561, respectively, as obtained experimentally by Idun and Darwin (1995).

In the derivation of this theoretical relation, Hadje-Ghaffari et al. limited the maximum value of the bar rib face angle, γ , for the uncoated bars, based on the studies by Rehm (1961) and Lutz and Gergely (1967), who observed that, for uncoated bars with γ greater than 40° , the concrete in front of the bar ribs crushed at bond failure, producing ribs with an effective value of γ between 30° and 40° . In the current study, the bar rib face angle, γ , is limited to 40° , so the theoretical relation becomes

$$C/U = \frac{(\tan \gamma + \mu_c)(1 - \mu_u \tan 40^\circ)}{(\tan 40^\circ + \mu_u)(1 - \mu_c \tan \gamma)} \leq 1.0 \quad (9)$$

for γ greater than 40° .

As shown in Figs. 18 to 21, the theoretical relation consists of three distinct parts. The first part, which is nonlinear, represents γ less than 40° . This part of the relation shows that C/U increases very slightly as γ increases from 0° to about 20° , and then decreases very slightly as γ increases up to 40° . The second part of the relation, which is linear, represents γ between 40° and

about 43° . In this part of the relation, C/U increases nearly linearly as γ increases. In the third part of the relation, for $\gamma > 43^\circ$, $C/U = 1.0$, meaning that epoxy coating should not affect bond strength if γ is greater than 43° .

In Figs. 18 and 20, the average value of C/U for each bar type is plotted as a function of the rib face angle, for the specimens without and with stirrups, respectively. In Figs. 19 and 21, the value of C/U for each matched pair of specimens is plotted as a function of the rib face angle, for the specimens without and with stirrups, respectively, to provide a full picture of the test results. It is interesting to note the close agreement between test results and the theoretical relation, especially in Figs. 18 and 19. It is suggested that this theoretical relation may serve as a useful tool in the study of the effect of γ on C/U .

Casting Position — In addition to the bottom-cast bar splice tests, two groups of top-cast bar specimens with both epoxy-coated and uncoated bars and matching bottom-cast bar specimens were cast and tested using 5C3 and 8N1 bars. The test results are summarized in Table 8. Concrete slump was 4 in. (100 mm) for the 5C3 bars and 3 3/4 in. (95 mm) for the 8N1 bars. The test results show that there is not a significant “top-bar effect” for either coated or uncoated bars. The splice strength ratios for coated bottom-cast bars (C_b) to coated top-cast bars (C_t) are 1.120 and 1.000 for 5C3 bars and 8N1 bars, respectively, while the splice strength ratios for uncoated bottom-cast bars (U_b) to uncoated top-cast bars (U_t) are 0.993 and 1.033 for 5C3 bars and 8N1 bars, respectively. The “top-bar effect” for the 5C3 and 8N1 bars is much less than that reflected by 1.3, the development length modification factor for top bars required by the ACI Building Code (318-95).

There is also not a significant difference in C/U between the bottom-cast and the top-cast bars. The values of C/U for 5C3 bars, bottom-cast and top-cast, are 1.067 and 0.946, respectively. The values of C/U for 8N1 bars, bottom-cast and top-cast, are 0.896 and 0.925, respectively. It is interesting to note that, for 8N1 bars, C/U for the top-cast bars is even higher than the bottom-cast bars.

The splice strength ratios of the uncoated bottom-cast bar to the coated top-cast bars, U_b/C_t , are 1.050 and 1.116 for 5C3 and 8N1 bars, respectively. These values are much less than the upper value of the ACI development length modification factor of 1.7 for epoxy-coated top-cast bars with a concrete cover less than $3 d_b$ or a clear spacing less than $6 d_b$. These results sug-

gest that, as demonstrated in earlier studies on conventional bars (Treece and Jirsa 1987, 1989; Hadje-Ghaffari et al. 1992, 1994), the effects of casting position and epoxy coating on splice strength of coated high relative rib area bars are not cumulative.

The test results in Table 8 contrast sharply with (1) the average splice strength ratio, C/U of 0.69 for the 17 epoxy-coated top-cast bar specimens without transverse reinforcement by Treece and Jirsa (1987, 1989) and (2) the average splice strength ratio of 0.78 for the 12 epoxy-coated top-cast bar specimens with transverse reinforcement by Hamad and Jirsa (1993). However, the low number of top-cast tests in the current study indicates that more research is needed on the effect of the casting position on the bond strength of high R_r epoxy-coated reinforcing steel to concrete.

SUMMARY AND CONCLUSIONS

This report describes the testing of 47 beam splice specimens containing high relative rib area bars. Forty-four specimens were cast as matched pairs containing epoxy-coated and uncoated bars. Seven pairs contained splices with confining reinforcement and fifteen pairs contained splices without confining reinforcement. Two pairs of specimens were top-cast and twenty pairs were bottom-cast. No. 5, No. 8, and No. 11 (16, 25, and 36 mm) bars with relative rib areas ranging from 0.101 to 0.141 were evaluated.

The analyses of the effects of relative rib area and transverse reinforcement on the splice strength combine the current test results with those of seven matched pairs tested by Choi et al. (1990, 1991) and fifteen matched pairs tested by Hester et al. (1991, 1993). The following conclusions are based on the analyses presented in this report.

1. The detrimental effect of epoxy coating on splice strength decreases as relative rib area increases. The relative improvement in splice strength for epoxy-coated high relative rib area reinforcement is obtained whether or not the splices are confined with transverse reinforcement. The development length modification factor for the epoxy-coated high relative rib area bars can be reduced as much as 20 percent compared to current requirement, from 1.5 to 1.2.

2. Confining transverse reinforcement does not affect the relative splice strength of epoxy-coated bars to uncoated bars. A single development length modification factor can be used in design for epoxy-coated splices with and without transverse reinforcement.
3. The "top-bar effect" on splice strength of high relative rib area bars seems to be much less than that of conventional bars. Results, however, are limited.
4. The close agreement between results from the current tests and the theoretical relation between bar rib face angle, γ , and splice strength ratio, C/U , developed by Hadje-Ghaffari, Darwin and McCabe (1991):

$$C/U = \frac{(\tan\gamma + \mu_c)(1 - \mu_u \tan\gamma)}{(\tan\gamma + \mu_u)(1 - \mu_c \tan\gamma)}$$

suggests that it may serve as a useful tool in the study of the effect of γ on C/U .

REFERENCES

AASHTO Highway Sub-Committee on Bridges and Structures. 1992. *Standard Specifications for Highway Bridges*, 15th Edition, American Associate of State Highway and Transportation Officials, Washington, DC, 686 pp.

ACI Committee 318. 1995. *Building Code Requirements for Structural Concrete (ACI 318-95) and Commentary - ACI 318R-95*, American Concrete Institute, Farmington Hills, MI, 369 pp.

ASTM "Standard Specification for Chemical Admixtures for Concrete, (ASTM C 494-92)" *1995 Annual Book of ASTM Standards*, Vol. 4.02, American Society of Testing and Materials, Philadelphia, PA, pp. 254-262.

ASTM "Standard Specification for Deformed and Plain Billet-Steel Bars for Concrete Reinforcement. (ASTM A 615/A 615M-95b)," *1996 Annual Book of ASTM Standards*, Vol. 1.04, American Society of Testing and Materials, Philadelphia, PA, pp. 302-306.

ASTM "Standard Specification for Epoxy-Coated Reinforcing Bars, (ASTM A 775/A775M-95)" *1996 Annual Book of ASTM Standards*, Vol. 1.04, American Society of Testing and Materials, Philadelphia, PA, pp. 408-414.

Choi, Oan Chul; Hadje-Ghaffari, Hossain; Darwin, David; and McCabe, Steven L. 1990. "Bond of Epoxy-Coated Reinforcement to Concrete: Bar Parameters," *SL Report No. 90-1*, University

of Kansas Center for Research, Lawrence, Kansas, Jan., 43 pp.

Choi, Oan Chul; Hadje-Ghaffari, Hossain; Darwin, David; and McCabe, Steven L. 1990. "Bond of Epoxy-Coated Reinforcement to Concrete: Bar Parameters," *ACI Materials Journal*, Vol. 88, No. 2, March-April, pp. 207-217.

Clark, A.-P. (1946) "Comparative Bond Efficiency of Deformed Concrete Reinforcing Bars," *ACI Journal, Proceedings* Vol. 43, No. 4, Dec., pp. 381-400

Darwin, D. and Graham, E. K. 1993a. "Effect of Deformation Height and Spacing on Bond Strength of Reinforcing Bars," *SL Report 93-1*, University of Kansas Center for Research, Lawrence, Kansas, Jan., 68 pp.

Darwin, D. and Graham, E. K. 1993b. "Effect of Deformation Height and Spacing on Bond Strength of Reinforcing Bars," *ACI Structural Journal*, Nov.-Dec., Vol. 90, No. 6, pp. 646-657.

Darwin, D.; Tholen, M. L.; Idun, E. K.; and Zuo, J. 1995a. "Splice Strength of High Relative Rib Area Reinforcing Bars," *SL Report 95-3*, University of Kansas Center for Research, Lawrence, Kansas, May, 58 pp.

Darwin, D.; Zuo, J.; Tholen, M. L.; and Idun, E. K. 1995b. "Development Length Criteria for Conventional and High Relative Rib Area Reinforcing Bars," *SL Report 95-4*, University of Kansas Center for Research, Lawrence, Kansas, May, 70 pp.

Darwin, D.; Tholen, M. L.; Idun, E. K.; and Zuo, J. 1996a. "Splice Strength of High Relative Rib Area Reinforcing Bars," *ACI Structural Journal*, Vol. 93, No. 1, Jan.-Feb., pp. 95-107

Darwin, D.; Zuo, J.; Tholen, M. L.; and Idun, E. K. 1996b. "Development Length Criteria for Conventional and High Relative Rib Area Reinforcing Bars," *ACI Structural Journal*, Vol. 93, No. 3, May-June, in press

Draper, N. R. and Smith, H. 1981. *Applied Regression Analysis*, Second Edition, John Wiley & Sons, Inc., pp. 241-249.

Hadje-Ghaffari, Hossain; Darwin, David; and McCabe, Steven L. 1991. "Effect of Epoxy Coating on Bond of Reinforcing Steel to Concrete," *SM Report No. 28*, University of Kansas Center for Research, Lawrence, Kansas, July, 288 pp.

Hadje-Ghaffari, Hossain; Darwin, David; and McCabe, Steven L. 1992. "Bond of Epoxy-Coated Reinforcement to Concrete: Cover, Casting Position, Slump, and Consolidation," *SL Report 92-3*, University of Kansas Center for Research, Lawrence, Kansas, July, 42 pp.

Hadje-Ghaffari, Hossain; Choi, Oan Chul; Darwin, David; and McCabe, Steven L. 1994. "Bond of Epoxy-Coated Reinforcement to Concrete: Cover, Casting Position, Slump, and Consolidation," *ACI Structural Journal*, Vol. 91, No. 1, Jan.-Feb., pp. 59-68.

Hamad, Bilal S. and Jirsa, James O. 1993. "Strength of Epoxy-Coated Reinforcing Bar Splices Confined with Transverse Reinforcement," *ACI Structural Journal*, Vol. 90, No. 1, Jan.-Feb., pp. 77-88.

Hester, Cynthia J.; Salamizavaregh, Shahin; Darwin, David; and McCabe, Steven L. 1991. "Bond of Epoxy-Coated Reinforcement to Concrete: Splices." *SL Report 91-1*, University of Kansas Center for Research, Lawrence, Kansas, May, 66 pp.

Hester, Cynthia J.; Salamizavaregh, Shahin; Darwin, David; and McCabe, Steven L. 1993. "Bond of Epoxy-Coated Reinforcement to Concrete: Splices." *ACI Structural Journal*, Vol. 90, No. 1, Jan.-Feb., pp. 89-102.

Idun, Emmanuel K. and Darwin, David. 1995. "Improving the Development Characteristics of Steel Reinforcing Bars," *SM Report No. 41*, University of Kansas Center for Research, Lawrence, Kansas, August, 256 pp.

Lutz, L. A. and Gergely, P. 1967. "Mechanics of Bond and Slip of Deformed Bars in Concrete," *ACI Journal, Proceedings* Vol. 64, No. 11, Nov., pp. 711-721

Lutz, L. A., "Analysis of Stress in Concrete near a Reinforcing Bar due to Bond and Transverse Cracking," *ACI Journal, Proceedings* Vol. 67, No. 10, Oct. 1970, pp. 778-787.

Rehm, G. 1961. "Über die Grundlagen des Verbundes Zwischen Stahl und Beton," *Deutscher Ausschuss für Stahlbeton*. No. 1381, pp. 59, (C & CA Library Translation No. 134, 1968. "The Basic Principle of the Bond between Steel and Concrete,").

Soretz, S.; and Holzenbein, H. 1979. "Influence of Rib Dimensions of Reinforcing Bars on Bond and Bendability," *ACI Journal, Proceedings* Vol. 76, No. 1, Jan., pp. 111-127.

Treece, Robert A. and Jirsa, James O. 1987. "Bond Strength of Epoxy-Coated Reinforcing Bars," *PMFSEL Report No. 87-1*, Phil M. Ferguson Structural Engineering Laboratory, Univ. of Texas at Austin, Jan., 85 pp.

Treece, Robert A. and Jirsa, James O. 1989. "Bond Strength of Epoxy-Coated Reinforcing Bars," *ACI Materials Journal*, Vol. 86, No. 2, Mar.-Apr., pp. 167-174.

Table 1
Splice Specimen Properties and Test Results

Specimen No. *	Bar ** Designation	R _r	n	Coating Thick. (mils)	l _s (in)	b (in)	h (in)	d _b (in)	c _{so} (in)	c _{si} (in)	c _b (in)	d (in)	l _t (ft)	l _c (ft)	f _c ¹ (psi)	N	d _s (in)	f _{yt} (ksi)	P (kips)	M _u (k-in)	f _s ^{***} (ksi)
1.3	8C1	0.101	3	0.00	16.0	16.07	16.21	1.000	2.032	1.438	1.938	13.75	13.0	4.0	5020	0	-	-	26.74	1310	45.01
1.4	8C1	0.101	3	12.80	16.0	16.11	16.20	1.000	2.032	1.375	1.938	13.74	13.0	4.0	5020	0	-	-	21.93	1079	37.09
2.5	8F1	0.140	2	0.00	24.0	12.13	16.01	1.000	2.063	1.856	1.813	13.67	16.0	6.0	5250	0	-	-	20.69	1138	58.67
2.6	8F1	0.140	2	16.80 ⁺	24.0	12.12	16.19	1.000	2.000	1.917	1.938	13.71	16.0	6.0	5250	0	-	-	17.41	961	49.37
4.5	8C1	0.101	2	0.00	24.0	12.12	16.15	1.000	2.063	1.936	1.844	13.79	16.0	6.0	4090	0	-	-	18.02	994	51.06
4.6	8C1	0.101	2	12.00	24.0	12.16	16.23	1.000	2.094	1.926	2.000	13.72	16.0	6.0	4090	0	-	-	14.57	808	41.72
6.5	8F1	0.140	2	0.00	24.0	12.10	16.13	1.000	2.000	1.906	1.969	13.63	16.0	6.0	4220	0	-	-	18.71	1031	53.59
6.6	8F1	0.140	2	16.80 ⁺	24.0	12.15	16.13	1.000	2.032	1.875	1.969	13.63	16.0	6.0	4220	0	-	-	17.30	955	49.63
10.1	8N3	0.119	2	12.40	26.0	12.15	16.16	1.000	2.016	1.907	1.896	13.72	16.0	6.0	4250	0	-	-	20.36	1120	57.79
10.2	8N3	0.119	2	0.00	26.0	12.13	16.25	1.000	2.063	1.875	1.933	13.78	16.0	6.0	4250	0	-	-	21.66	1191	61.17
13.3	5C2	0.109	3	9.90	16.0	12.15	15.52	0.625	2.047	1.000	1.325	13.86	13.0	4.0	4110	0	-	-	12.84	636	53.91
13.4	5C2	0.109	3	0.00	16.0	12.19	15.60	0.625	2.094	1.016	1.354	13.92	13.0	4.0	4110	0	-	-	14.38	710	59.96
14.3	5C2	0.109	3	0.00	17.0	12.14	15.51	0.625	2.032	1.031	1.295	13.89	13.0	4.0	4200	0	-	-	15.06	743	62.84
14.4	5C2	0.109	3	10.00	17.0	12.14	15.59	0.625	2.063	1.000	1.320	13.94	13.0	4.0	4200	0	-	-	13.76	680	57.34
15.5	11F3	0.127	2	0.00	40.0	18.05	16.12	1.410	3.063	2.984	1.908	13.47	16.0	6.0	5250	0	-	-	36.65	2013	54.12
15.6	11F3	0.127	2	6.80	40.0	18.07	16.10	1.410	2.922	3.063	1.932	13.42	16.0	6.0	5250	0	-	-	32.45	1787	48.19
16.1	11F3	0.127	2	6.80	40.0	18.04	15.93	1.410	3.063	2.906	1.833	13.35	16.0	6.0	5180	0	-	-	32.68	1799	48.83
16.2	11F3	0.127	2	0.00	40.0	18.07	16.28	1.410	3.016	2.969	1.895	13.64	16.0	6.0	5180	0	-	-	35.92	1974	52.38
18.2	11F3	0.127	2	5.30	40.0	18.07	16.14	1.410	2.984	3.000	1.922	13.48	16.0	6.0	4700	6	0.375	64.55	38.88	2134	57.48
18.3	11F3	0.127	2	0.00	40.0	18.05	16.08	1.410	3.031	3.000	1.911	13.43	16.0	6.0	4700	6	0.375	64.55	46.85	2564	69.33
20.5	8N3	0.119	3	11.2 ⁺	40.0	12.03	15.63	1.000	1.500	0.660	1.243	13.89	16.0	6.0	5080	0	-	-	25.87	1419	49.14
20.6	8N3	0.119	3	0.00	40.0	12.08	15.60	1.000	1.516	0.672	1.300	13.80	16.0	6.0	5080	0	-	-	29.61	1621	56.51
21.1	8N3	0.119	3	0.00	24.0	12.05	15.66	1.000	1.766	0.485	1.470	13.69	16.0	6.0	4330	6	0.625	62.98	37.27	2033	71.79
21.2	8N3	0.119	3	9.75	24.0	12.14	15.76	1.000	1.813	0.492	1.462	13.80	16.0	6.0	4330	6	0.625	62.98	35.15	1918	67.14
21.3	8N3	0.119	3	0.00	25.0	12.10	16.13	1.000	1.610	0.578	1.942	13.69	16.0	6.0	4330	5	0.625	62.98	38.43	2096	73.97
21.4	8N3	0.119	3	11.70	25.0	12.06	16.17	1.000	1.524	0.614	1.850	13.82	16.0	6.0	4330	5	0.625	62.98	35.35	1929	67.43
21.5	8N3	0.119	2	0.00	25.0	12.14	15.54	1.000	1.641	2.219	1.412	13.63	16.0	6.0	4330	5	0.500	64.92	26.67	1460	76.11
21.6	8N3	0.119	2	9.70	25.0	12.14	15.50	1.000	1.516	2.172	1.376	13.62	16.0	6.0	4330	5	0.500	64.92	22.49	1235	64.33
22.2 [^]	11F3	0.127	2	5.70	32.0	12.06	15.67	1.410	2.313	0.688	1.436	13.53	16.0	6.0	6300	8	0.375	71.25	68.63	2569	70.10
22.4 [^]	11F3	0.127	2	8.40	33.0	12.06	15.65	1.410	1.282	1.250	1.390	13.53	16.0	6.0	6300	6	0.375	71.25	66.66	2497	68.02
22.6 [^]	11F3	0.127	2	8.40	33.0	17.87	16.47	1.410	3.438	2.172	2.724	13.56	16.0	-	6700	0	-	-	94.16	3536	66.57

Table 1
Splice Specimen Properties and Test Results (continued)

Specimen No. *	Bar ** Designation	R _r	n	Coating Thick. (mils)	l _s (in)	b (in)	h (in)	d _b (in)	c _{so} (in)	c _{si} (in)	c _b (in)	d (in)	l (ft)	l _c (ft)	f _c [†] (psi)	N	d _s (in)	f _{yt} (ksi)	P (kips)	M _u (k-in)	f _s ^{***} (ksi)
23a.1	8N3	0.111	3	0.00	21.0	18.28	16.09	1.000	2.164	1.852	1.931	13.04	16.0	6.0	9080	4	0.375	71.25	42.51	2326	79.01
23a.2	8N3	0.111	3	11.60	21.0	18.18	16.17	1.000	2.063	1.860	1.933	13.66	16.0	-	9080	4	0.375	71.25	33.82	1857	62.73
23b.1	8N3	0.113	3	0.00	17.5	12.15	16.22	1.000	1.469	0.711	1.951	13.74	16.0	6.0	8370	5	0.500	64.92	41.87	2281	78.46
23b.2	8N3	0.113	3	11.90	17.5	12.10	16.11	1.000	1.454	0.711	1.903	13.76	16.0	-	8370	5	0.500	64.92	37.21	2029	70.13
23b.3	8N3	0.113	2	0.00	19.5	18.24	16.32	1.000	3.032	3.860	3.057	13.71	16.0	6.0	8370	0	-	-	24.02	1328	71.57
23b.4	8N3	0.113	2	11.30	19.5	18.18	16.11	1.000	3.047	3.813	3.041	12.76	16.0	-	8370	0	-	-	23.17	1282	70.17
23b.5 [^]	11F3	0.127	2	0.00	25.0	12.03	16.24	1.410	2.032	1.125	1.939	12.57	16.0	6.0	4500	5	0.500	64.92	32.37	1951	53.32
23b.6 [^]	11F3	0.127	2	8.60	25.0	12.05	16.10	1.410	2.001	1.125	1.905	13.60	16.0	-	4500	5	0.500	64.92	26.4	1604	44.22
24.1	8N1	0.127	2	0.00	32.0	12.14	16.21	1.000	2.000	1.875	1.903	13.49	16.0	6.0	4300	0	-	-	21.54	1185	61.12
24.2	8N1	0.127	2	9.50	32.0	12.15	16.17	1.000	2.000	1.875	1.878	13.81	16.0	-	4300	0	-	-	19.36	1067	54.74
24.3 ^{^^}	8N1	0.127	2	0.00	32.0	12.08	16.04	1.000	2.000	1.875	2.000	13.79	16.0	6.0	4300	0	-	-	20.56	1132	59.19
24.4 ^{^^}	8N1	0.127	2	10.90	32.0	12.07	16.04	1.000	2.000	1.875	2.102	13.54	16.0	-	4300	0	-	-	18.84	1039	54.76
25.1	5C3	0.14	3	0.00	16.5	12.19	16.27	0.625	1.985	1.024	1.556	13.44	16.0	6.0	4490	0	-	-	14.59	808	65.72
25.2	5C3	0.142	3	6.00	16.5	12.16	16.12	0.625	2.016	0.992	1.530	14.40	16.0	-	4490	0	-	-	15.45	854	70.10
25.3 ^{^^}	5C3	0.139	3	0.00	16.5	12.12	16.14	0.625	2.032	0.985	1.520	14.28	16.0	6.0	4490	0	-	-	14.65	811	66.16
25.4 ^{^^}	5C3	0.142	3	9.50	16.5	12.28	16.12	0.625	2.047	0.961	1.495	14.31	16.0	-	4490	0	-	-	13.92	772	62.85

- * Specimen No.
G.P, G = group number (1-25), P = casting order in the group (1-6)
- ** Bar Designation
#AA, # = bar size (No.5, No.8, No.11), AA = bar manufacturer and deformation pattern
C2, C3: Chaparral Steel bars
N1, N3: North Star Steel bars
F1, F3: Florida Steel (AmeriSteel) bars
- *** Bar stress is computed using working stress method
- [^] Specimens were tested using different test set-up (as shown in Fig. 5 and Fig. 6)
- ^{^^} Specimens were cast with more 12 inch concrete below the tested bars
- + Average coating thickness belonging to bar designation

1 in. = 25.4 mm; 1 mil = 0.0254 mm; 1 psi = 6.89 kPa; 1 ksi = 6.89 MPa; 1 k-in. = 0.113 kN-m; 1 ft = 305 mm

Table 2
Properties of Reinforcing Bars⁺

Bar * Designation	Yield Strength (ksi)	Nominal Diameter (in.)	Weight (lb/ft)	% Light or Heavy	Rib Spacing (in.)	Rib Height ASTM (in.)	Avg** (in.)	Relative Rib Area	Coating Thickness*** (mils)
5C2	61.8	0.625	1.013	2.9%L	0.275	0.042	0.041	0.109	9.9
5C3	63.0	0.625	1.033	1.0%L	0.258	0.047	0.043	0.141	7.8
8C1	67.7	1.000	2.529	5.3%L	0.504	0.064	0.060	0.101	12.5
8F1	75.4	1.000	2.600	2.6%L	0.471	0.078	0.074	0.140	16.8
8N1	79.7	1.000	4.733	2.4%H	0.441	0.073	0.058	0.120	10.2
8N3	80.6	1.000	2.730	2.2%H	0.487	0.072	0.068	0.119	12.1
11F3	77.8	1.410	5.145	3.2%L	0.615	0.090	0.088	0.127	7.1

+ All values are for uncoated bars except coating thickness

* Bar Designation

#AA, # = bar size (No.5, No.8, No.11), AA = bar manufacturer and deformation pattern

C2, C3:

N1, N3: Chaparral Steel bars

F1, F3: North Star Steel bars

** Average r Florida Steel (AmeriSteel) bars

*** Average coating thickness for epoxy-coated bars belonging to bar designation

1 ksi = 6.89 MPa; 1 in = 25.4 mm; 1 lb/ft = 1.49 kg/m; 1 mil = 0.0254 mm

Table 3
Concrete Mix Proportions (lb/yd³) and Properties

Group	w/c Ratio	Cement (lb/yd ³)	Water (lb/yd ³)	Fine Agg.* (lb/yd ³)	Coarse Agg. Type	Coarse Agg. Amount (lb/yd ³)	Silica Fume** (lb/yd ³)	wr (oz)	^Superplasticizer (oz/yd ³)		Slump (in.)	Concrete Temperature (F ⁰)	Air Content (%)	Test Age (days)	Cylinder Strength (psi)
									Type F	Type G					
1	0.41	550	225	1564	L	1588	0	0.0	0	0	2.00	80.0	3.5	14	5020
2	0.36	575	205	1556	L	1588	0	3.0	0	0	0.75	91.5	3.1	7	5250
4	0.36	575	205	1556	L	1588	0	3.0	0	0	1.75	95.0	4.5	5	4090
6	0.36	575	205	1556	L	1588	0	3.0	0	0	2.25	77.0	4.7	5	4220
10	0.42	578	240	1512	B	1670	0	0.0	0	0	2.50	91.0	2.3	10	4250
13	0.36	575	205	1556	L	1588	0	3.0	0	0	2.50	91.0	5.2	6	4110
14	0.44	511	225	1564	L	1661	0	0.0	0	0	2.50	90.0	2.9	10	4200
15	0.44	511	225	1564	L	1661	0	0.0	0	0	2.50	83.0	2.3	19	5250
16	0.44	511	225	1564	L	1661	0	0.0	0	0	3.25	59.0	3.1	22	5180
18	0.44	511	225	1564	L	1661	0	0.0	0	0	2.50	65.0	3.7	30	4700
20	0.44	511	225	1564	L	1661	0	0.0	0	0	2.25	66.0	3.4	19	5080
21	0.44	511	225	1564	L	1661	0	0.0	0	0	2.50	74.0	3.2	12	4330
22	0.35	886	310	1209	B	1586	0	0.0	0	0	2.25	93.0	2.1	8	6300
														14	6700
23a	0.33	548	182	1427	L	1803	83	0.0	132	44	3.50	66.0	1.9	8	9080
23b1 ⁺	0.33	548	182	1427	L	1803	83	0.0	132	44	4.50	56.0	1.6	8	8370
23b2 ⁺	0.44	511	225	1564	L	1661	0	0.0	0	0	3.00	51.0	3.0	10	4500
24	0.44	511	225	1564	L	1661	0	0.0	0	58	4.00	87.0	2.6	9	4300
25	0.44	511	225	1564	L	1661	0	0.0	0	58	3.75	90.0	3.9	13	4490

- * Kansas River Sand - Lawrence Sand Co., Lawrence, KS
Bulk Specific Gravity (SSD) = 2.62; Absorption = 0.5%; Fineness Modulus = 2.89;
- ** Silica fume - Master Builders Technologies, Inc.
- L Crushed Limestone - Fogel's Quarry, Ottawa, KS
Bulk Specific Gravity (SSD) = 2.58; Absorption = 2.7%; Max. Size = 3/4 in.;
Unit Weight = 90.5 lb/ft³
- B Basalt - Iron Mountain Trap Rock Company
Bulk Specific Gravity (SSD) = 2.64; Absorption = 0.44%; Max. Size = 3/4 in.;
Unit Weight = 95.5 lb/ft³
- wr Water Reducer per 100 lb Cement
- ^ Superplasticizer ASTM C 494 TYPE F or G -- Master Builders Technologies, Inc.
- + 23b1 was used for specimen 23b.1 - 23b.4, and 23b2 for specimen 23b.5, 23b.6

1 lb/yd³ = 0.5933 kg/m³; 1 oz = 29.57 cm³; 1 psi = 6.89 kPa; 1 in. = 25.4 mm

Table 4
Comparison of Splice Strength for Bottom-Cast Epoxy-Coated (C) and Uncoated (U)
High R_r Bars

Bar Size	Bar Designation	R _r [*]	Specimen No.	Thickness of Coating (mil)	Transverse Reinforcement	Bar Stress (ksi)	f _s ^{***} (ksi)	C ^{**} U
No. 5	5C2	0.109	13.4	0.0	W/O	59.96	58.56	0.906
			13.3	9.9	W/O	53.91	58.08	
			14.3	0.0	W/O	62.84	61.53	
			14.4	10.0	W/O	57.34	60.94	
	5C3	0.141	25.1	0.0	W/O	63.13	65.72	1.081
			25.2	6.0	W/O	66.7	70.10	
No.8	8C1	0.101	1.3	0.0	W/O	45.01	42.04	0.834
			1.4	12.8	W/O	37.09	41.54	
			4.5	0.0	W/O	51.06	53.54	
			4.6	12.0	W/O	41.72	55.56	
	8F1	0.140	2.5	0.0	W/O	58.67	56.58	0.820
			2.6	16.8	W/O	49.37	58.03	
			6.5	0.0	W/O	53.59	55.34	
			6.6	16.8	W/O	49.63	55.43	
	8N1	0.120	24.1	0.0	W/O	61.12	67.25	0.901
			24.2	9.5	W/O	54.74	66.82	
	8N3	0.119	10.2	0.0	W/O	61.17	58.32	0.955
			10.1	12.4	W/O	57.79	57.67	
			20.6	0.0	W/O	56.51	59.69	
			20.5	11.2	W/O	49.14	59.11	
			21.1	0.0	W/	71.79	84.05	
			21.2	9.8	W/	67.14	84.07	
			21.3	0.0	W/	73.97	80.88	
			21.4	11.7	W/	67.43	80.72	
			21.5	0.0	W/	76.11	84.67	
			21.6	9.7	W/	64.33	83.78	
			23a.1	0.0	W/	79.01	79.10	
			23a.2	11.6	W/	62.73	79.00	
			23b.1	0.0	W/	78.46	70.34	
			23b.2	11.9	W/	70.13	70.14	
23b.3	0.0	W/O	71.57	72.96				
23b.4	11.3	W/O	70.17	73.06				
No.11	11F3	0.127	15.5	0.0	W/O	54.12	57.33	0.893
			15.6	6.8	W/O	48.19	57.18	
			16.2	0.0	W/O	52.38	56.88	
			16.1	6.8	W/O	48.83	56.40	
			18.3	0.0	W/	69.33	71.20	
			18.2	5.3	W/	57.48	71.18	
			23b.5	0.0	W/	53.32	52.17	
			23b.6	8.6	W/	44.22	52.09	
Average								0.894
STD								0.0697
COV								0.0780

* R_r = relative rib area

** C/U = normalized splice strengths ratio of coated to uncoated bars

*** f_s = predicted bar stress, Eq. (1) or (2)

1 mil = 0.0254 mm; 1 ksi = 6.89 MPa

Table 5 (Without Stirrups)
Comparison of Splice Strength for Bottom-Cast Epoxy-Coated (C) and Uncoated (U)
High R_r Bars

Bar Size	Bar Designation	R _c [*]	Specimen No.	Thickness of Coating (mils)	Bar Stress (ksi)	f _s ^{***} (ksi)	C ^{**} U
No. 5	5C2	0.109	13.4	0.0	59.96	58.56	
			13.3	9.9	53.91	58.08	0.906
			14.3	0.0	62.84	61.53	
			14.4	10.0	57.34	60.94	0.921
	5C3	0.141	25.1	0.0	63.13	65.72	
			25.2	6.0	66.7	70.10	1.081
No. 8	8C1	0.101	1.3	0.0	45.01	42.04	
			1.4	12.8	37.09	41.54	0.834
			4.5	0.0	51.06	53.54	
			4.6	12.0	41.72	55.56	0.787
	8F1	0.140	2.5	0.0	58.67	56.58	
			2.6	16.8	49.37	58.03	0.820
			6.5	0.0	53.59	55.34	
			6.6	16.8	49.63	55.43	0.925
	8N1	0.120	24.1	0.0	61.12	67.25	
			24.2	9.5	54.74	66.82	0.901
	8N3	0.119	10.2	0.0	61.17	58.32	
			10.1	12.4	57.79	57.67	0.955
			20.6	0.0	56.51	59.69	
			20.5	11.2	49.14	59.11	0.878
			23b.3	0.0	71.57	72.96	
			23b.4	11.3	70.17	73.06	0.979
No. 11	11F3	0.127	15.5	0.0	54.12	57.33	
			15.6	6.8	48.19	57.18	0.893
			16.2	0.0	52.38	56.88	
			16.1	6.8	48.83	56.40	0.940
Average							0.909
STD							0.0750
COV							0.0825

* R_r = relative rib area

** C/U = normalized splice strengths ratio of coated to uncoated bars

*** f_s = predicted bar stress, Eq. (1) or (2)

1 mil = 0.0254 mm; 1 ksi = 6.89 MPa

Table 6 (With Stirrups)
Comparison of Splice Strength for Bottom-Cast Epoxy-Coated (C) and Uncoated (U)
High R_r Bars

Bar Size	Bar Designation	R_y^*	Specimen No.	Thickness of Coating (mils)	Bar Stress (ksi)	f_s^{***} (ksi)	C^{**} U
No.8	8N3	0.119	21.1	0.0	71.79	84.05	
			21.2	9.8	67.14	84.07	0.935
			21.3	0.0	73.97	80.88	
			21.4	11.7	67.43	80.72	0.913
			21.5	0.0	76.11	84.67	
			21.6	9.7	64.33	83.78	0.854
			23a.1	0.0	79.01	79.10	
			23a.2	11.6	62.73	79.00	0.795
			23b.1	0.0	78.46	70.34	
			23b.2	11.9	70.13	70.14	0.896
No.11	11F3	0.127	18.3	0.0	69.33	71.20	
			18.2	5.3	57.48	71.18	0.829
			23b.5	0.0	53.32	52.17	
			23b.6	8.6	44.22	52.09	0.831
Average							0.865
STD							0.0511
COV							0.0590

* R_r = relative rib area

** C/U = normalized splice strengths ratio of coated to uncoated bars

*** f_s = predicted bar stress, Eq. (1) or (2)

1 mil = 0.0254 mm; 1 ksi = 6.89 MPa

Table 7
Previous Beam Splice Test Results

Specimen Label *	n	Coating Thick. (mils)	l_s (in)	b (in)	h (in)	d_b (in)	c_{s0} (in)	c_{si} (in)	c_b (in)	d (in)	l (ft)	l_c (ft)	f_c' (psi)	N	d_s (in)	M_u (k-in)	f_t^{**} (ksi)	R_r
Hester et al (1991, 1993) W/O Stirrups																		
8C3-16-0-U	3	0.0	16.00	16	16	1.0	2.0	1.5	1.84	13.658	13.0	4.0	6200	0	-	1376	46.5	0.071
8C3-16-0-C	3	11.2	16.00	16	16	1.0	2.0	1.5	1.75	13.750	13.0	4.0	6200	0	-	1146	38.5	0.071
8S3-16-0-U	3	0.0	16.00	16	16	1.0	2.0	1.5	2.04	13.460	13.0	4.0	6020	0	-	1361	47.0	0.07
8S3-16-0-C	3	9.9	16.00	16	16	1.0	2.0	1.5	2.06	13.440	13.0	4.0	6020	0	-	911	30.9	0.07
8S3-16-0-U	3	0.0	16.00	16	16	1.0	2.0	1.5	2.10	13.400	13.0	4.0	6450	0	-	1228	42.7	0.07
8S3-16-0-C	3	10.7	16.00	16	16	1.0	2.0	1.5	2.11	13.390	13.0	4.0	6450	0	-	884	30.8	0.07
8C3-16-0-U	3	0.0	16.00	16	16	1.0	2.0	1.5	2.05	13.450	13.0	4.0	5490	0	-	1158	39.7	0.071
8C3-16-0-C	3	8.6	16.00	16	16	1.0	2.0	1.5	2.01	13.490	13.0	4.0	5490	0	-	931	31.8	0.071
8C3-22 3/4-0-U	3	0.0	22.75	16	16	1.0	2.0	1.5	2.15	13.350	13.0	4.0	5850	0	-	1489	51.6	0.071
8C3-22 3/4-0-C	3	9.0	22.75	16	16	1.0	2.0	1.5	2.00	13.500	13.0	4.0	5850	0	-	952	33.4	0.071
*8C3-16-0-C	2	0.0	16.00	16	16	1.0	2.0	4.0	2.12	13.380	13.0	4.0	5240	0	-	885	45.2	0.071
*8C3-16-0-U	2	11.4	16.00	16	16	1.0	2.0	4.0	2.12	13.380	13.0	4.0	5240	0	-	759	38.7	0.071
Hester et al. (1991, 1993) W/stirrups																		
8N3-16-2-U	3	0.0	16.00	16	16	1.0	2.0	1.5	2.00	13.500	13.0	4.0	5990	2	0.375	1604	56.5	0.078
8N3-16-2-C	3	9.6	16.00	16	16	1.0	2.0	1.5	2.00	13.500	13.0	4.0	5990	2	0.375	1214	42.7	0.078
8C3-16-2-U	3	0.0	16.00	16	16	1.0	2.0	1.5	1.83	13.670	13.0	4.0	6200	2	0.375	1305	44.2	0.071
8C3-16-2-C	3	8.7	16.00	16	16	1.0	2.0	1.5	1.78	13.720	13.0	4.0	6200	2	0.375	1124	38.0	0.071
8S3-16-2-U	3	0.0	16.00	16	16	1.0	2.0	1.5	2.08	13.420	13.0	4.0	6020	2	0.375	1348	46.6	0.07
8S3-16-2-C	3	9.8	16.00	16	16	1.0	2.0	1.5	2.07	13.430	13.0	4.0	6020	2	0.375	921	32.0	0.07
8S3-16-2-U	3	0.0	16.00	16	16	1.0	2.0	1.5	2.04	13.460	13.0	4.0	6450	2	0.375	1384	47.4	0.07
8S3-16-2-C	3	9.8	16.00	16	16	1.0	2.0	1.5	2.00	13.500	13.0	4.0	6450	2	0.375	932	32.1	0.07
8S3-16-3-U	3	0.0	16.00	16	16	1.0	2.0	1.5	2.10	13.400	13.0	4.0	6450	3	0.375	1456	50.4	0.07
8S3-16-3-C	3	8.9	16.00	16	16	1.0	2.0	1.5	2.03	13.470	13.0	4.0	6450	3	0.375	887	30.8	0.07
8C3-16-3-U	3	0.0	16.00	16	16	1.0	2.0	1.5	2.06	13.440	13.0	4.0	5490	3	0.375	1244	43.2	0.071
8C3-16-3-C	3	8.0	16.00	16	16	1.0	2.0	1.5	2.06	13.440	13.0	4.0	5490	3	0.375	1024	34.7	0.071
8C3-22 3/4-3-U	3	0.0	22.75	16	16	1.0	2.0	1.5	2.17	13.330	13.0	4.0	5850	3	0.375	1620	56.2	0.071
8C3-22 3/4-3-C	3	8.6	22.75	16	16	1.0	2.0	1.5	2.13	13.370	13.0	4.0	5850	3	0.375	1027	35.6	0.071
8C3-22 3/4-4-U	3	0.0	22.75	16	16	1.0	2.0	1.5	2.16	13.340	13.0	4.0	5850	4	0.375	1595	55.6	0.071
8C3-22 3/4-4-C	3	9.9	22.75	16	16	1.0	2.0	1.5	2.18	13.320	13.0	4.0	5850	4	0.375	1112	38.5	0.071
8C3-16-3-U	2	0.0	16.00	16	16	1.0	2.0	4.0	2.03	13.470	13.0	4.0	5240	3	0.375	1019	51.5	0.071
8C3-16-3-C	2	9.9	16.00	16	16	1.0	2.0	4.0	2.08	13.420	13.0	4.0	5240	3	0.375	759	38.7	0.071

Table 7 (continued)
Previous Beam Splice Test Results

Specimen Label *	n	Coating Thick. (mils)	l_s (in)	b (in)	h (in)	d_b (in)	c_{so} (in)	c_{si} (in)	c_b (in)	d (in)	l (ft)	l_c (ft)	f_c' (psi)	N	d_s (in)	M_u (k-in)	f_s^{**} (ksi)	R_r
Choi et al (1990, 1991)																		
5N0-12-0-U	3	0.0	12.0	15.75	16	0.625	2.0	2.0	1.0	14.688	12.0	4.0	5360	0	-	813	65.3	0.086
5N0-12-0-C	3	9.5	12.0	15.75	16	0.625	2.0	2.0	1.0	14.688	12.0	4.0	5360	0	-	609	49.0	0.086
6S0-12-0-U	2	0.0	12.0	11.00	16	0.750	2.0	2.0	1.0	14.625	12.0	4.0	6010	0	-	543	45.8	0.060
6S0-12-0-C	2	8.3	12.0	11.00	16	0.750	2.0	2.0	1.0	14.625	12.0	4.0	6010	0	-	511	43.1	0.060
6C0-12-0-U	2	0.0	12.0	11.00	16	0.750	2.0	2.0	1.0	14.625	12.0	4.0	6010	0	-	610	51.4	0.079
6C0-12-0-C	2	8.8	12.0	11.00	16	0.750	2.0	2.0	1.0	14.625	12.0	4.0	6010	0	-	466	39.3	0.079
8S0-16-0-U	2	0.0	16.0	12.00	16	1.000	2.0	2.0	1.5	14.000	12.0	4.0	5980	0	-	854	43.1	0.064
8S0-16-0-C	2	9.4	16.0	12.00	16	1.000	2.0	2.0	1.5	14.000	12.0	4.0	5980	0	-	768	38.7	0.064
8N0-16-0-U	2	0.0	16.0	12.00	16	1.000	2.0	2.0	1.5	14.000	12.0	4.0	5980	0	-	858	43.3	0.080
8N0-16-0-C	2	9.5	16.0	12.00	16	1.000	2.0	2.0	1.5	14.000	12.0	4.0	5980	0	-	737	37.2	0.080
11S0-24-0-U	2	0.0	24.0	13.65	16	1.410	2.0	2.0	2.0	13.295	14.0	6.0	5850	0	-	1459	40.2	0.071
11S0-24-0-C	2	9.3	24.0	13.65	16	1.410	2.0	2.0	2.0	13.295	14.0	6.0	5850	0	-	1053	29.0	0.071
11C0-24-0-U	2	0.0	24.0	13.65	16	1.410	2.0	2.0	2.0	13.295	14.0	6.0	5850	0	-	1372	37.8	0.069
11C0-24-0-C	2	10.3	24.0	13.65	16	1.410	2.0	2.0	2.0	13.295	14.0	6.0	5850	0	-	1128	31.1	0.069

*Specimen Label : #DS-L-N-B

= bar size

D = deformation pattern: S, C, N

S = stirrups bar size

L = splice length

N = number of stirrups

B = U - uncoated bars

C- coated bars

f_s^{**} = bar stresses at failure and calculated from ultimate moments (M_u) using working stress method.

1 in. = 25.4 mm; 1 mil = 0.0254 mm; 1 ft = 305 mm; 1 psi = 6.89 kPa; 1 ksi = 6.89 MPa; 1 k-in. = 0.113 kN-m

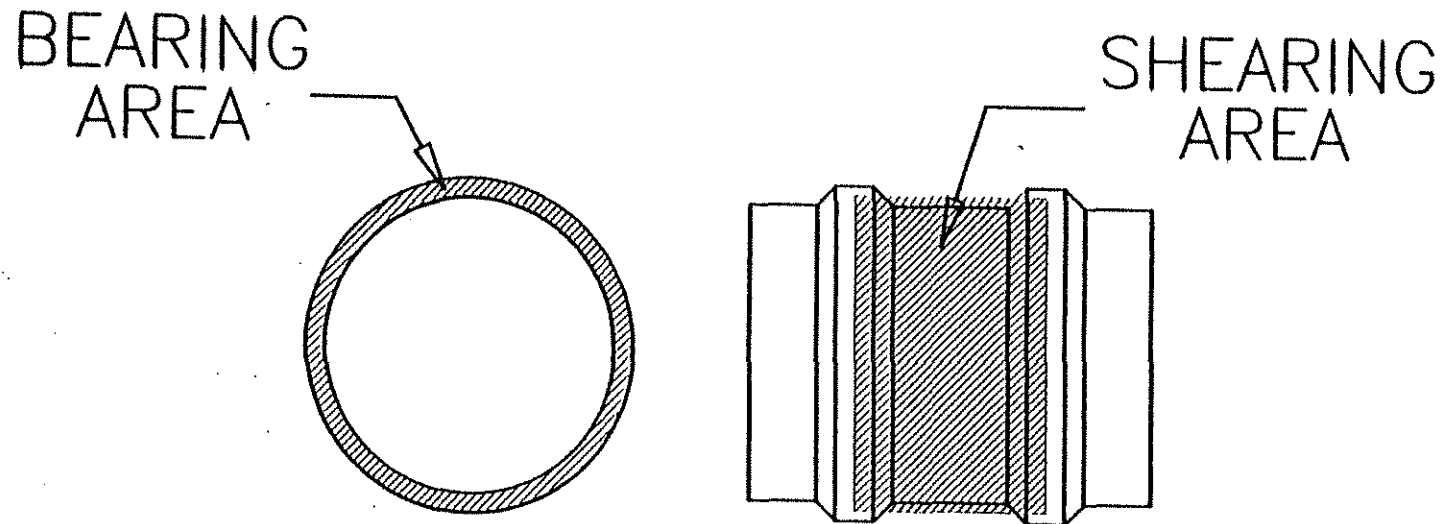
Table 8
Comparisons of Splice Strength for Epoxy Coated (C) and Uncoated (U)
Top Cast and Bottom Cast High R_r Bars

Bar Size	Bar Designation	R _r [*]	Specimen No.	Thickness of Coating (mils)	Cast Position	Transverse Reinforcement	Bar Stress (ksi)	bottom/top C _b /C _t or U _b /U _t	coated/uncoated C _b /U _b or C _t /U _t	U _b C _t
No. 5	5C3	0.141	25.1	0.0	bottom	W/O	65.72	0.993	-	1.050
			25.2	6.0	bottom	W/O	70.10	1.120	1.067	-
			25.3	0.0	top	W/O	66.16	-	-	-
			25.4	9.5	top	W/O	62.58	-	0.946	-
No.8	8N1	0.12	24.1	0.0	bottom	W/O	61.12	1.033	-	1.116
			24.2	9.5	bottom	W/O	54.74	1.000	0.896	-
			24.3	0.0	top	W/O	59.19	-	-	-
			24.4	10.9	top	W/O	54.76	-	0.925	-
MEAN								1.04	0.96	1.08

*R_r = relative rib area

**C_b, C_t and U_b, U_t = bottom cast, top cast splice strengths for epoxy coated and uncoated bars

1 ksi = 6.98 MPa; 1 mil = 0.0254 mm



$$R_r = \frac{\text{BEARING AREA}}{\text{SHEARING AREA}}$$

Fig. 1 Relative rib area illustration. Bearing area = projected rib area normal to bar axis.
Shearing area = product of the nominal bar perimeter and the center-to-center rib spacing.

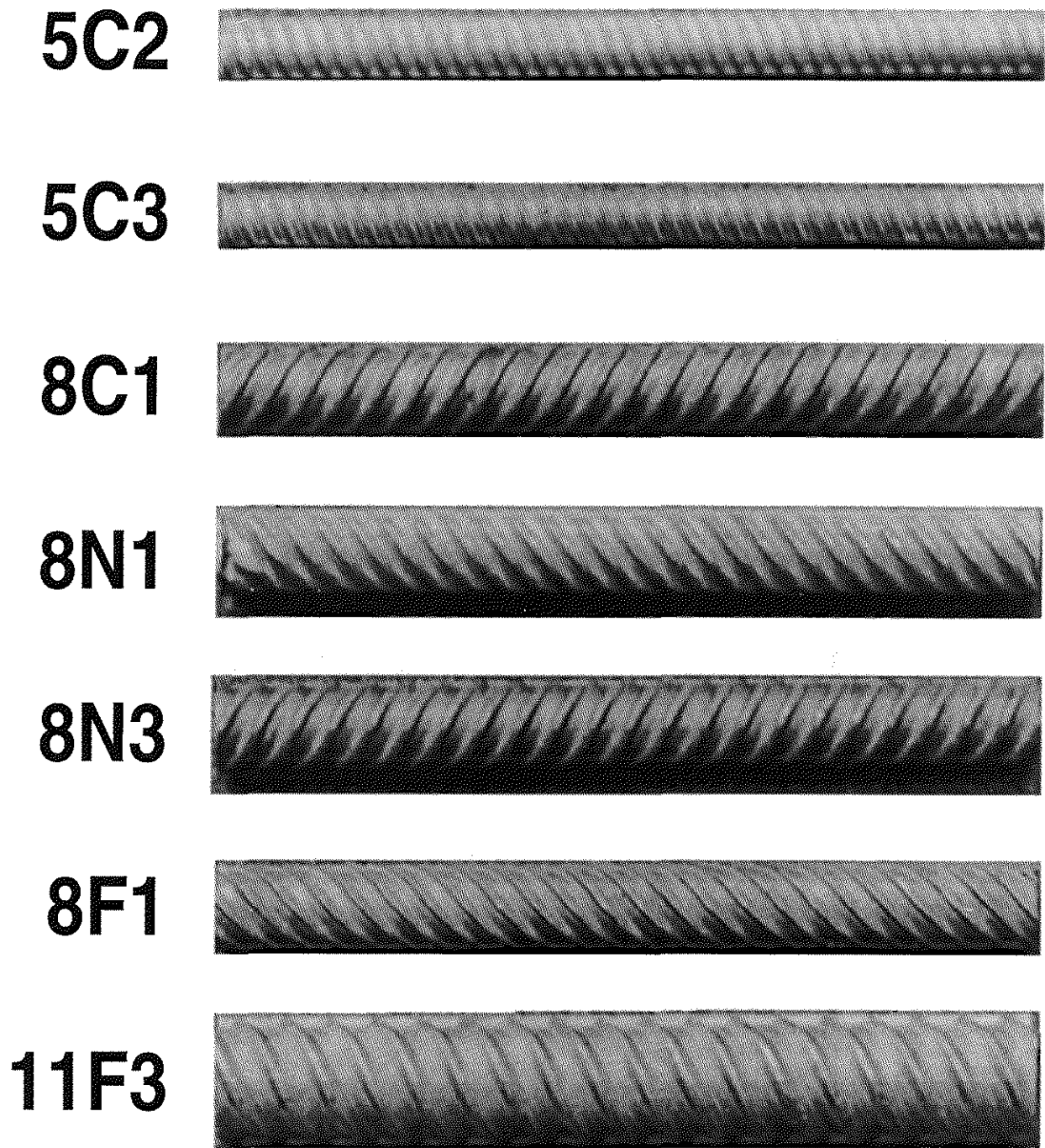


Fig. 2 Reinforcing bar deformation patterns

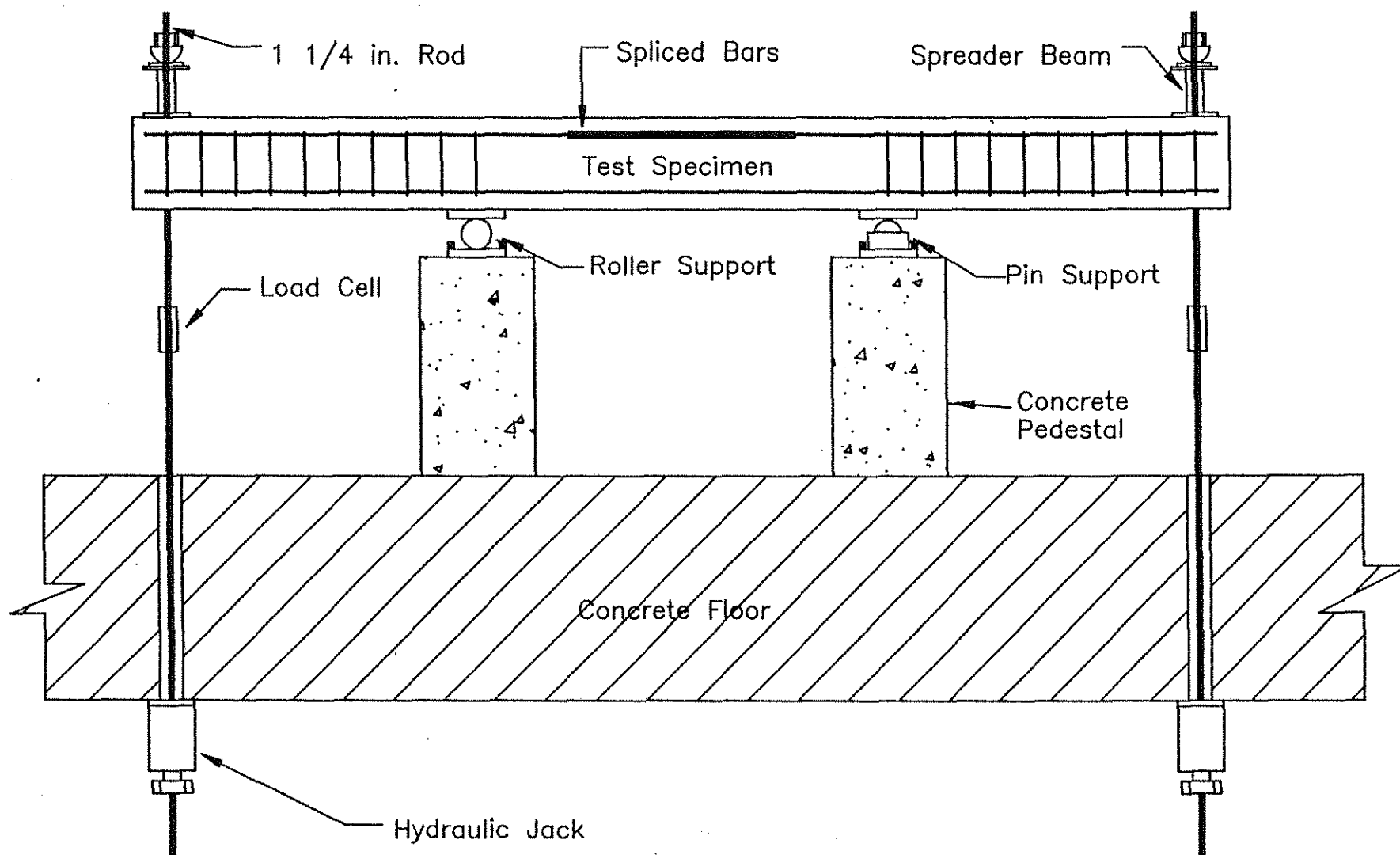


Fig. 3 Schematic of test apparatus

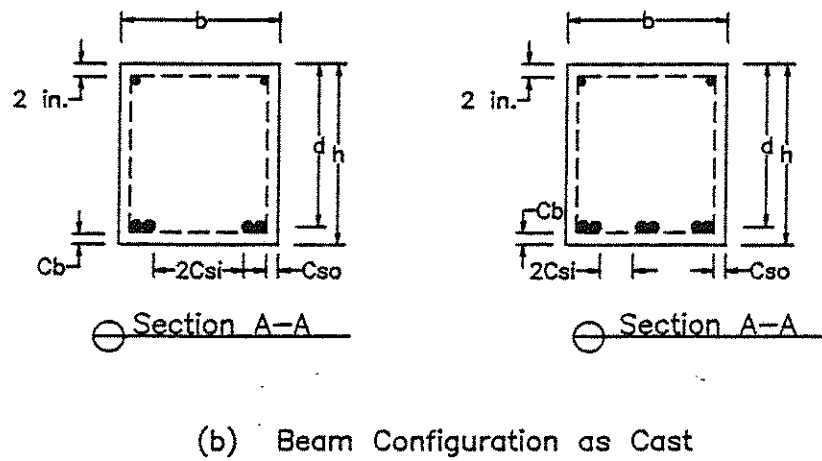
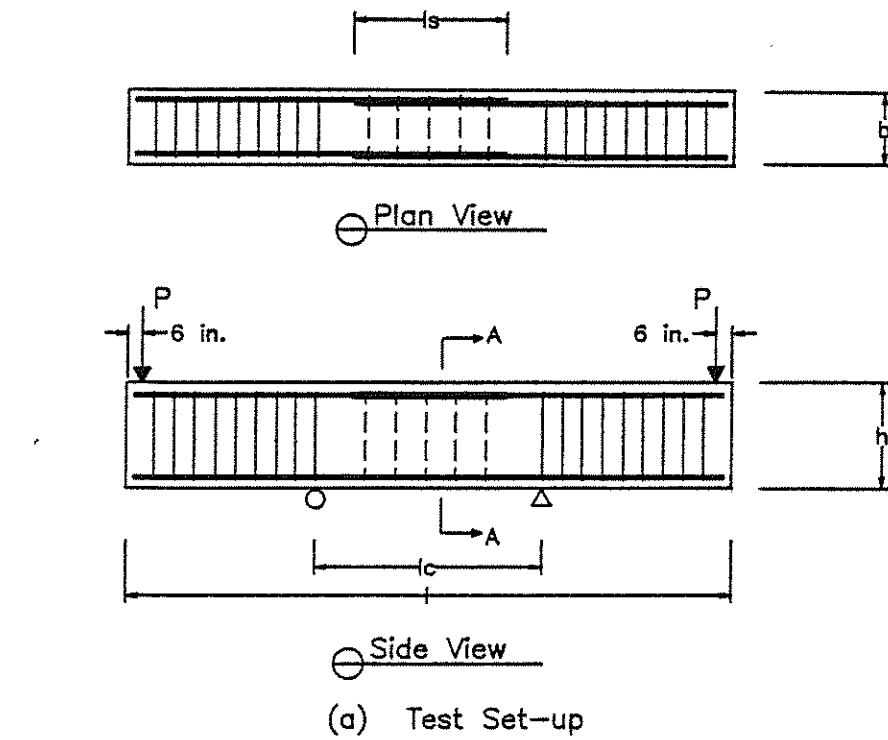


Fig. 4 Bottom-cast splice test specimens (1 in. = 25.4 mm)

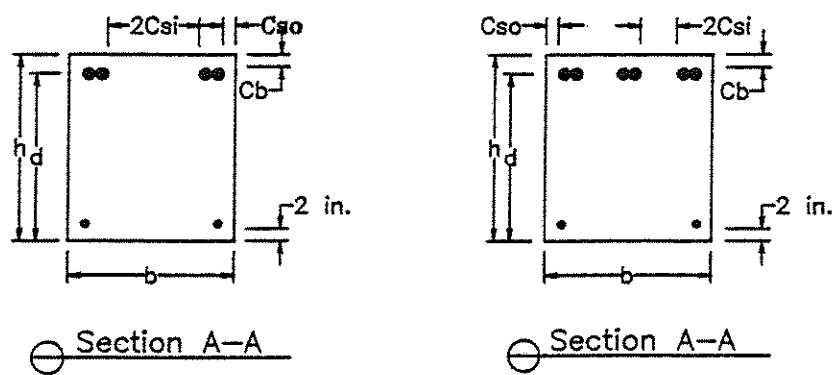
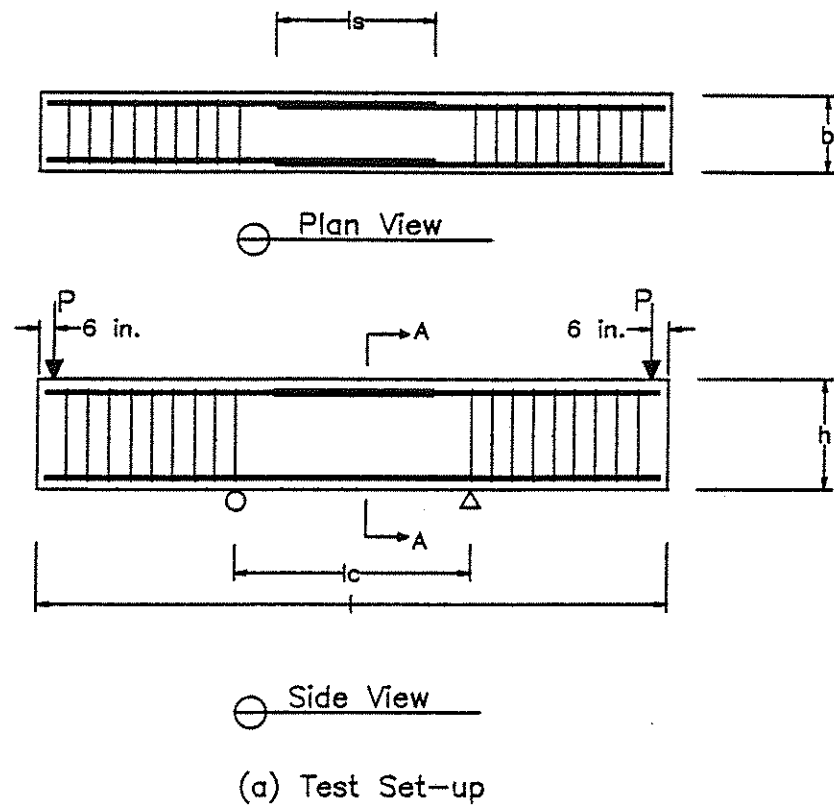


Fig. 5 Top-cast splice test specimens (1 in. = 25.4 mm)

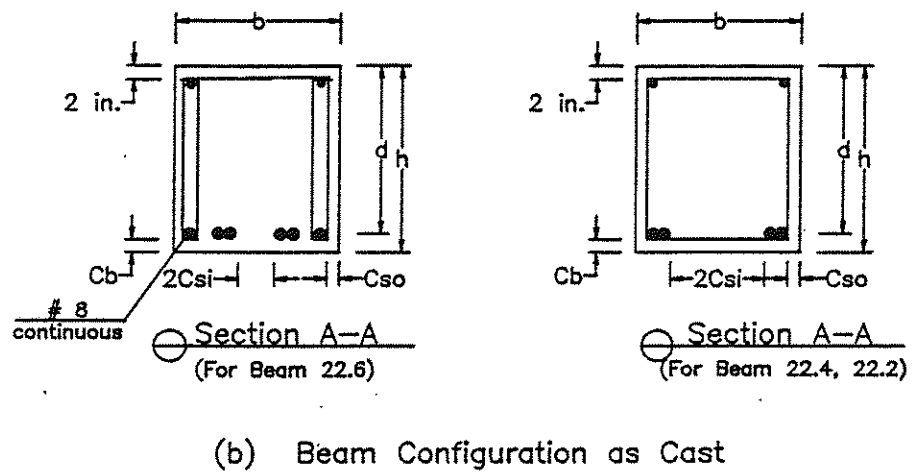
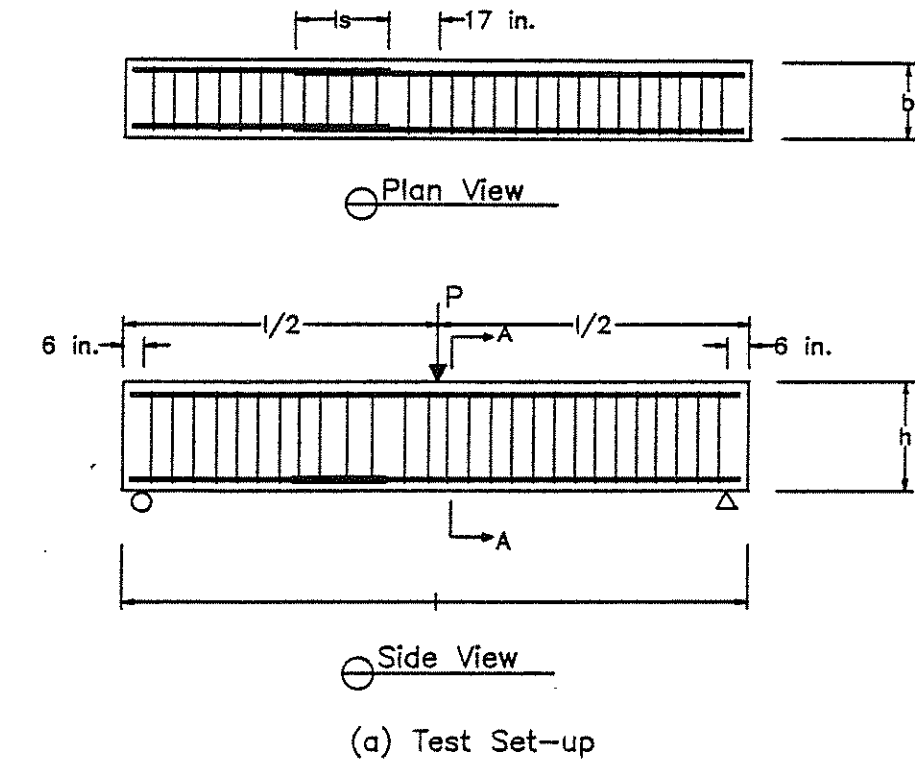
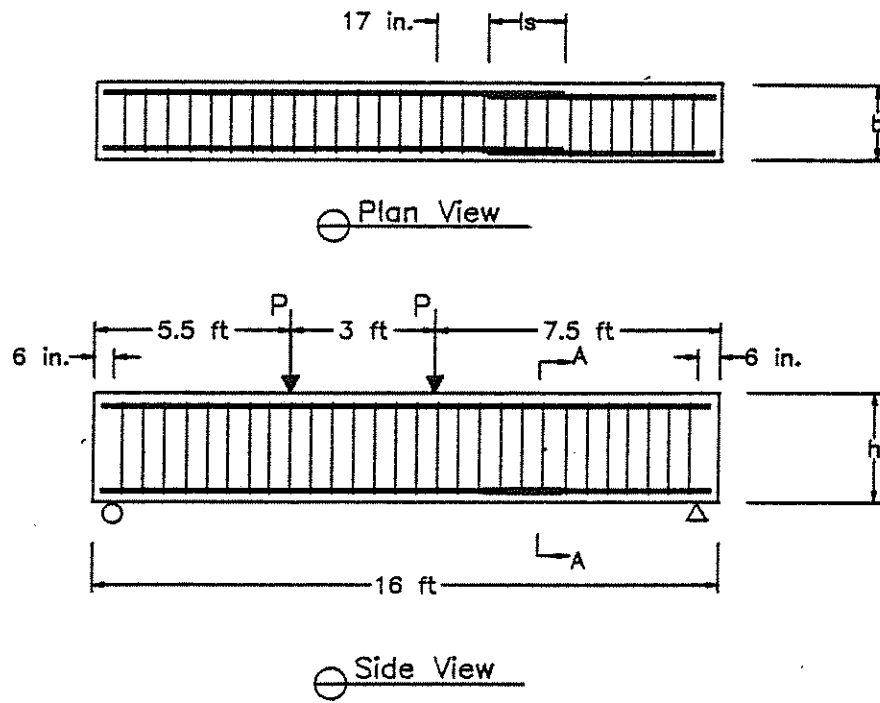
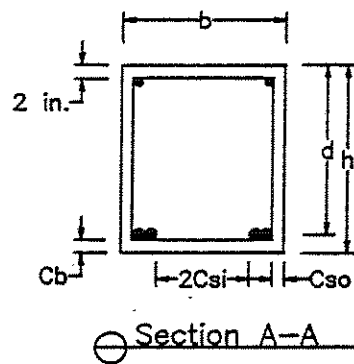


Fig. 6 Splice test specimens group 22 (1 in. = 25.4 mm)

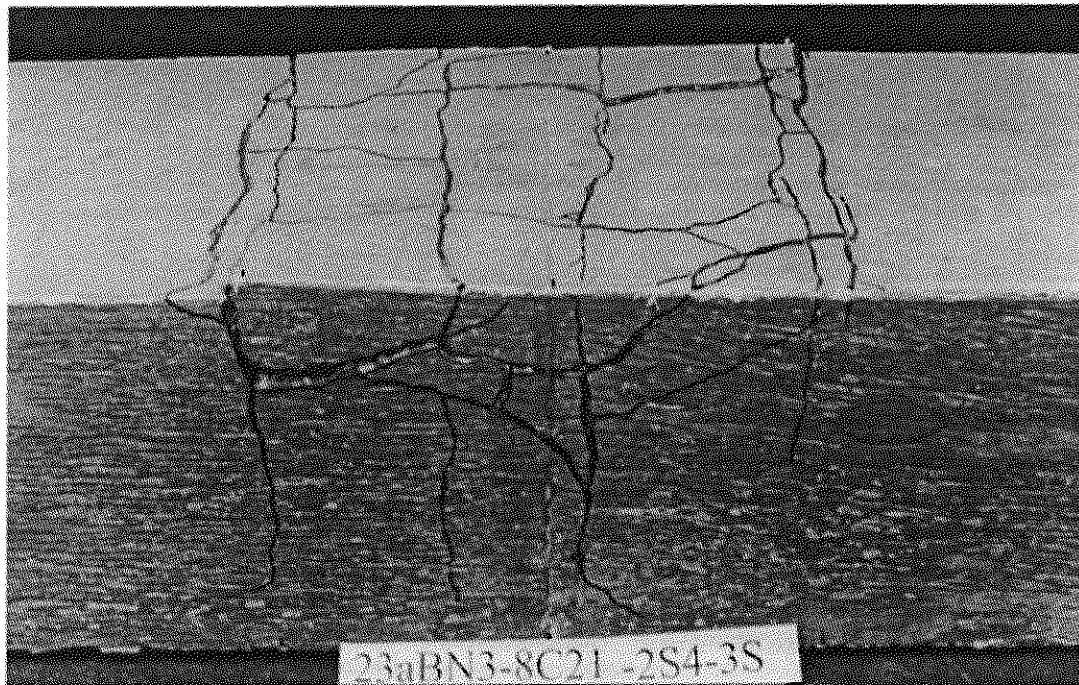


(a) Test Set-up

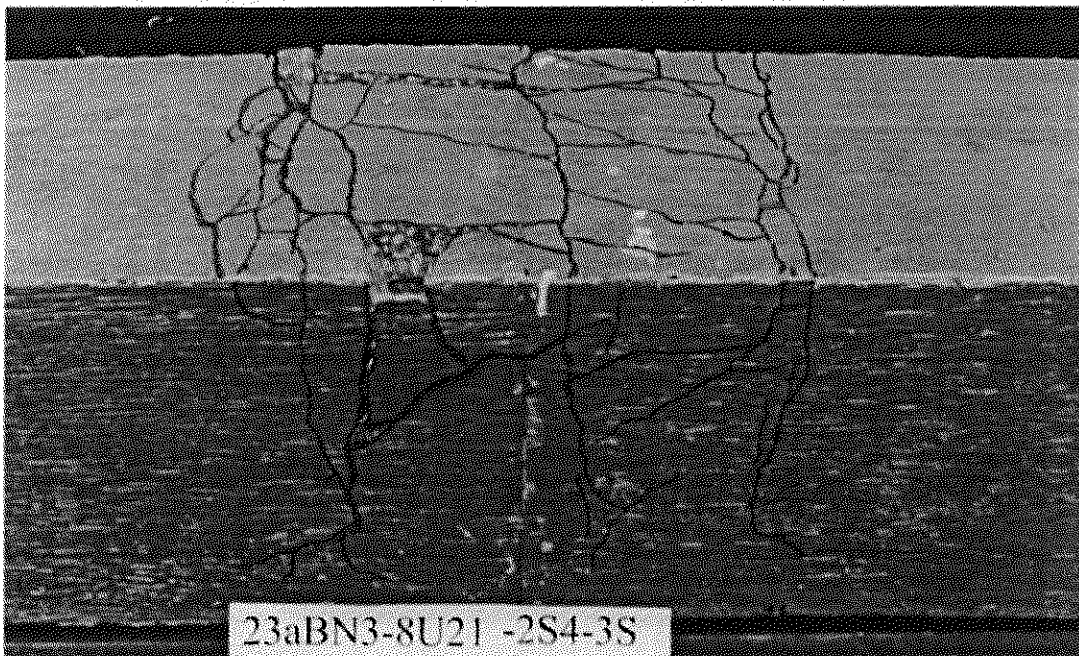


(b) Beam Configuration as Cast

Fig. 7 Splice test specimens 23b.5 and 23b.6 (1 in. = 25.4 mm)

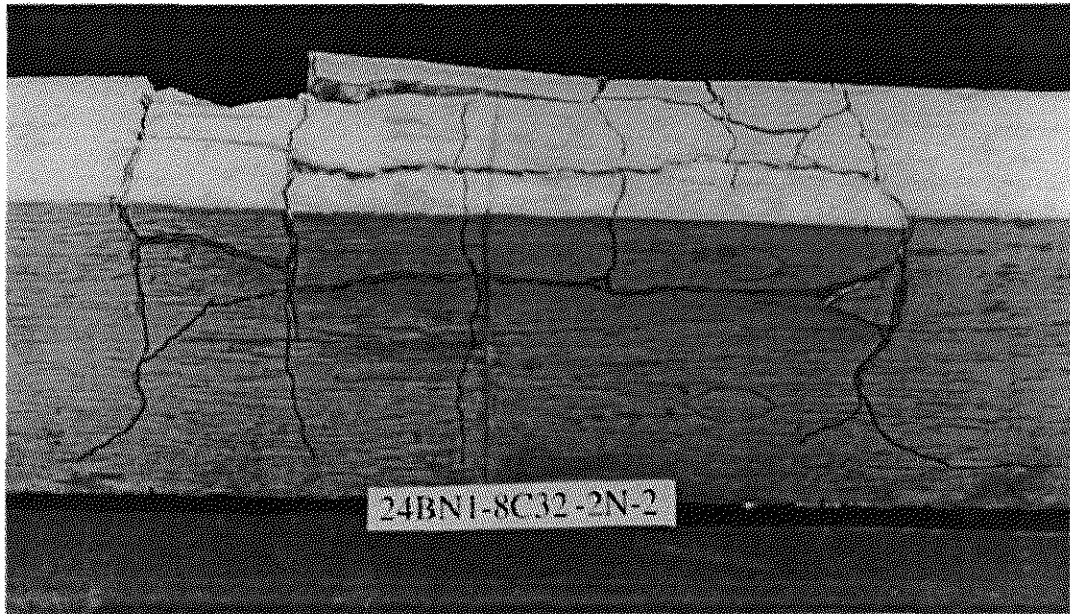


Epoxy-coated specimen

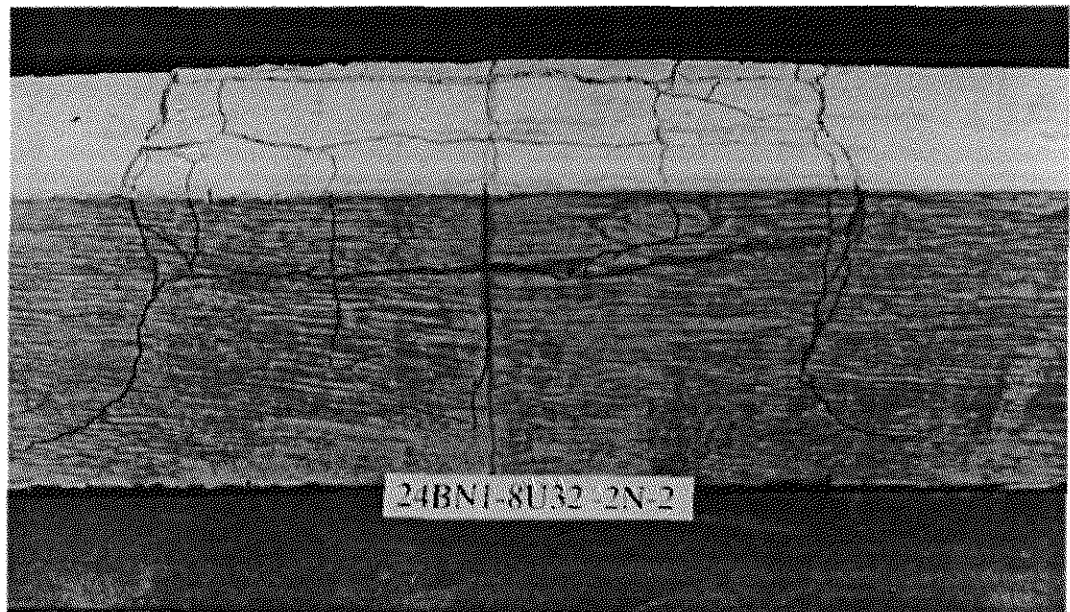


Uncoated specimen

Fig. 8(a) Cracked specimens with stirrups after failure



Epoxy-coated specimen



Uncoated specimen

Fig. 8(b) Cracked specimens without stirrups after failure

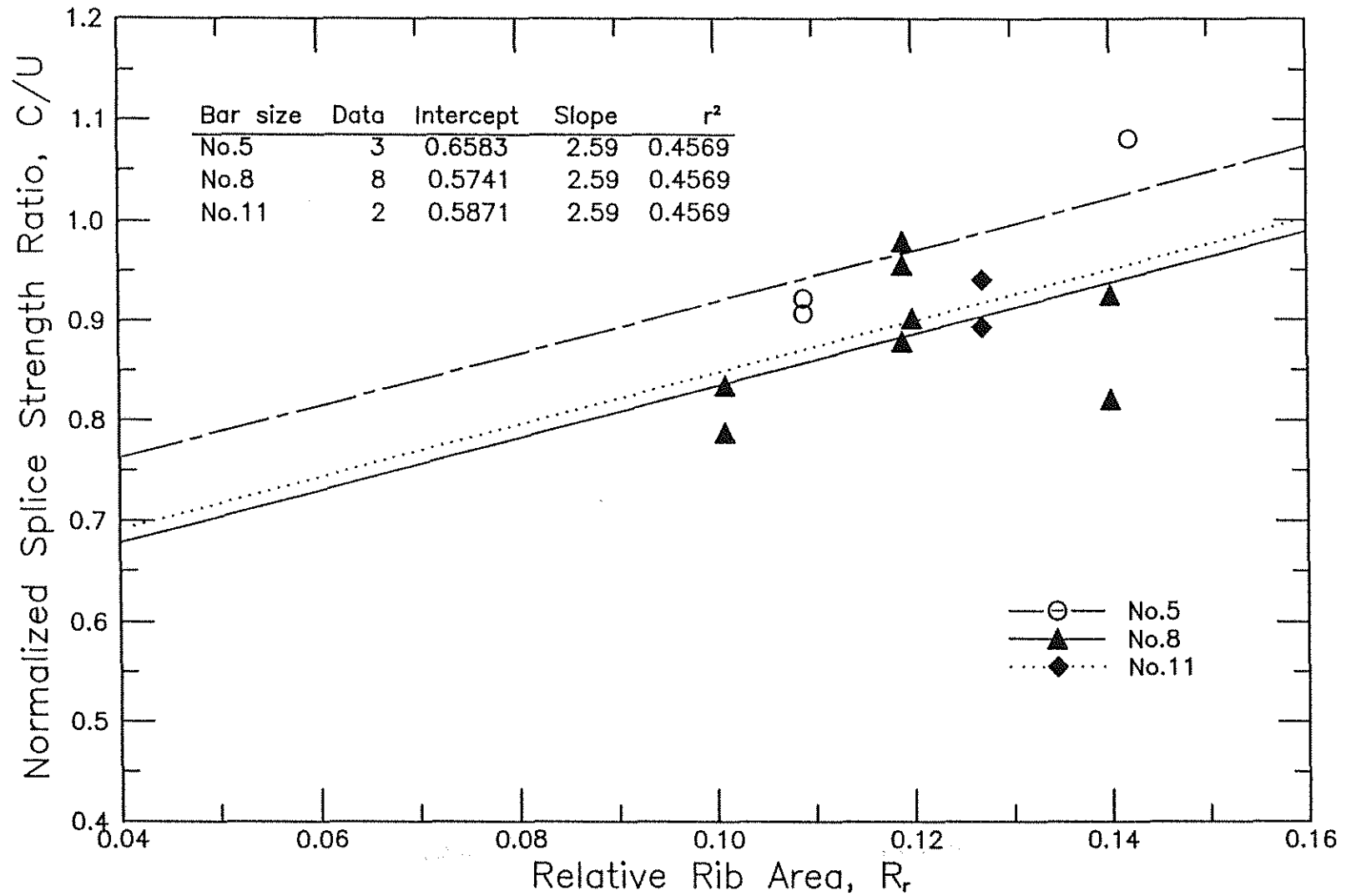


Fig. 9 Normalized splice strength ratio, C/U , versus relative rib area, R_r , for the specimens without stirrups tested in the current study

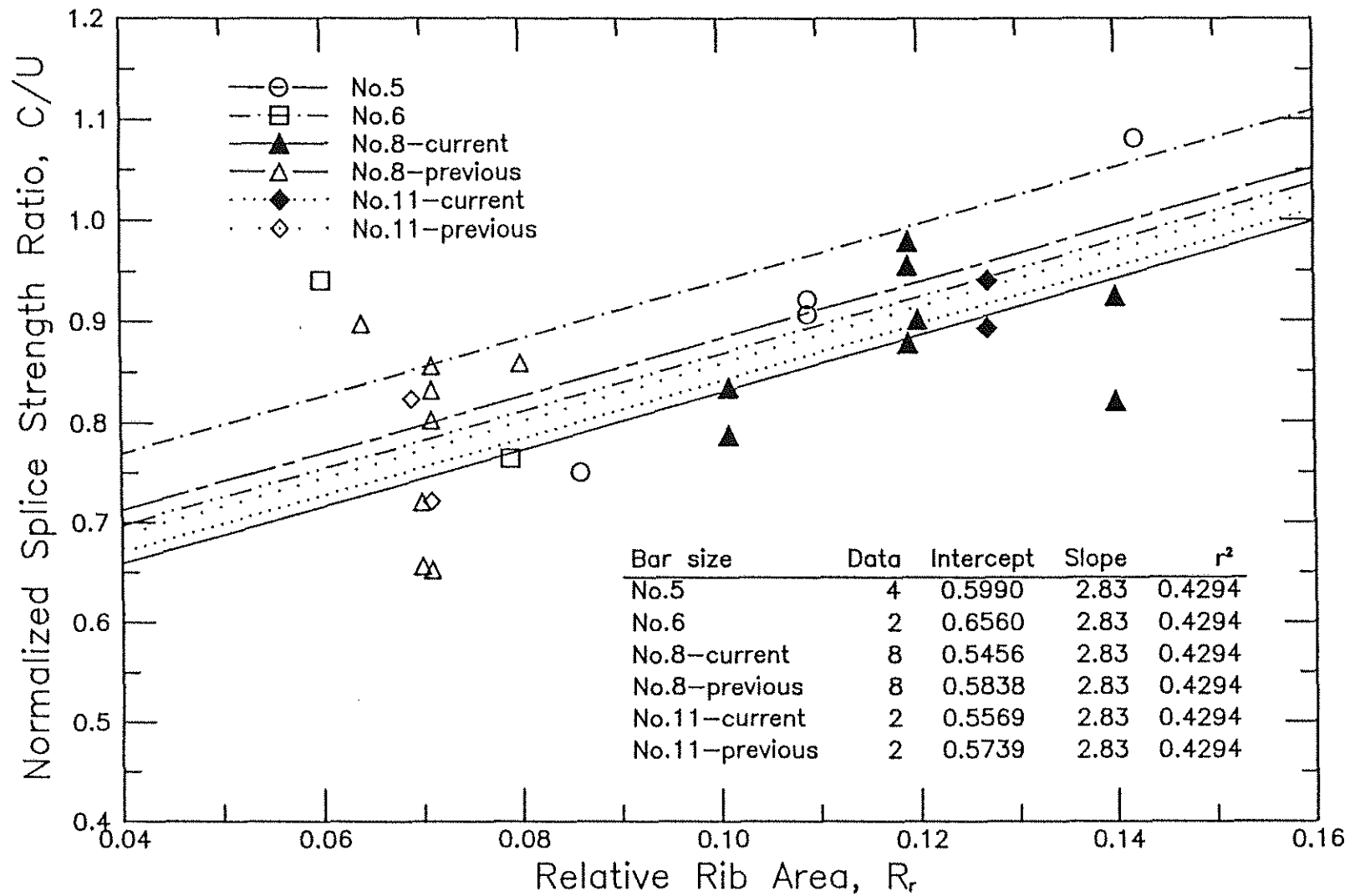


Fig. 10 Normalized splice strength ratio, C/U , versus relative rib area, R_r , for the specimens without stirrups tested in current and previous studies

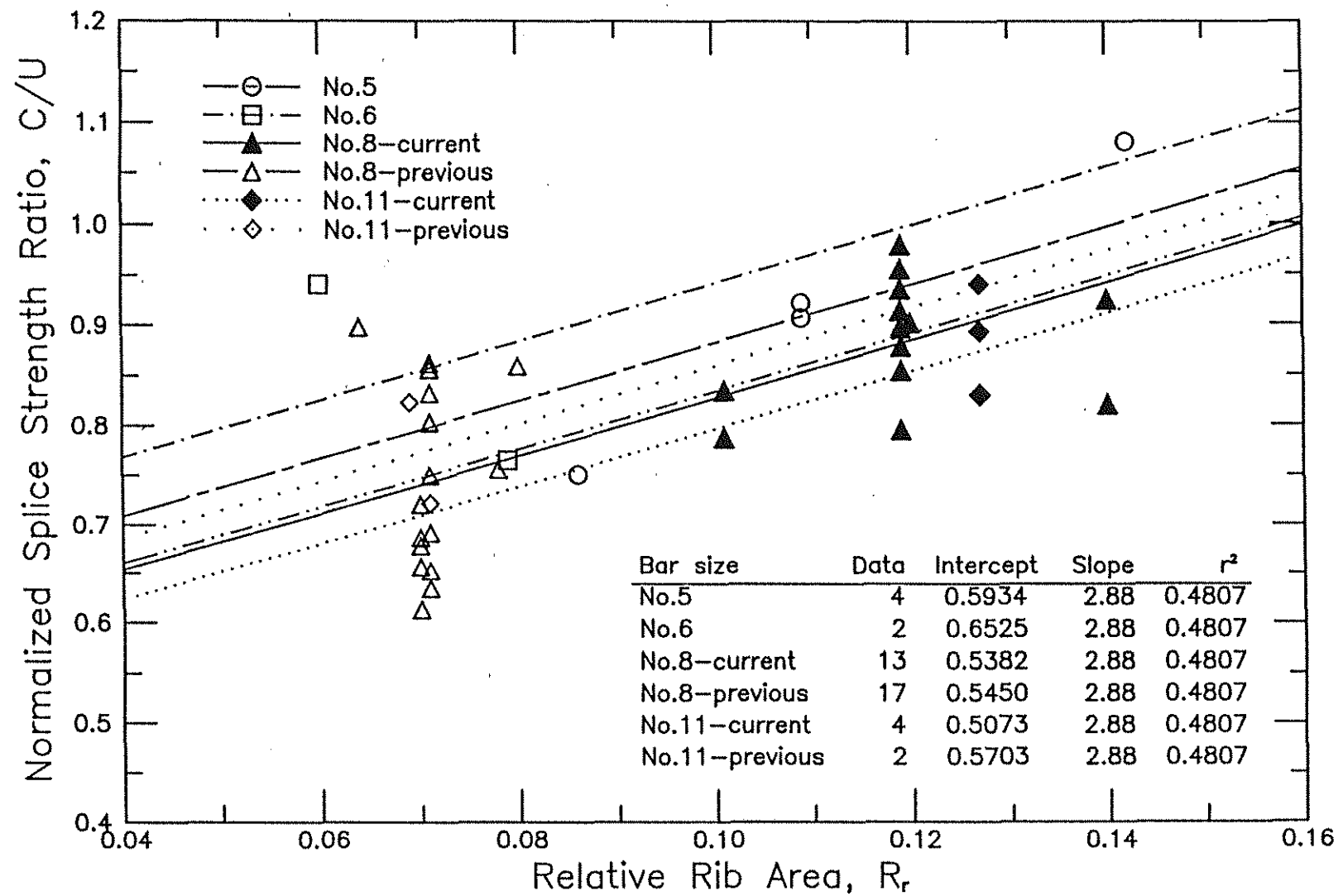


Fig. 11 Normalized splice strength ratio, C/U , versus relative rib area, R_r , for all specimens tested in current and previous studies

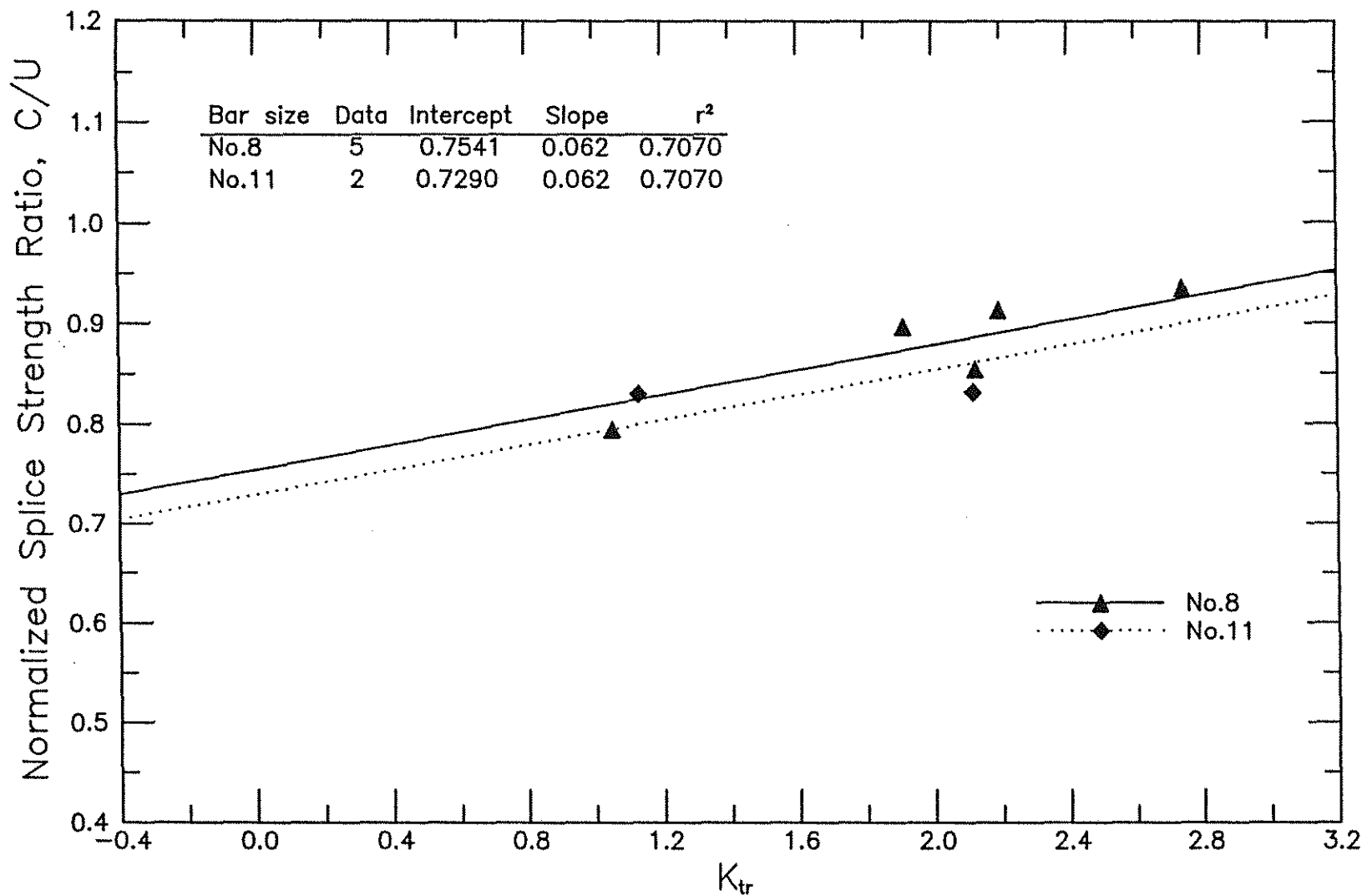


Fig. 12 Normalized splice strength ratio, C/U , versus K_{tr} for the specimens with stirrups tested in the current study
 (K_{tr} in in.) (1 in. = 25.4 mm)

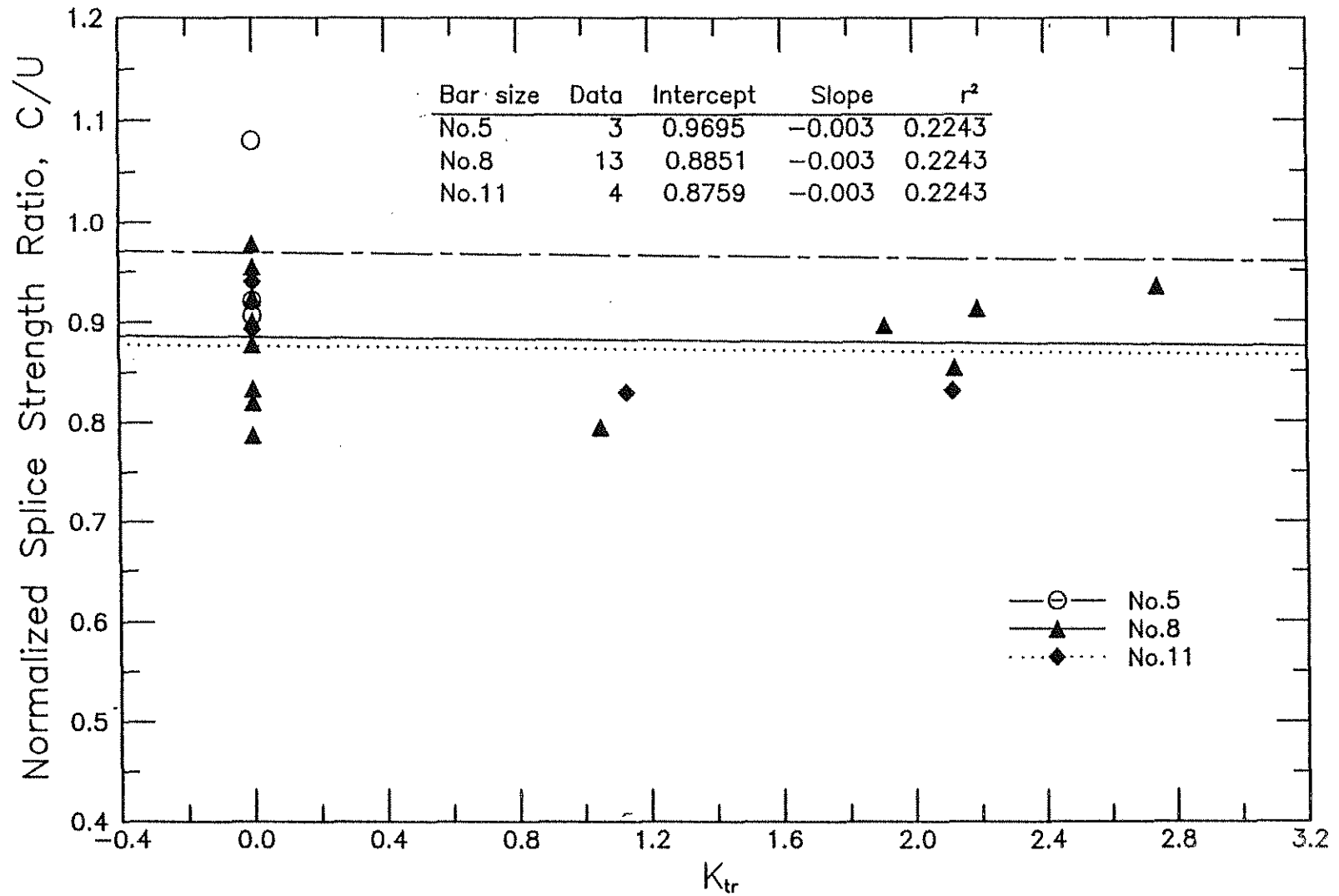


Fig. 13 Normalized splice strength ratio, C/U , versus K_{tr} for all specimens tested in the current study
 (K_{tr} in in.) (1 in. = 25.4 mm)

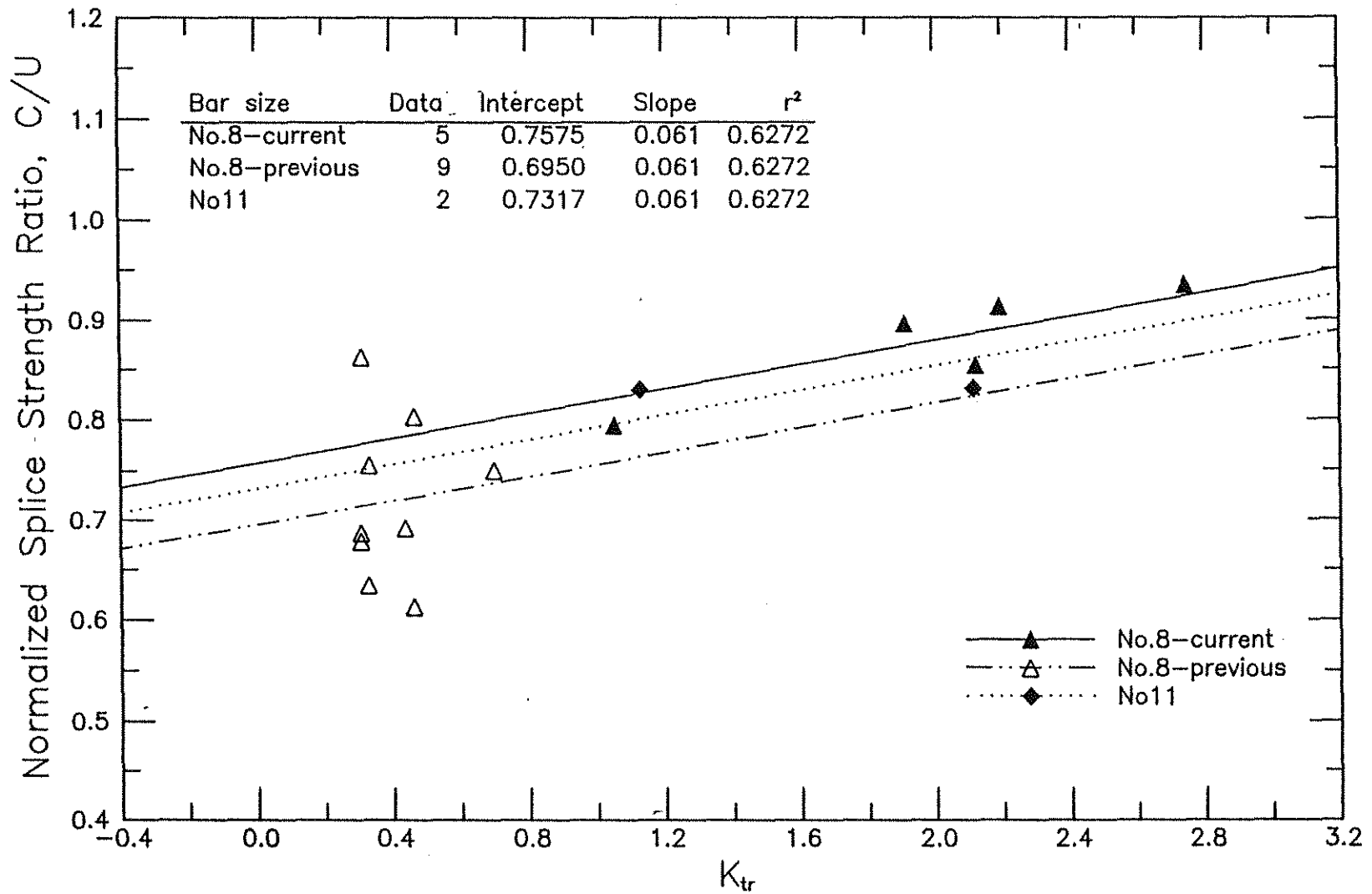


Fig. 14 Normalized splice strength ratio, C/U , versus K_{tr} for the specimens with stirrups tested in current and previous studies
(K_{tr} in in.) (1 in. = 25.4 mm)

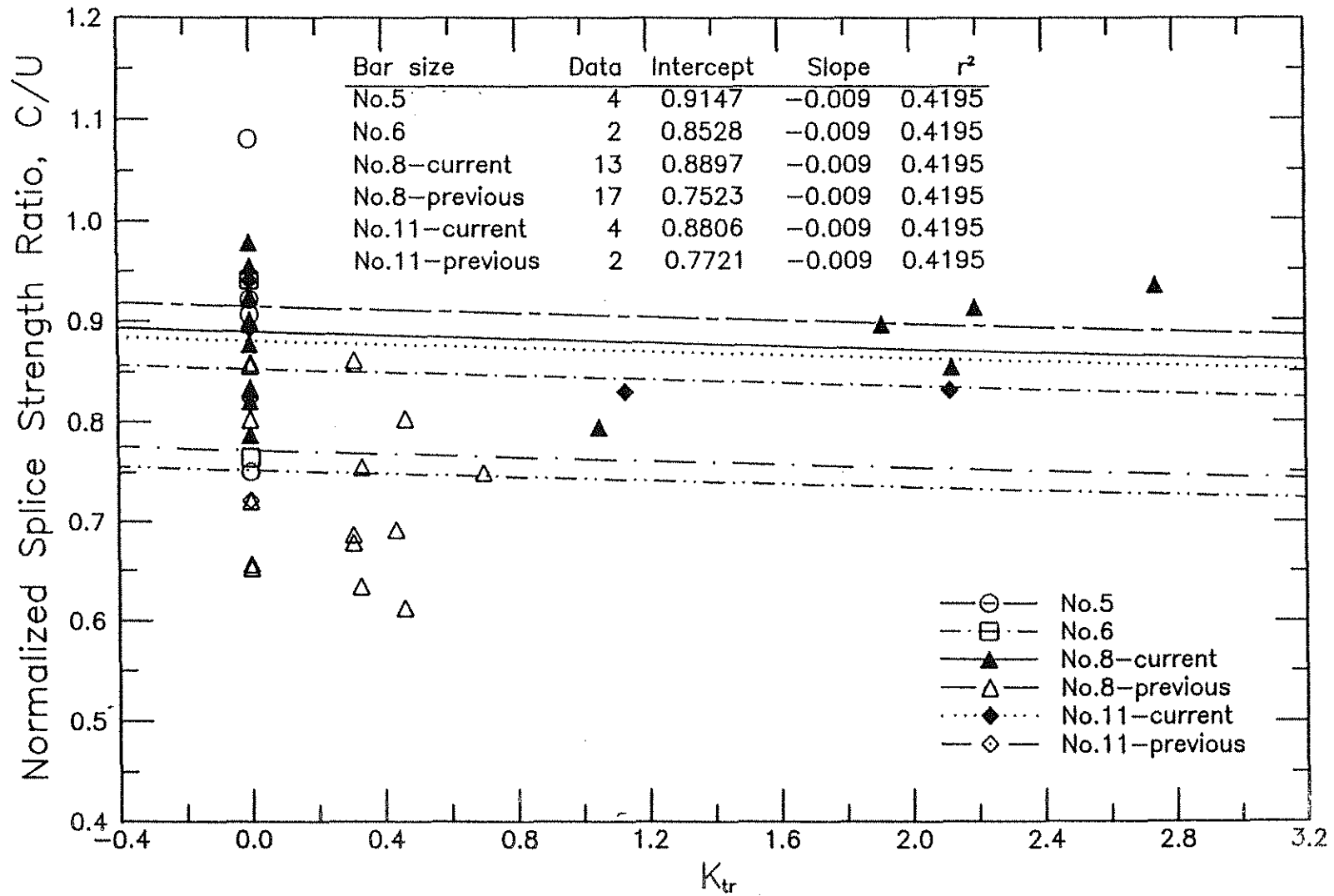


Fig. 15 Normalized splice strength ratio, C/U , versus K_{tr} for all specimens tested in current and previous studies
(K_{tr} in in.) (1 in. = 25.4 mm)

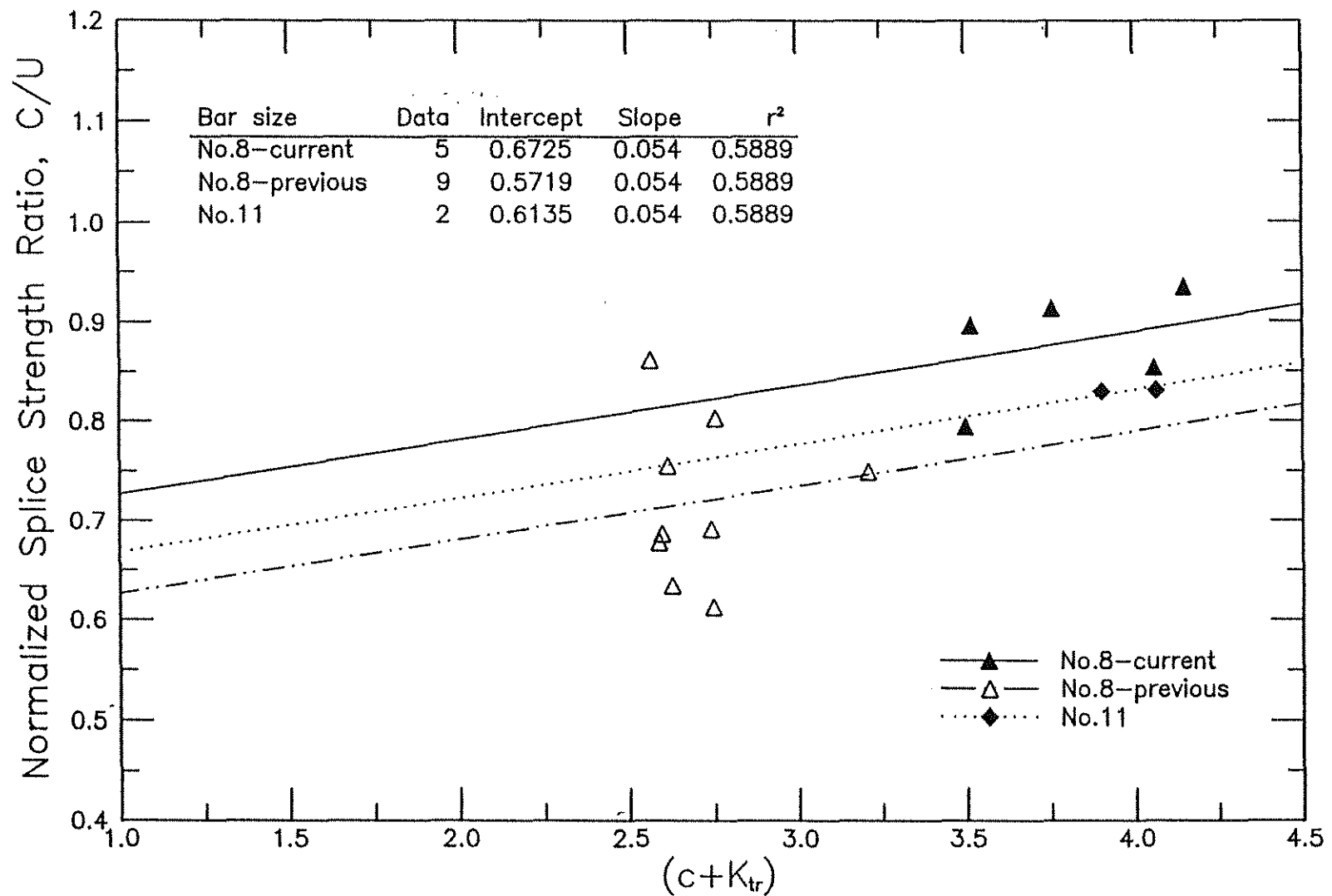


Fig. 16 Normalized splice strength ratio, C/U , versus $(c + K_{tr})$ for the specimens with stirrups tested in current and previous studies
(1 in. = 25.4 mm)

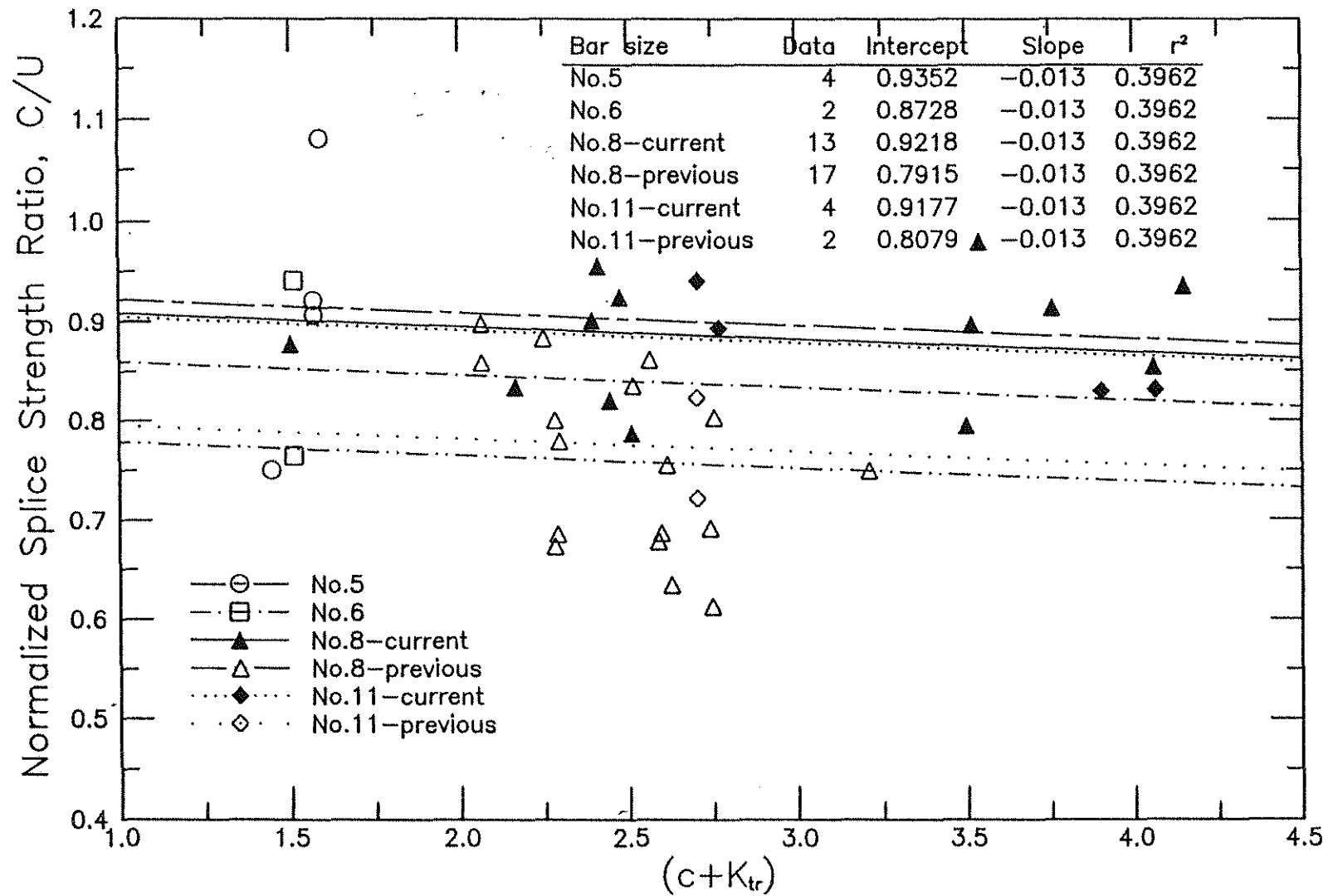


Fig. 17 Normalized splice strength ratio, C/U , versus $(c + K_{tr})$ for all specimens tested in current and previous studies
(1 in. = 25.4 mm)

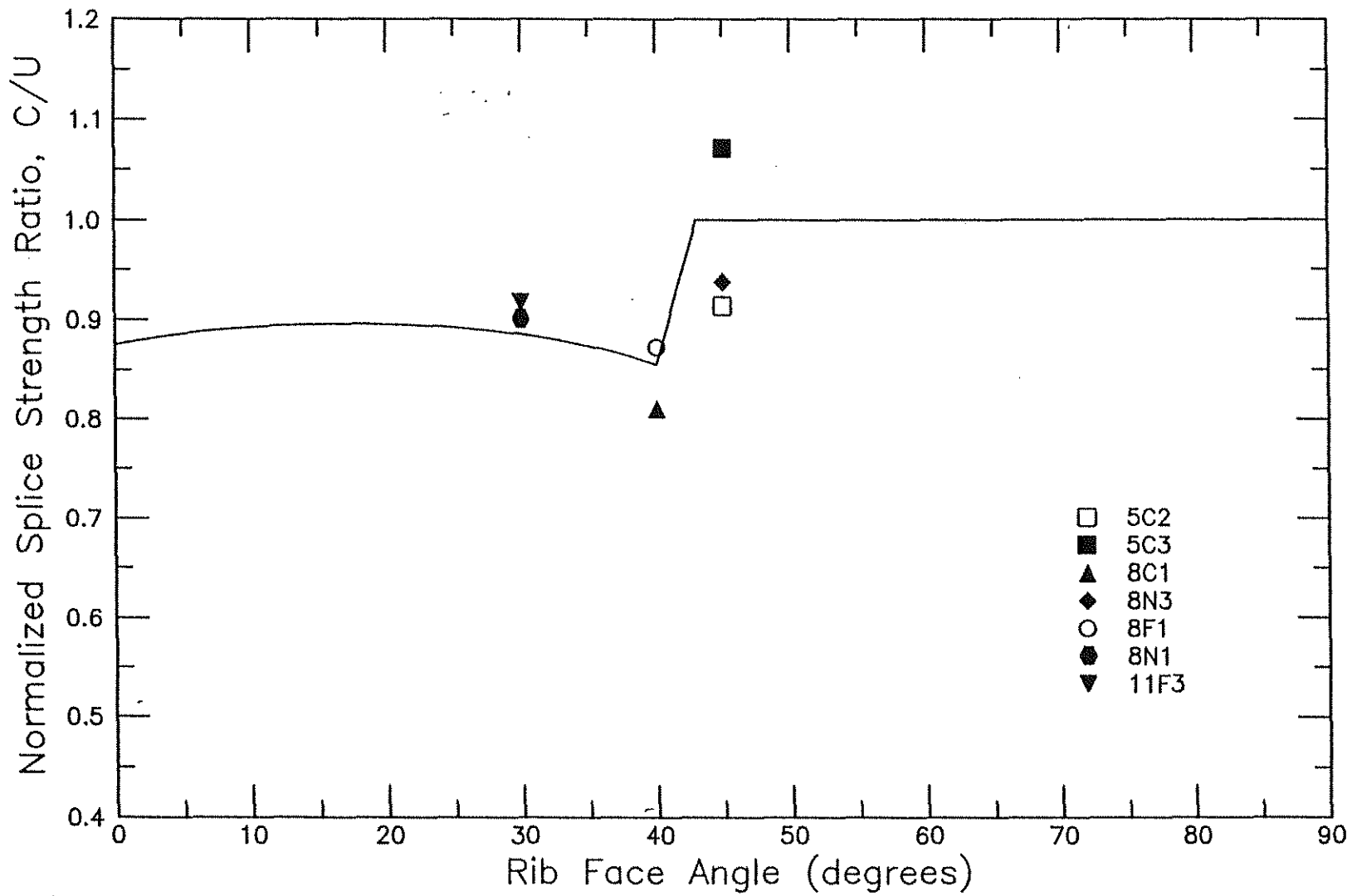


Fig. 18 Normalized splice strength ratio, C/U (average value for each bar type), versus rib face angle, γ , for the specimens without stirrups tested in the current study

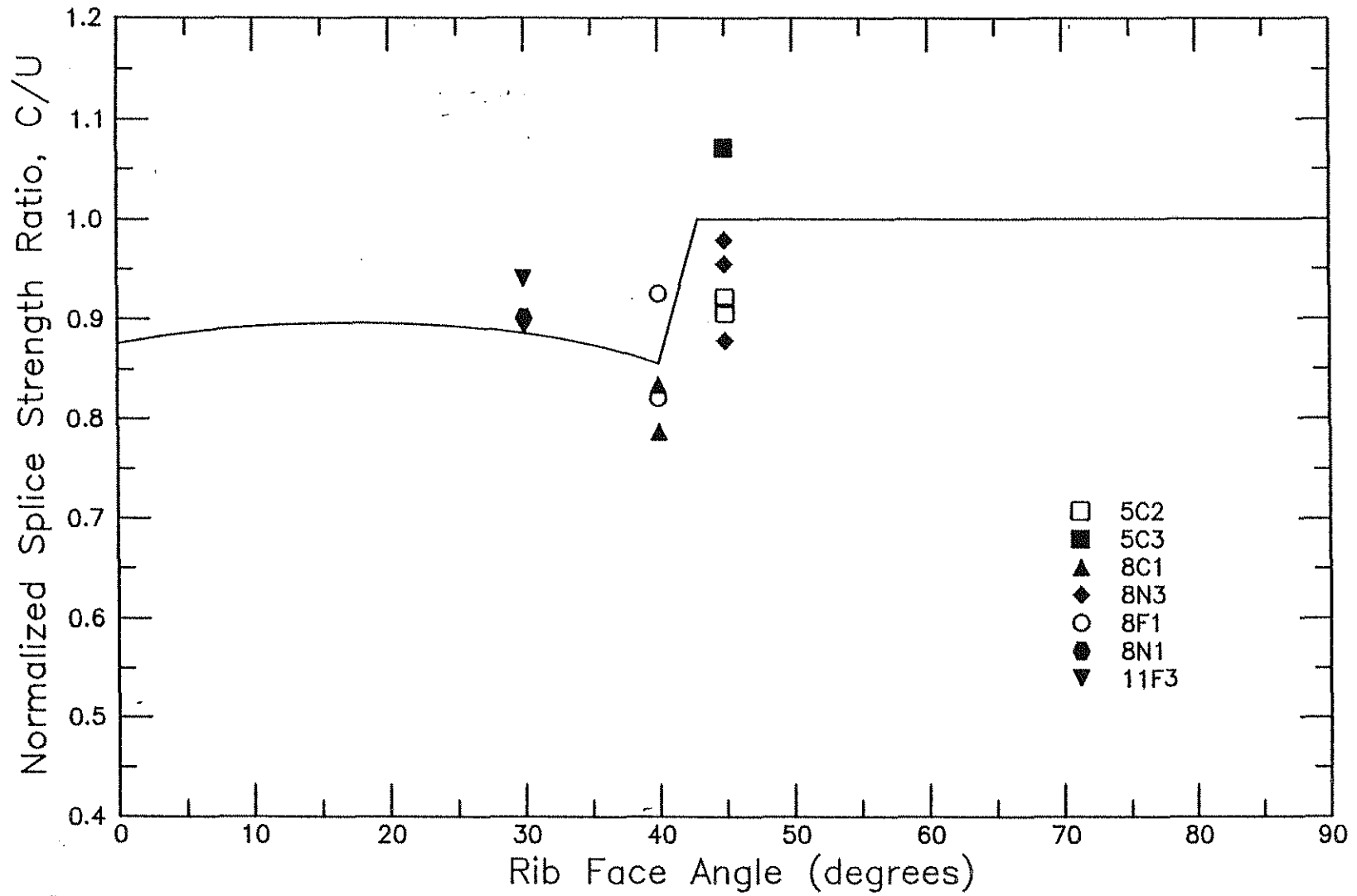


Fig. 19 Normalized splice strength ratio, C/U , versus rib face angle, γ , for the specimens without stirrups tested in the current study

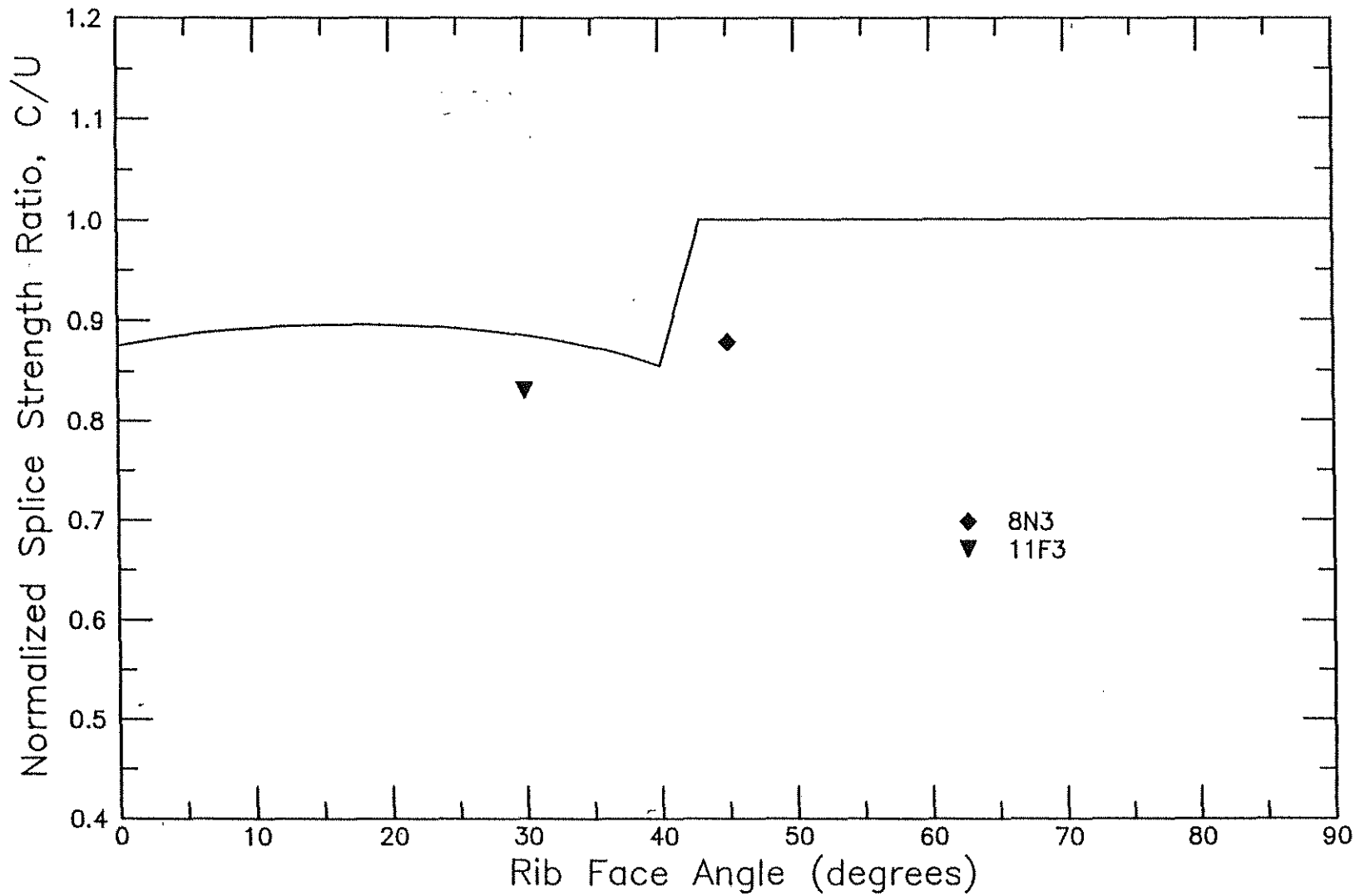


Fig. 20 Normalized splice strength ratio, C/U (average value for each bar type), versus rib face angle, γ , for the specimens with stirrups tested in the current study

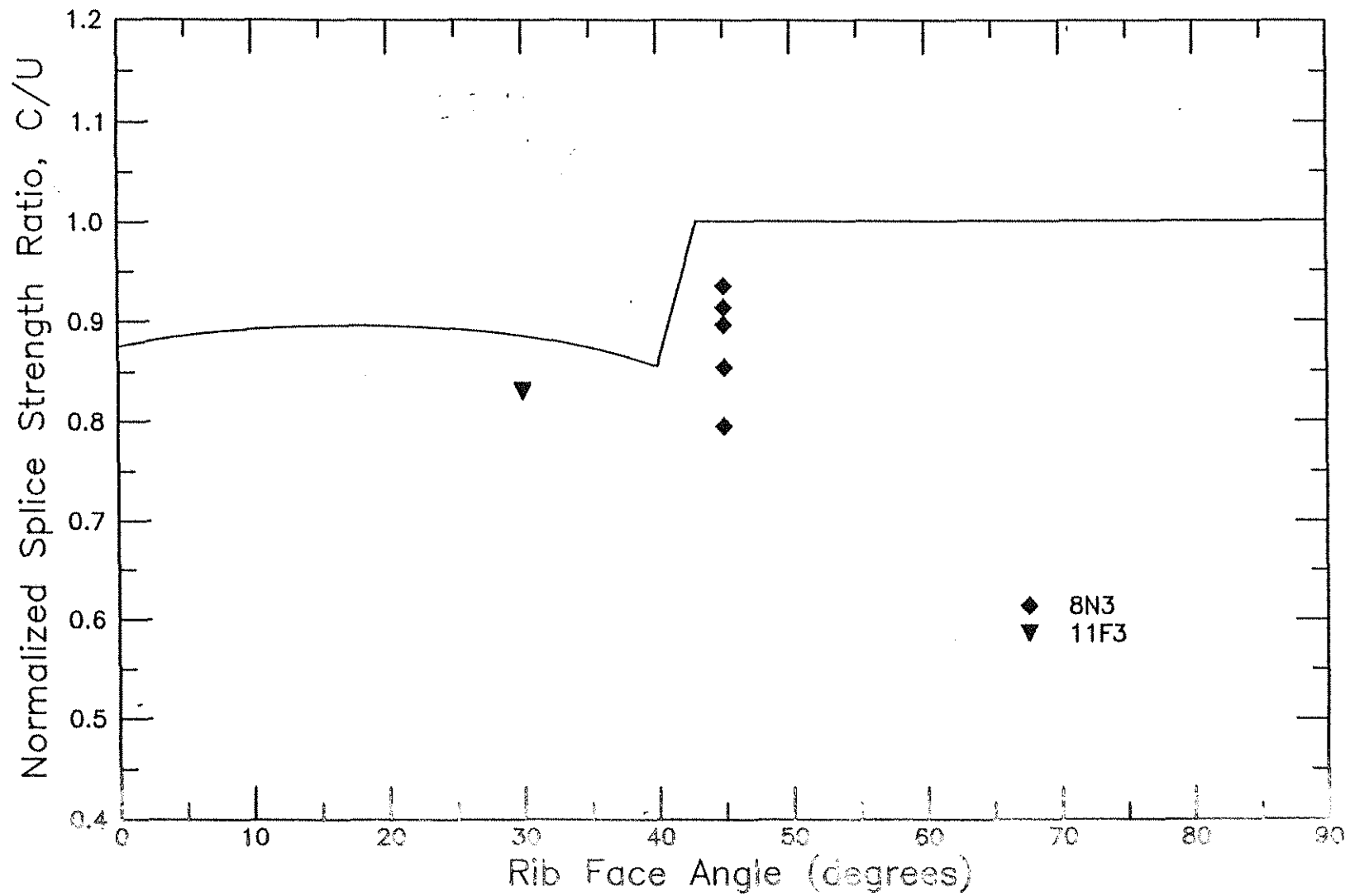


Fig. 21 Normalized splice strength ratio, C/U , versus rib face angle, γ , for the specimens with stirrups tested in the current study

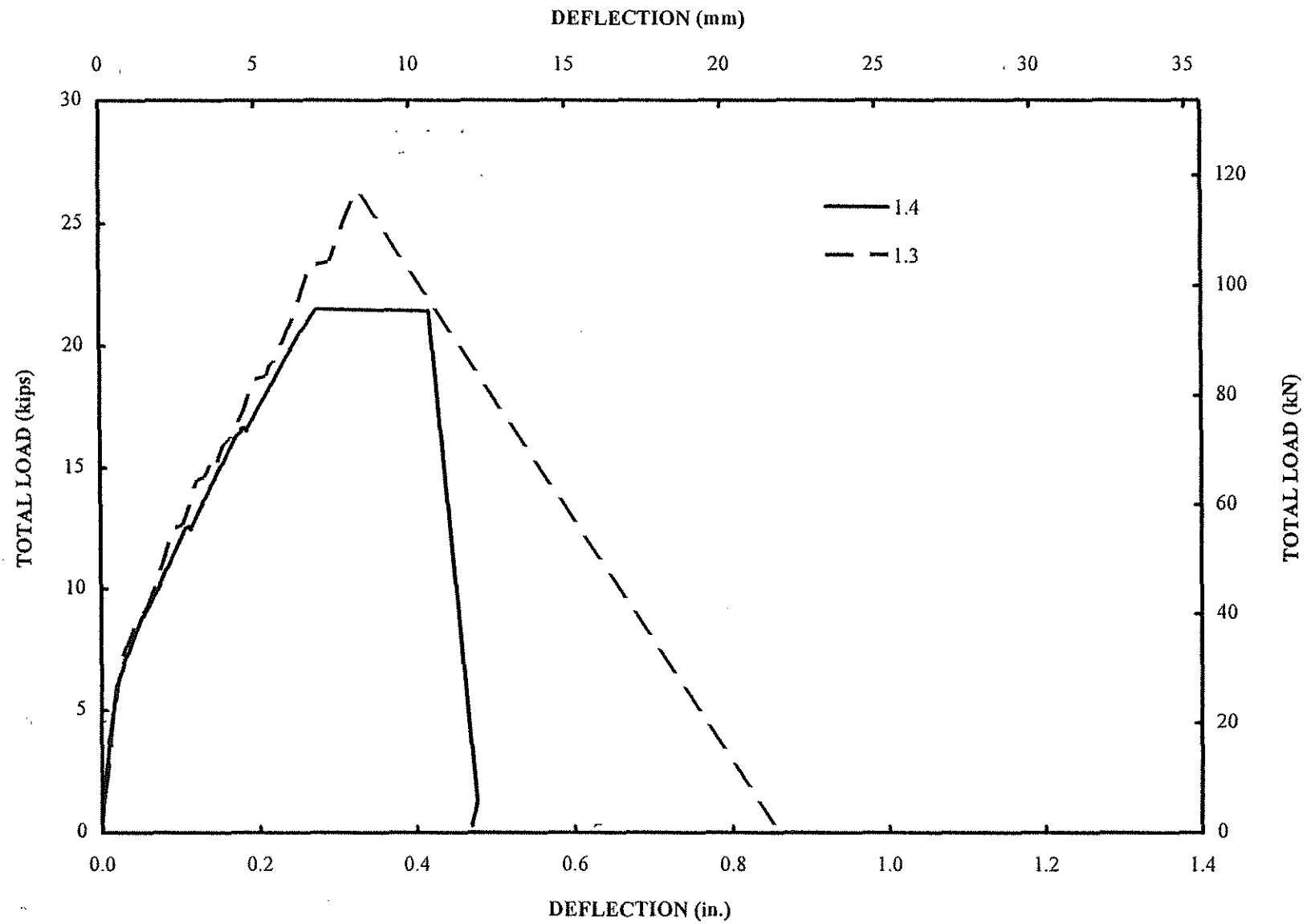


Fig A.1 Load-deflection curves for splice specimens in group 1 (1 in. = 25.4 mm, 1 kips = 4.45kN)

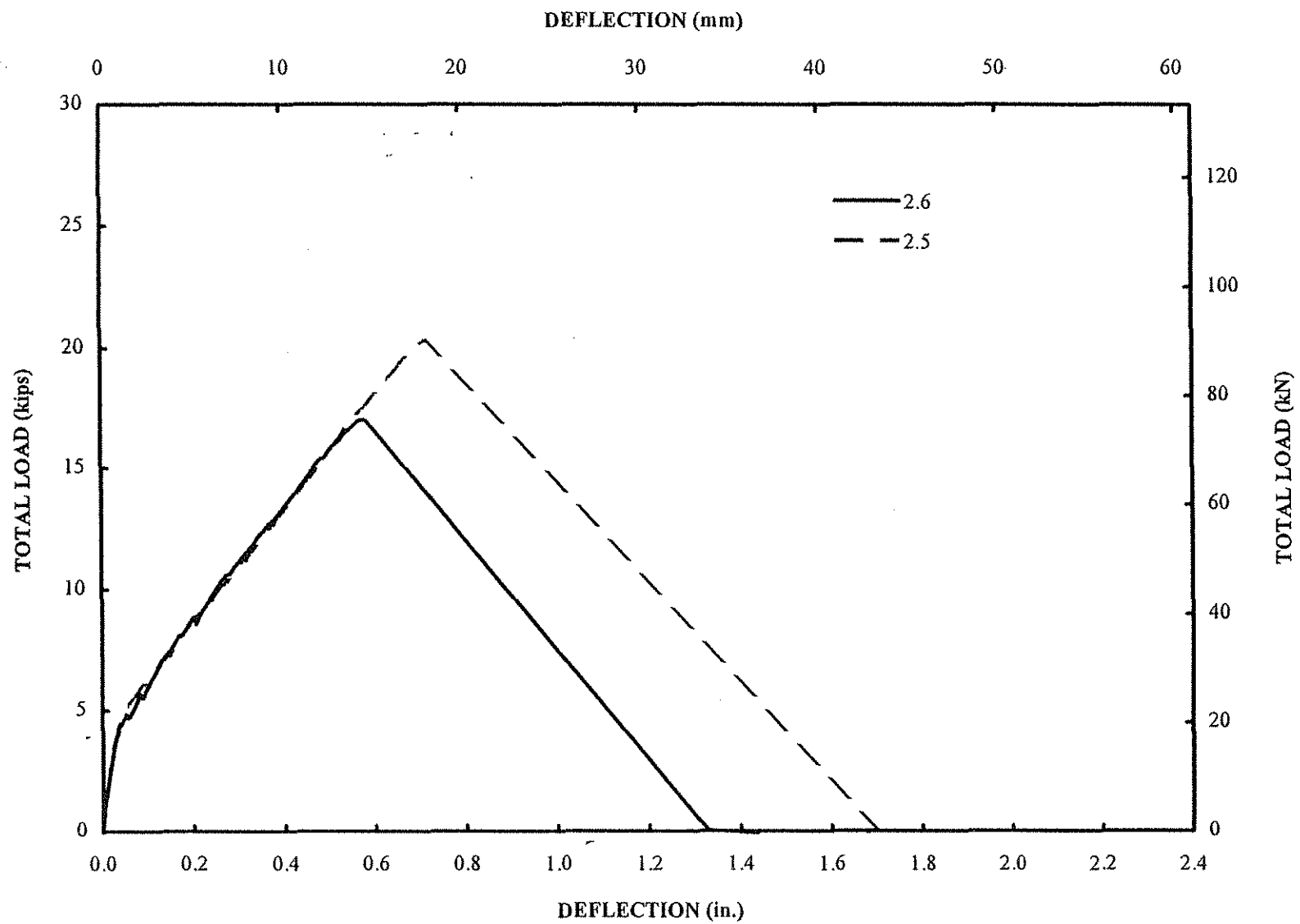


Fig A.2 Load-deflection curves for splice specimens in group 2 (1 in. = 25.4 mm, 1 kips = 4.45 kN)

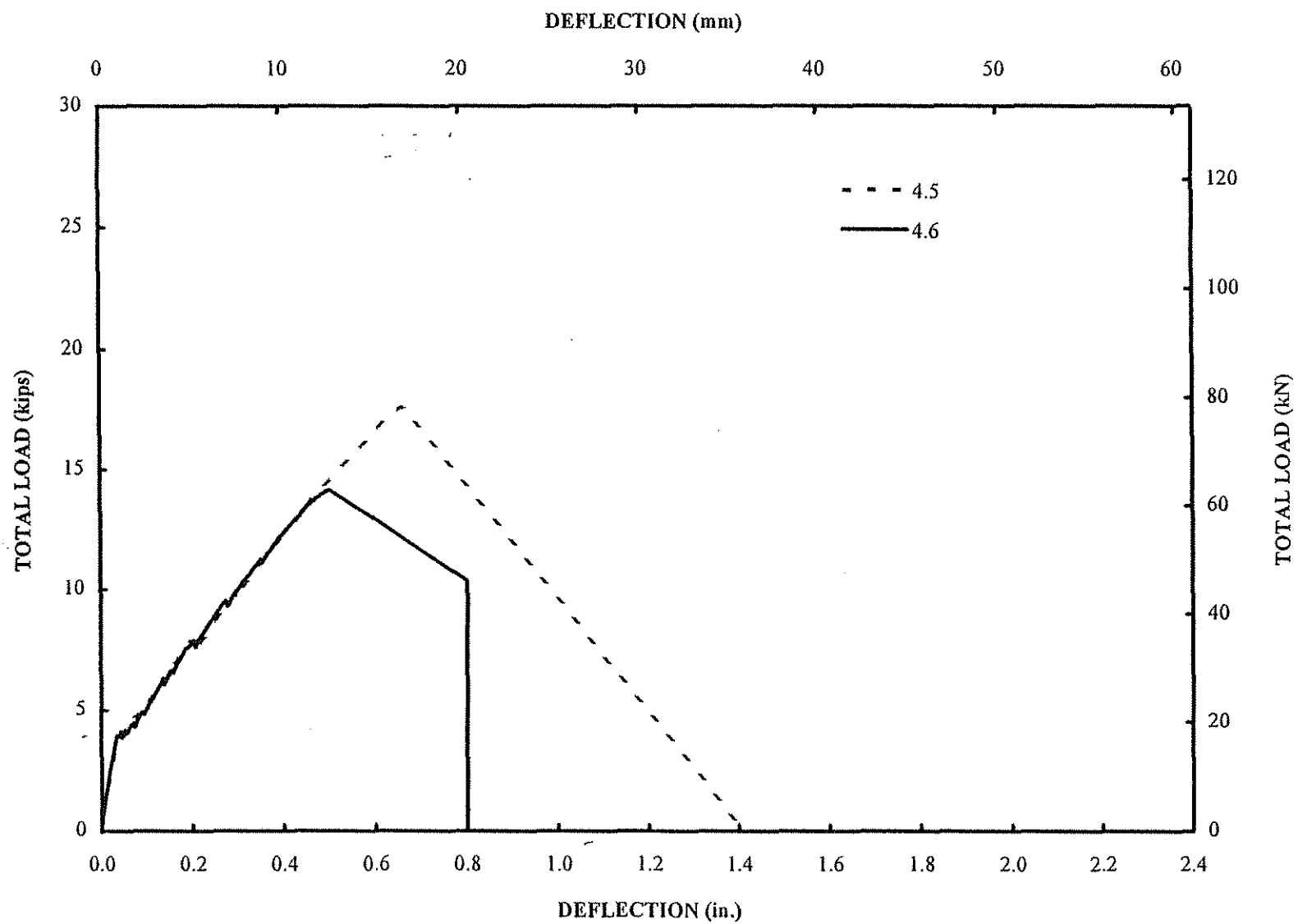


Fig A.3 Load-deflection curves for splice specimens in group 4 (1 in. = 25.4 mm, 1kips = 4.45kN)

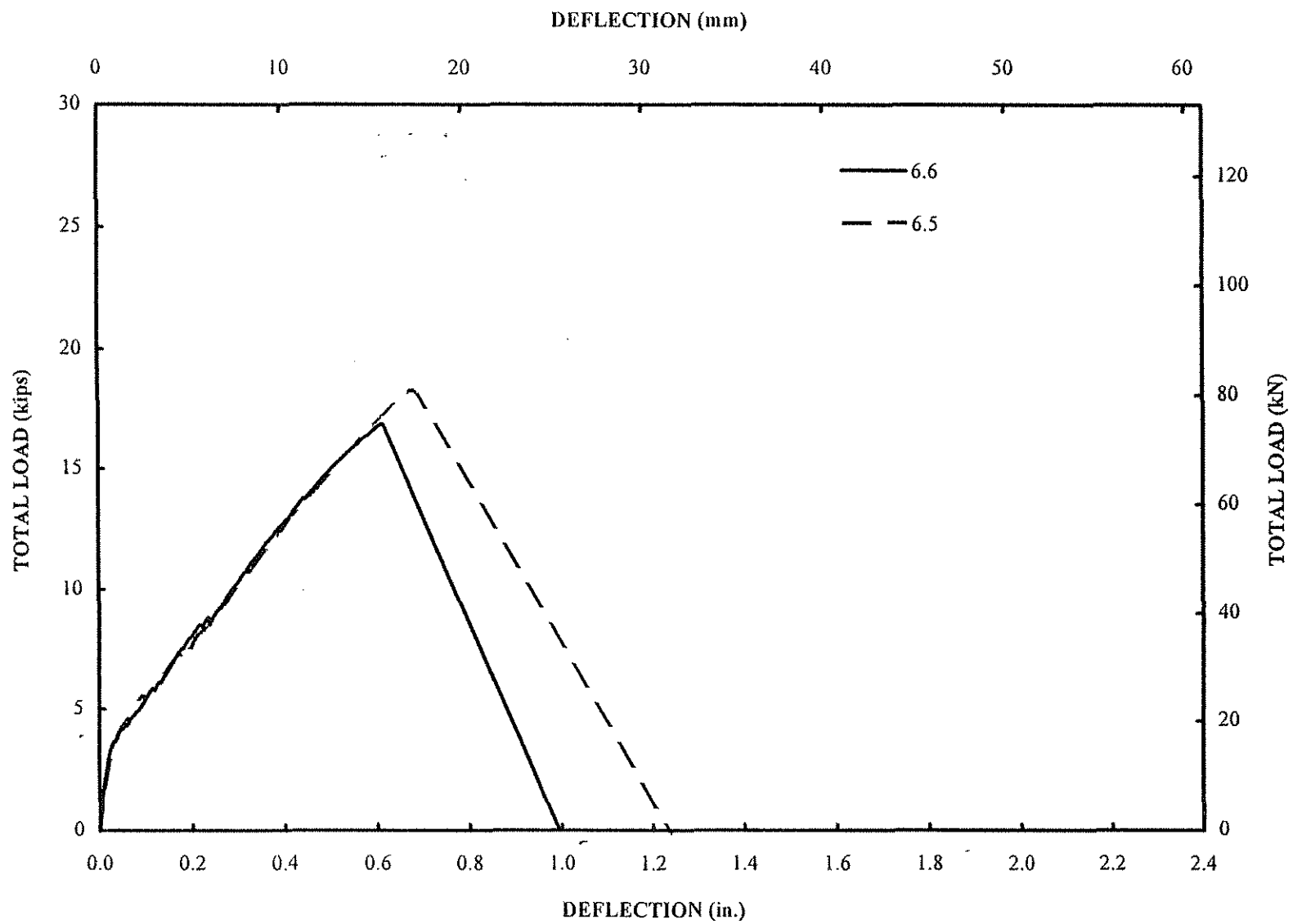


Fig A.4 Load-deflection curves for splice specimens in group 6 (1 in. = 25.4 mm, 1kips = 4.45 kN)

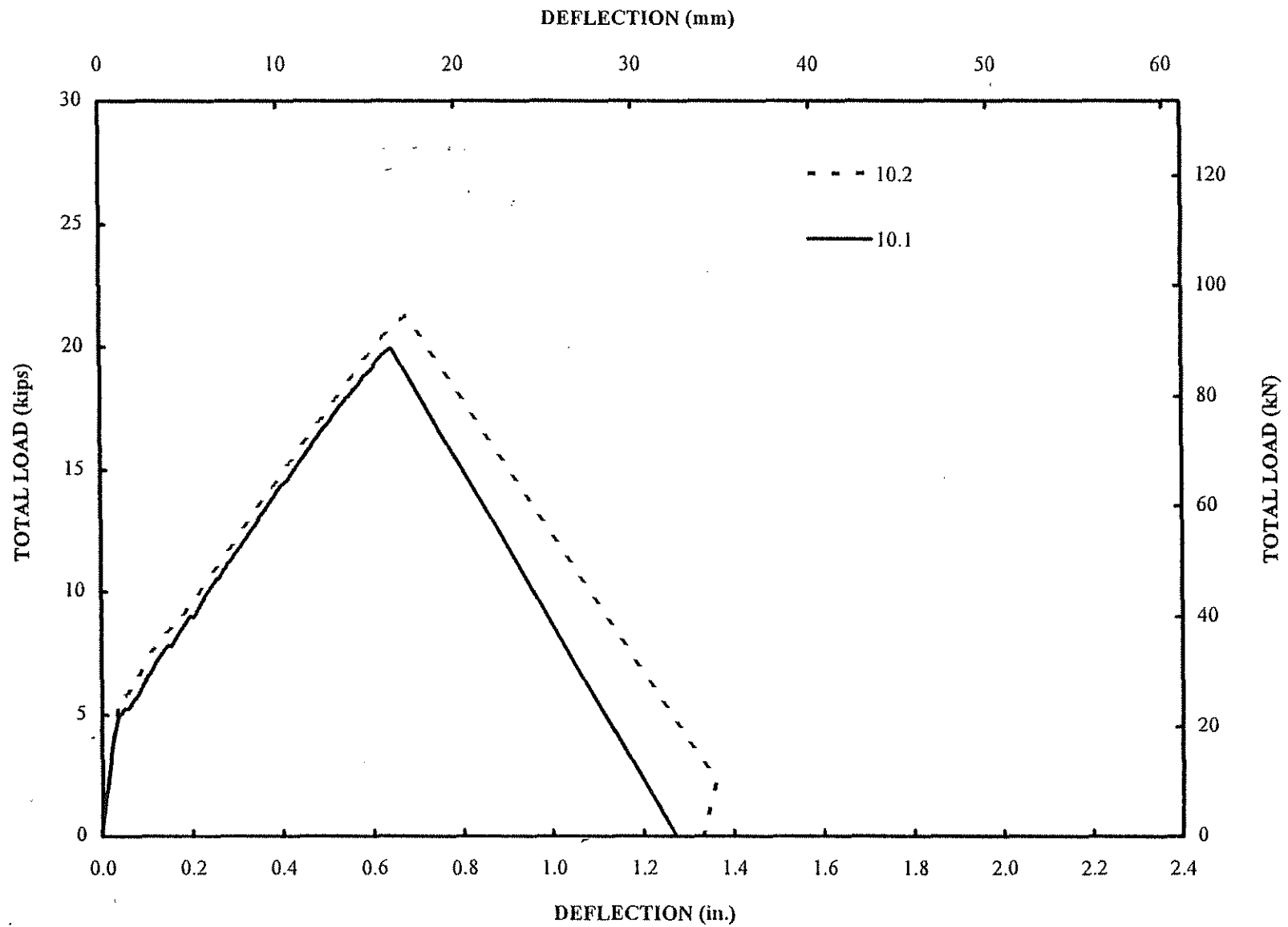


Fig A.5 Load-deflection curves for splice specimens in group 10 (1 in. = 25.4 mm, 1 kips = 4.45 kN)

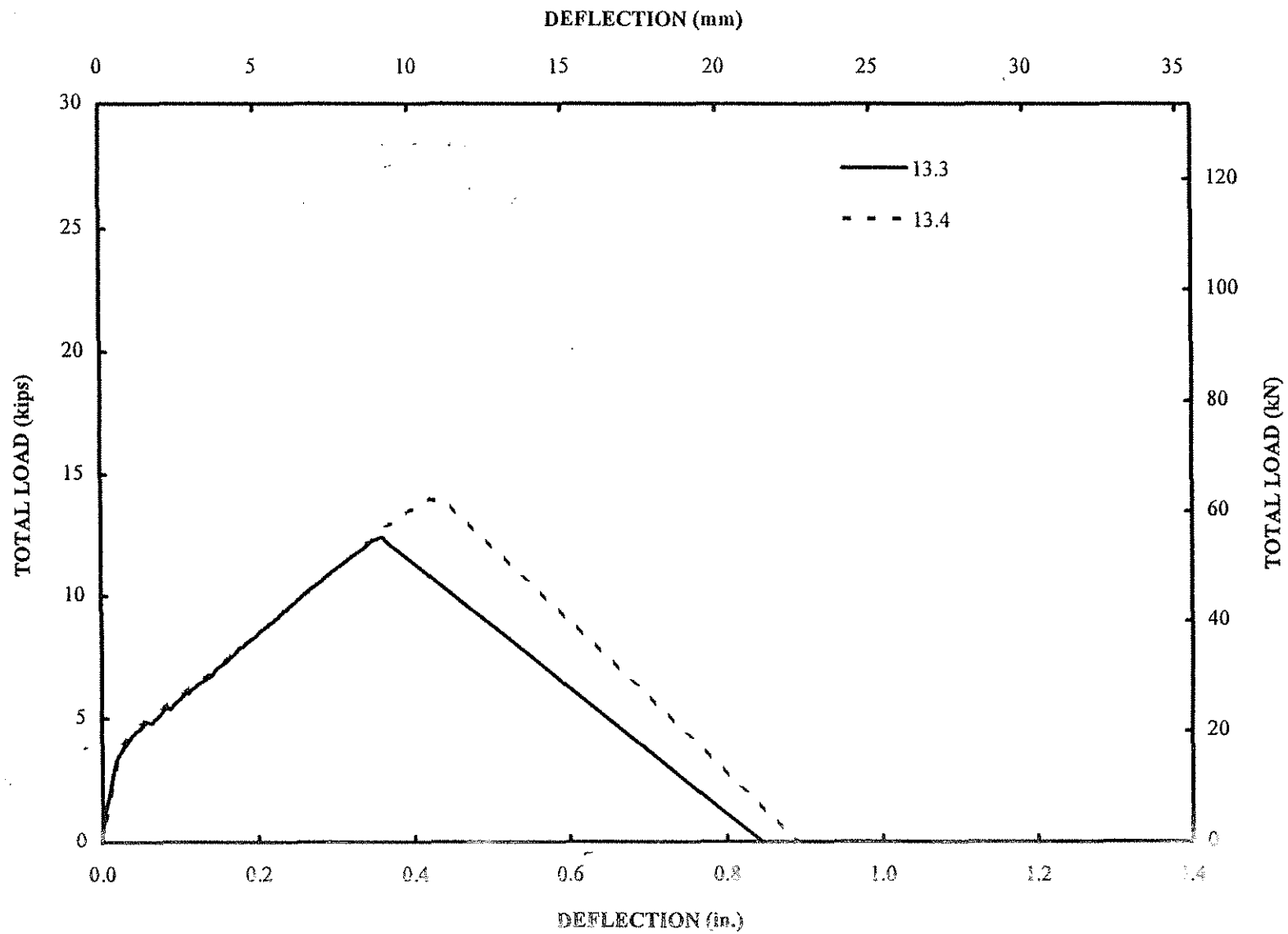


Fig A.6 Load-deflection curves for splice specimens in group 13 (1 in. = 25.4 mm, 1 kips = 4.45 kN)

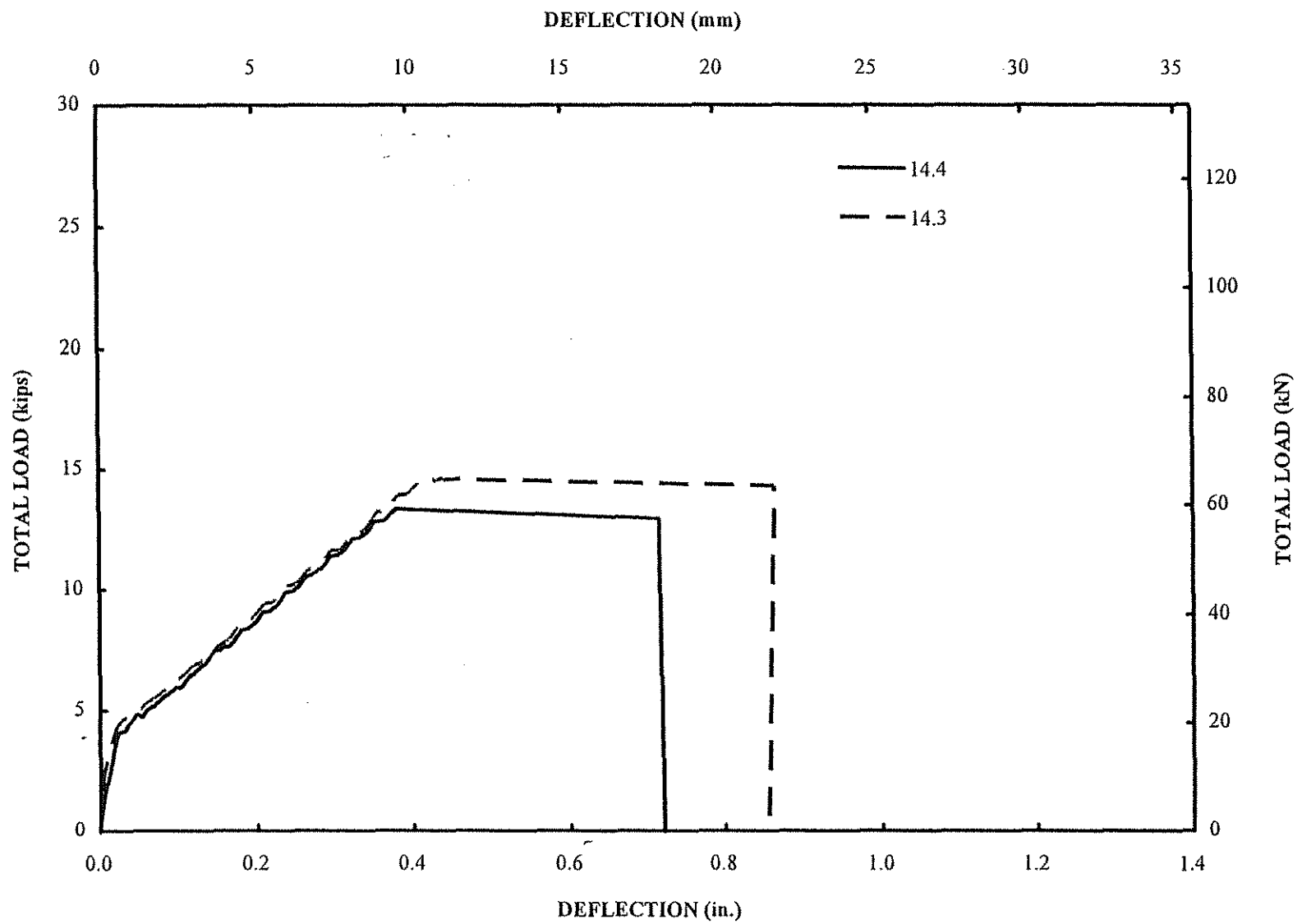


Fig A.7 Load-deflection curves for splice specimens in group 14 (1 in. = 25.4 mm, 1 kips = 4.45 kN)

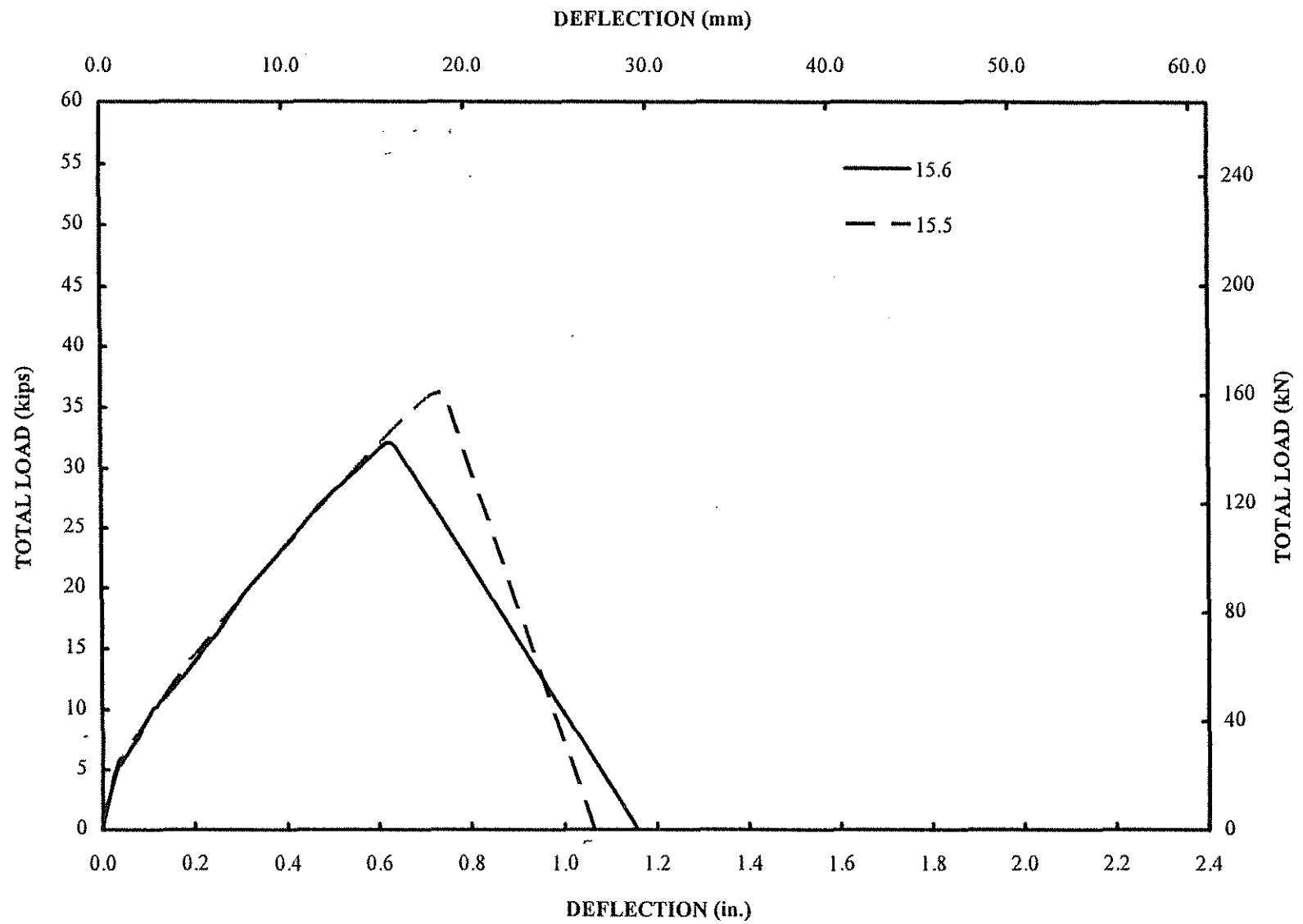


Fig A.8 Load-deflection curves for splice specimens in group 15 (1 in. = 25.4 mm, 1 kips = 4.45 kN)

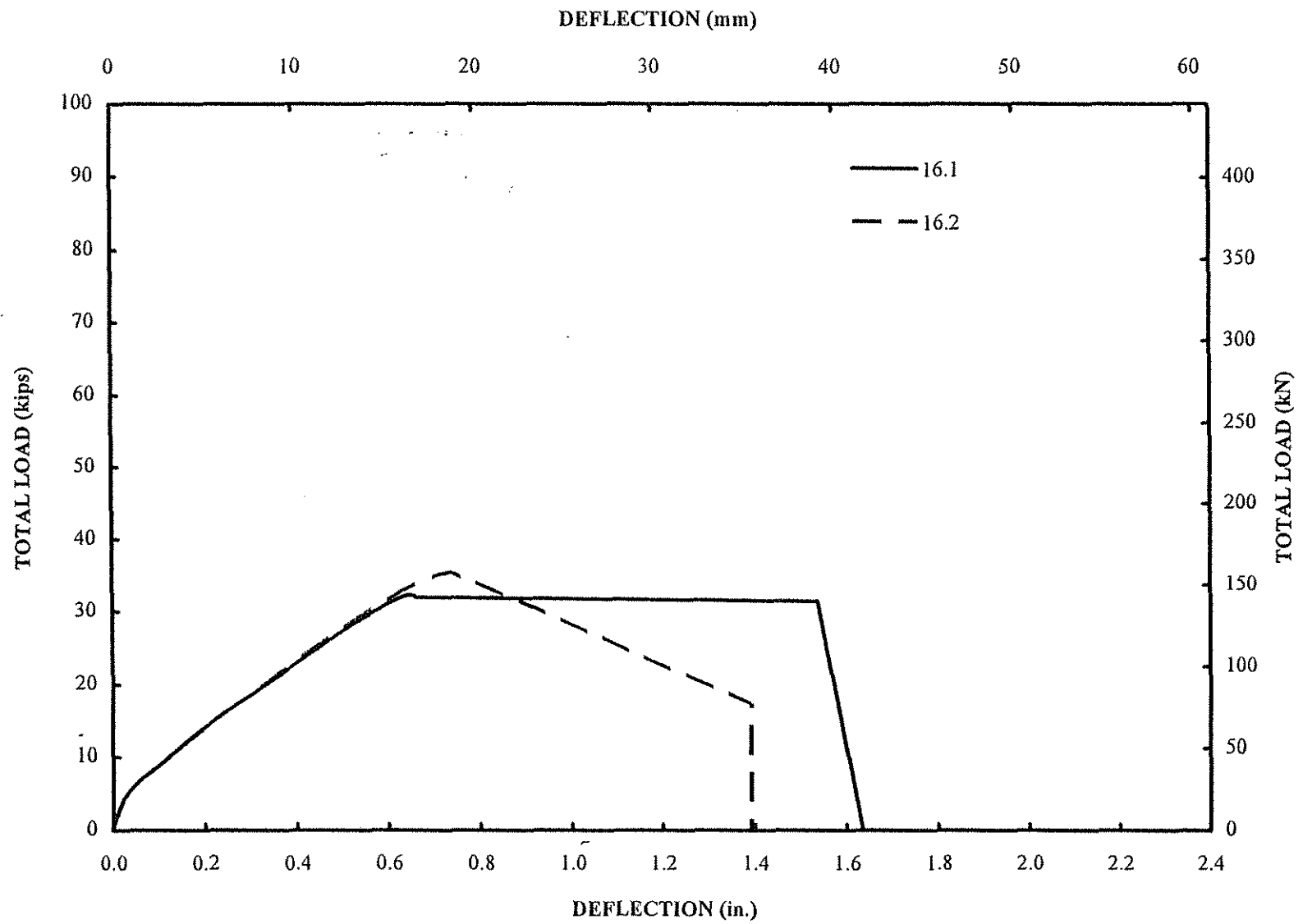


Fig A.9 Load-deflection curves for splice specimens in group 16 (1 in. = 25.4 mm, 1 kips = 4.45 kN)

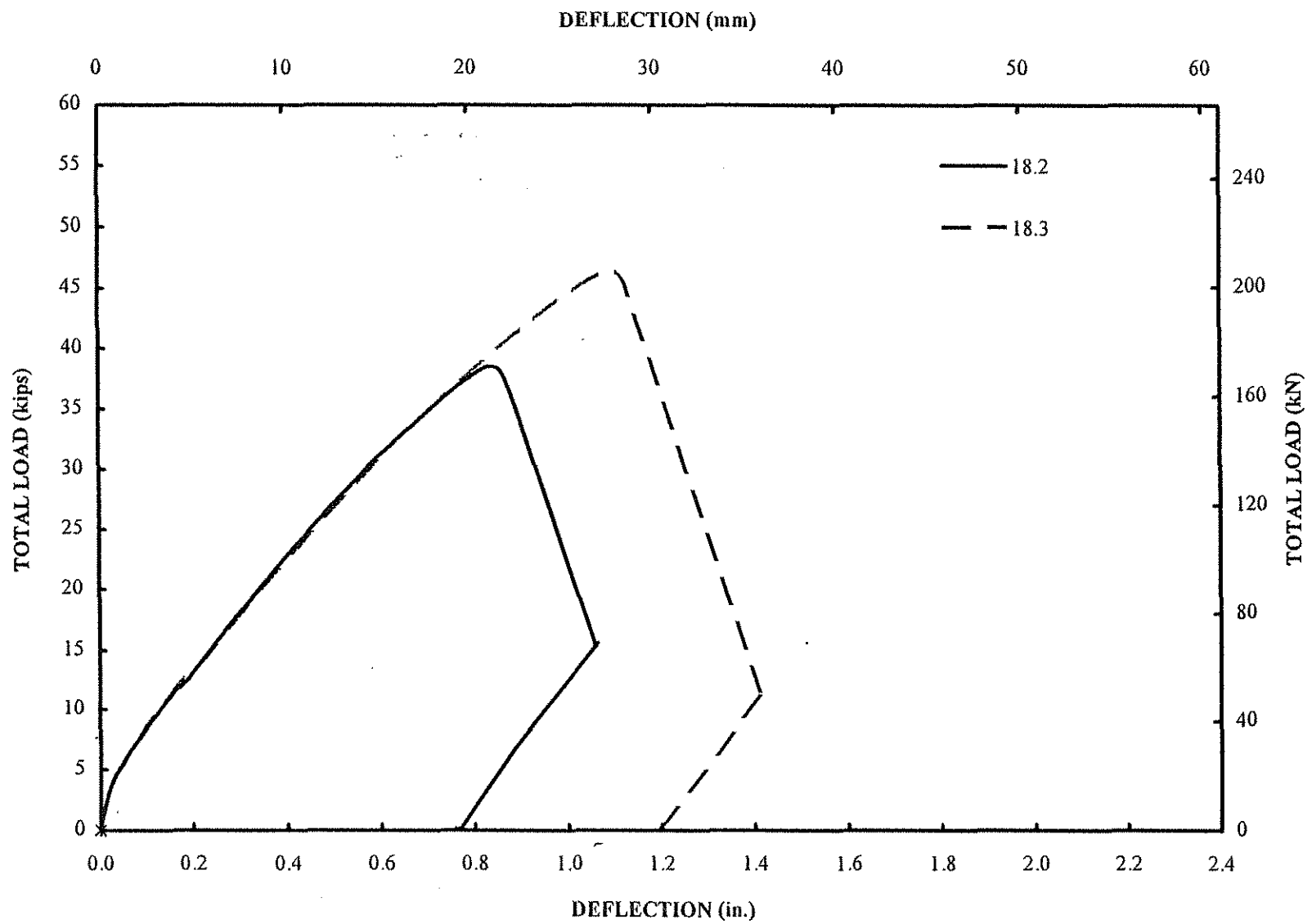


Fig A.10 Load-deflection curves for splice specimens in group 18 (1in. = 25.4 mm, 1 kips = 4.45 kN)

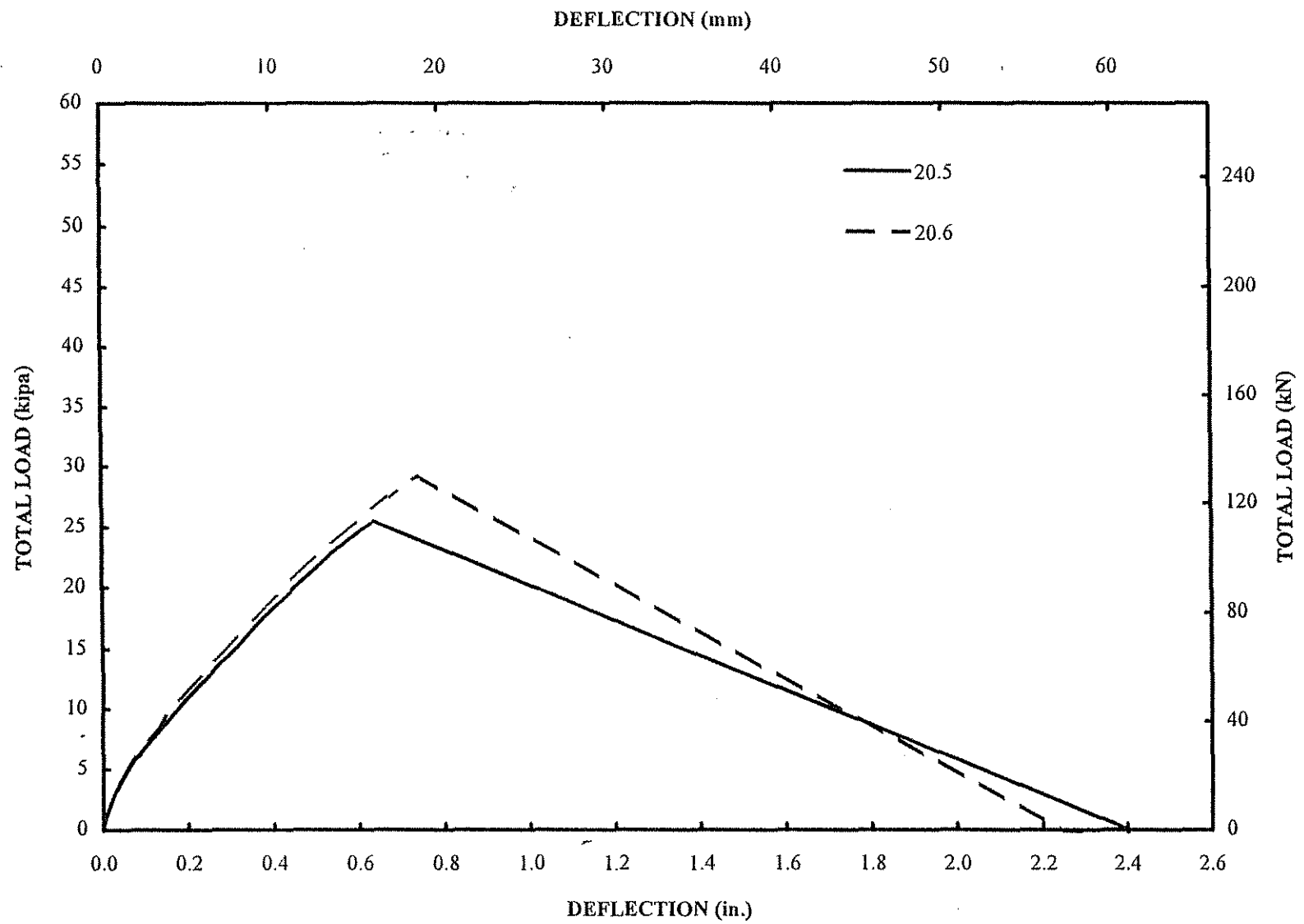


Fig A.11 Load-deflection curves for splice specimens in group 20 (1 in. = 25.4 mm, 1 kips = 4.45 kN)

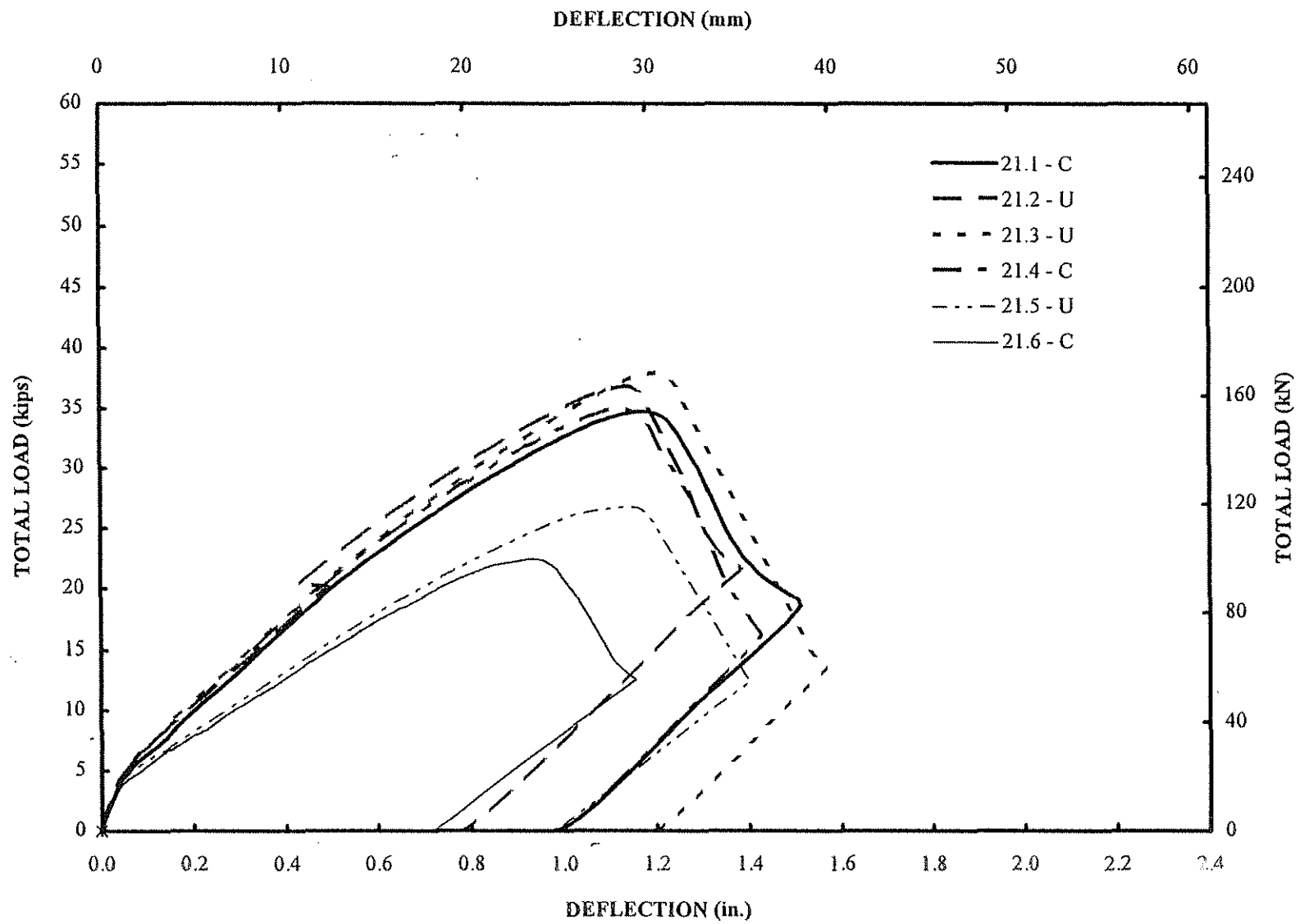


Fig A.12 Load-deflection curves for splice specimens in group 21 (1 in. = 25.4 mm, 1 kips = 4.45kN)

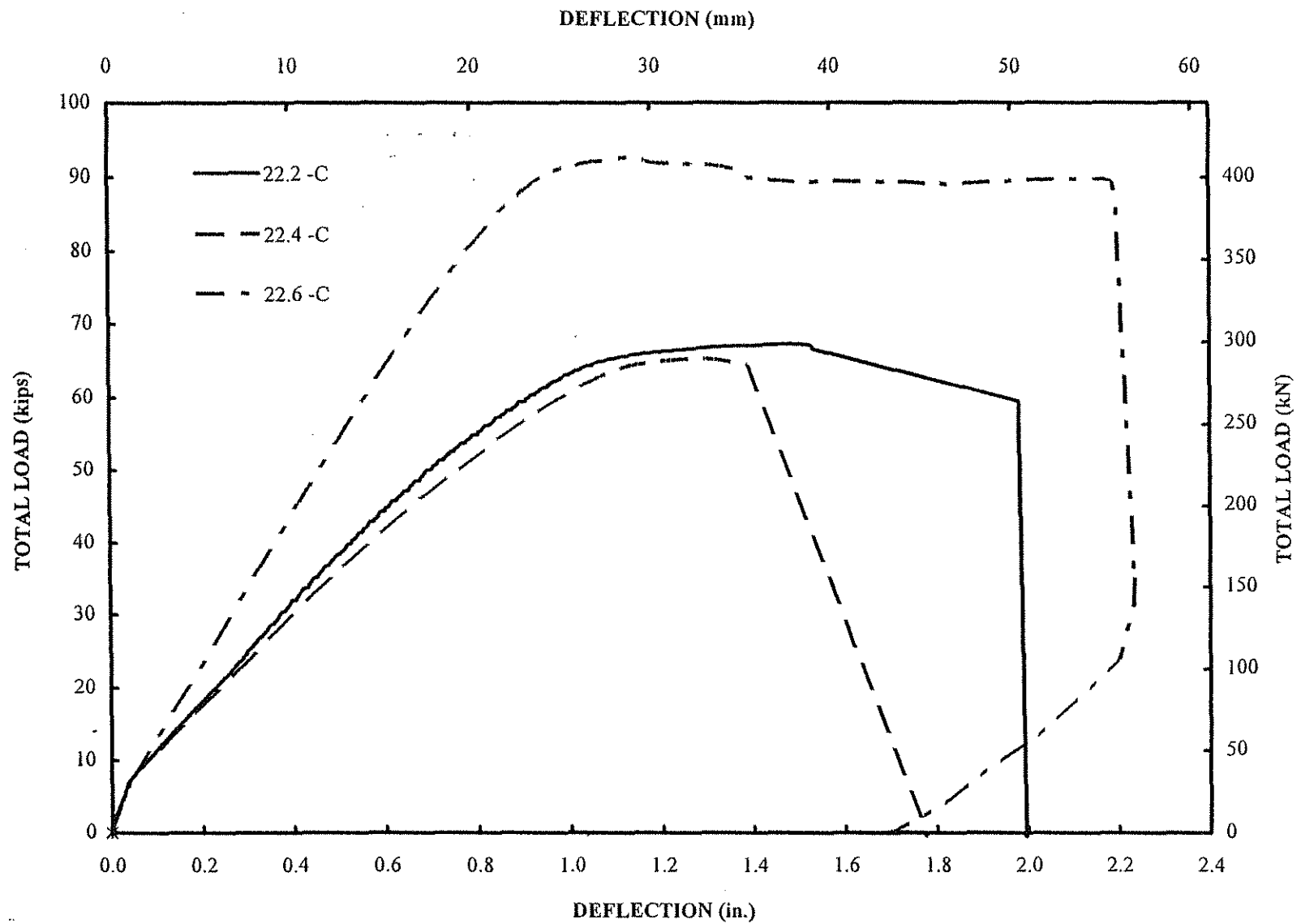


Fig A.13 Load-deflection curves for splice specimens in group 22 (1 in. = 25.4 mm, 1 kips = 4.45 kN)

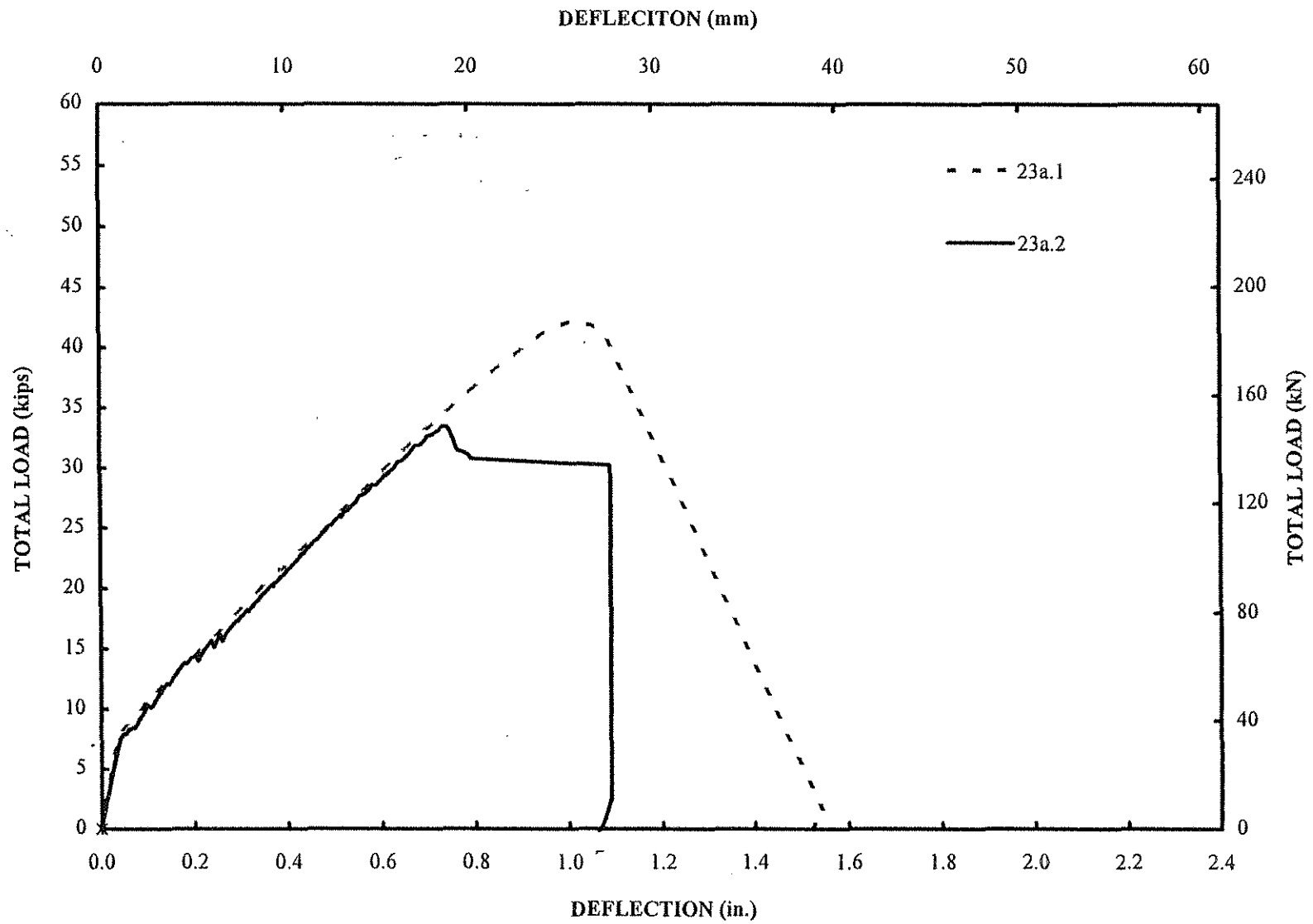


Fig A.14 Load-deflection curves for splice specimens in group 23a (1 in. = 25.4 mm, 1 kips = 4.45 kN)

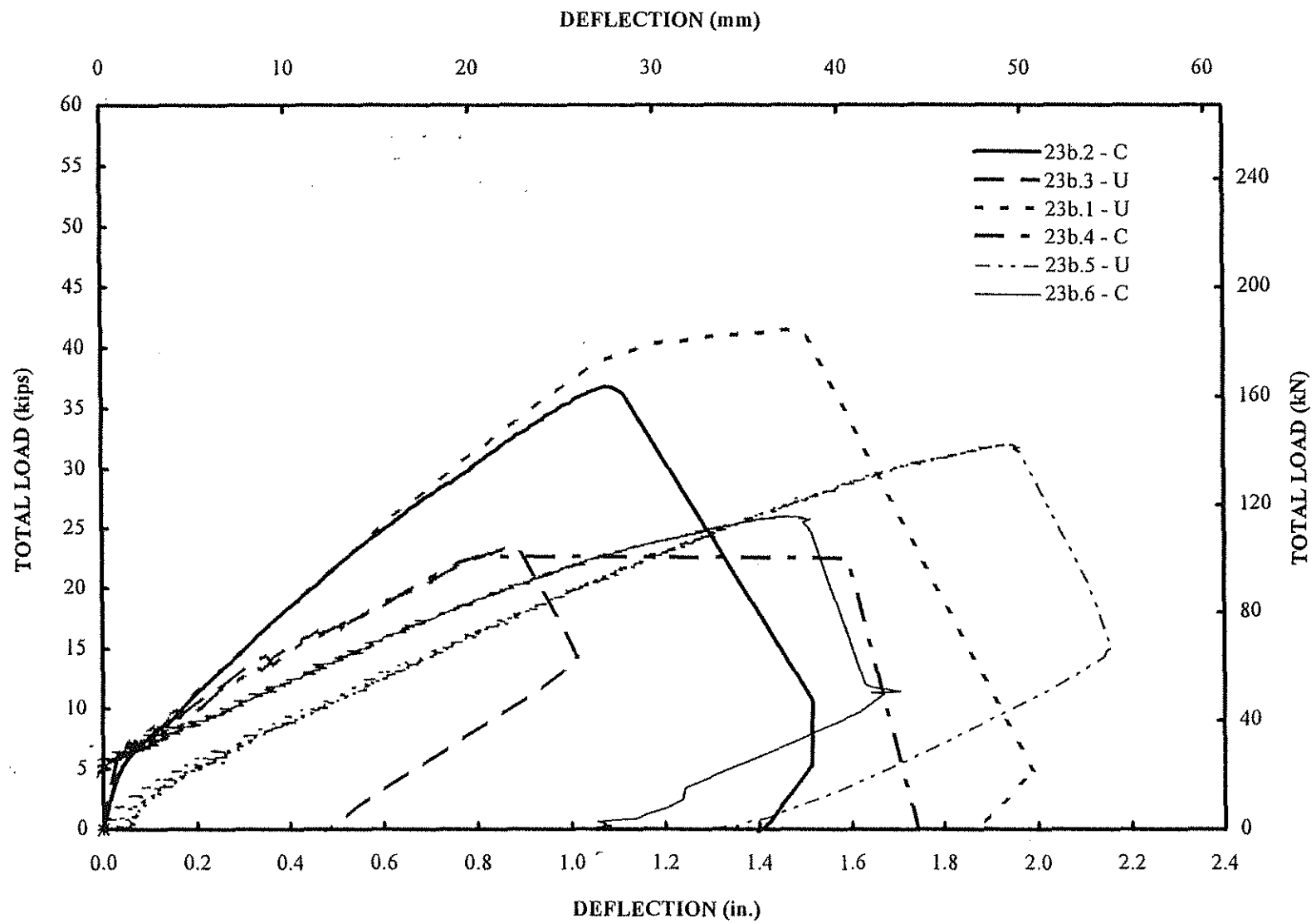


Fig A.15 Load-deflection curves for splice specimens in group 23b (1 in. = 25.4 mm, 1 kips = 4.45 kN)

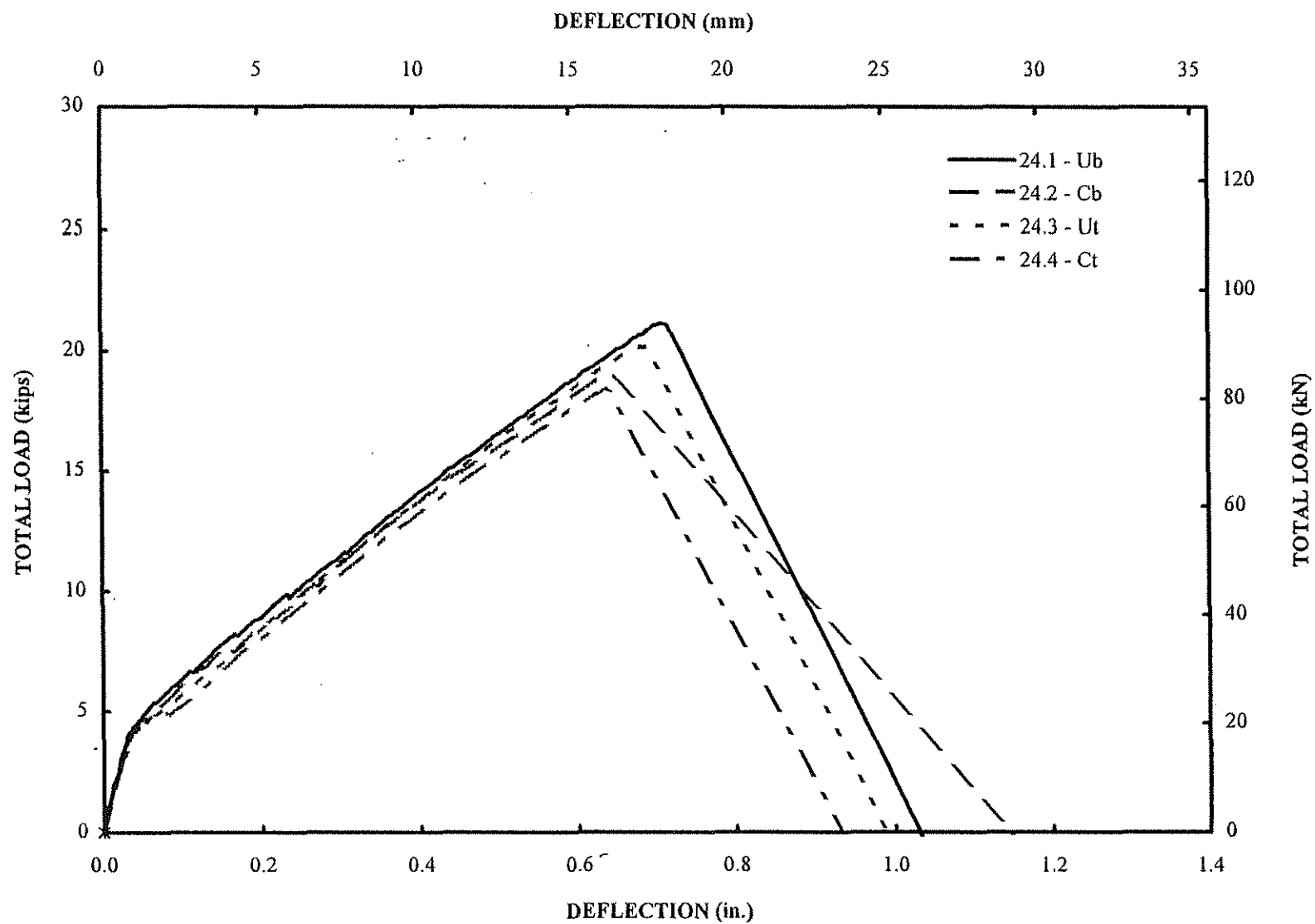


Fig A.16 Load-deflection curves for splice specimens in group 24. See Table 8 for symbols (1 in. = 25.4 mm, 1 kips = 4.45kN)

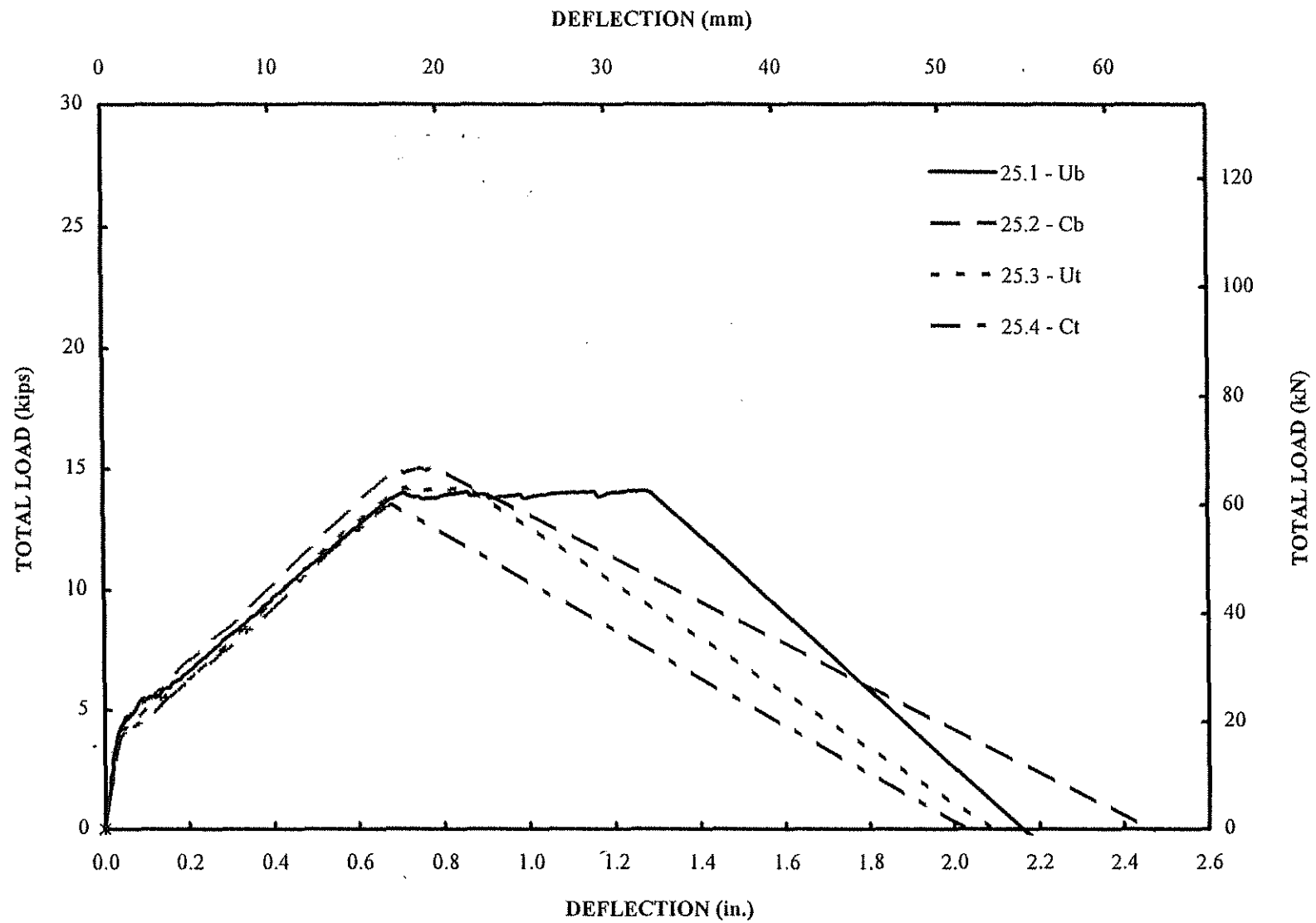


Fig A.17 Load-deflection curves for splice specimens in group 25. See Table 8 for symbols (1 in. = 25.4 mm, 1kips = 4.45 kN)

APPENDIX B
Comparison of Coating Thickness Measurement

Bar No.	Method	measurements (mils)															Mean	
		side	1	2	3	4	5	6	7	8	9	10	11	12	13	14	15	(mils)
#1, 8N0 L=36 in.	ASTM A 775	1	8.5	9.0	8.5	9.0	8.0	8.0	8.0	7.5	7.0	7.0	6.5	6.5	6.5	6.5	6.5	7.5
		2	9.0	8.5	8.0	7.5	8.0	8.5	7.0	6.5	6.0	6.0	5.5	6.5	6.0	5.5	5.5	6.9
		mean																7.2
	CURRENT	1	6.5	6.5	5.5	5.5	6.0	7.0	6.0	6.5	5.5	5.0	4.0	5.0	4.5	6.0	5.0	5.6
		2	7.5	7.5	8.0	8.0	8.0	8.0	8.0	7.0	7.5	6.0	6.0	6.5	6.5	7.0	6.5	7.2
		mean																6.4
Bar No.	Method	measurements (mils)															Mean	
		side	1	2	3	4	5	6	7	8	9	10	11	12	13	14	15	(mils)
#2, 8N0 L=36 in.	ASTM A 775	1	8.0	8.5	10.0	10.0	10.0	12.0	11.0	10.5	10.0	9.0	9.0	10.5	11.0	10.5	10.5	10.0
		2	8.0	8.0	8.0	8.5	8.5	8.5	8.0	8.0	8.0	8.5	8.0	9.0	9.0	8.0	10.0	8.4
		mean																9.2
	CURRENT	1	8.0	7.5	8.0	7.5	8.0	8.0	8.0	8.0	8.0	8.0	9.0	10.0	11.0	9.5	9.5	8.5
		2	10.0	11.0	11.0	10.5	12.0	11.5	12.0	12.0	11.0	11.0	11.0	12.0	12.0	12.5	12.0	11.4
		mean																10.0
Bar No.	Method	measurements (mils)															Mean	
		side	1	2	3	4	5	6	7	8	9	10	11	12	13	14	15	(mils)
#3, 8N0 L=36 in.	ASTM A 775	1	6.0	6.5	6.5	6.5	7.0	8.0	7.0	6.5	6.5	6.5	7.0	7.0	6.5	6.5	6.5	6.7
		2	6.0	6.0	6.5	6.5	7.0	6.0	7.0	7.5	6.0	6.5	6.5	6.5	6.0	6.0	6.5	6.4
		mean																6.6
	CURRENT	1	9.0	9.0	9.5	9.5	9.0	9.0	9.0	9.5	9.5	9.5	9.0	9.0	9.0	9.5	9.5	9.2
		2	9.5	9.0	9.0	9.0	8.5	9.0	9.0	8.5	8.0	8.0	9.0	8.0	8.5	8.5	9.5	8.7
		mean																9.0
Bar No.	Method	measurements (mils)															Mean	
		side	1	2	3	4	5	6	7	8	9	10	11	12	13	14	15	(mils)
#4, 8N0 L=18 in.	ASTM A 775	1	8.0	8.5	9.0	9.0	9.0	8.0	7.5	7.0	7.0	7.5	7.5	7.5	7.5	7.5	7.0	7.8
		2	8.0	8.0	8.5	8.0	8.0	8.0	8.0	7.5	7.0	7.5	8.0	7.5	7.0	7.0	7.0	7.7
		mean																7.8
	CURRENT	1	8.5	8.5	8.5	9.0	9.0	9.0	9.0	8.5	8.0	10.0	9.0	10.0	10.0	10.0	9.5	9.1
		2	10.0	9.5	10.0	10.5	10.0	10.5	10.5	9.0	10.1	10.5	11.0	11.0	12.0	11.5	11.5	10.5
		mean																9.8
OVERALL	MEAN	ASTM A 775															7.7	
		CURRENT															8.8	
	STD	ASTM A 775															1.320	
		CURRENT															1.830	
	COV	ASTM A 775															0.172	
		CURRENT															0.209	

1 mil = 0.0254 mm